Mohamed Ibrahim

# A New Extended Corresponding States Equation of State for Modelling CO2-Water Thermodynamics - A Compromise for CFD

Mohamed Ibrahim

Doctoral Thesis

**NTNU**
Norwegian University of
Science and Technology
Faculty of Engineering
Department of Energy and Process Engineering

◙ **NTNU**
Norwegian University of
Science and Technology

◙ NTNU

◙ **NTNU**
Norwegian University of
Science and Technology

Mohamed Ibrahim

# A New Extended Corresponding States Equation of State for Modelling CO2-Water Thermodynamics
# - A Compromise for CFD

Thesis for the degree of Philosophiae Doctor

Trondheim, September 2017

Norwegian University of Science and Technology
Faculty of Engineering
Department of Energy and Process Engineering

**NTNU**
Norwegian University of
Science and Technology

*In the name of Allah, the Entirely Merciful, the Especially Merciful*

*...and above every possessor of knowledge is the All-Knowing (Allah)*

*Holy Quran from verse (12:76)*

*...and say: O my Lord! increase me in knowledge.*

*Holy Quran from verse (20:114)*

*The prophet Muhammad prayer and peace of Allah be upon him said, Indeed Allah, His Angels, the inhabitants of the heavens and the earths - even the ant in his hole, even the fish - say Salat upon the one who teaches the people to do good.*

*Jami` at-Tirmidhi 2685, English translation: Vol. 5, Book 39, Hadith 2685*

*To the soul of my beloved father Ibrahim, sister Noha and grandmother Esmat Yousef,*
*I love and miss you so much...*
*To my beloved mother Khadiga Mansour, and my brilliant daughter Khadija Ibrahim*

# Abstract

This PhD work is part of the $CO_2$ Dynamics project in collaboration with Sintef Energy. We investigated the importance of accurate modelling of $CO_2$ thermodynamic properties for process design. The study was conducted for the application of depressurization of a $CO_2$ transport pipeline. In the study we investigated pure $CO_2$ and $CO_2$ mixtures, including the polar mixture of $CO_2$ - water. The study was conducted over pairs of pressure-temperature (PT) complying with two sets of experimental pipeline depressurization data. The results showed a significant impact of the quality of used equation of state (EoS), and the presence of impurities on the predicted thermodynamic behavior and speed of sound. Moreover, we conducted research on the capabilities of the extended corresponding states (ECS) EoS SPUNG when dealing with $CO_2$ - water mixtures. The SPUNG EoS was chosen as it was shown earlier to be a very promising EoS for Carbon Capture and Storage (CCS) non-polar mixtures. We started with a preliminary study followed by a detailed study that showed the potentials and limitations of the method. We also investigated the possibilities to improve or extend the limitations of the SPUNG EoS by changing the reference fluid. The found disadvantages of SPUNG EoS when dealing with $CO_2$ - water mixtures were that it poorly predicted the water-rich phase (even though better than SRK, and SRK-HV) and the $CO_2$ solubility at wide range of conditions. As part of the investigation of the potential of the method, we conducted a reference fluid sensitivity study, which revealed a significant dependency of the density predictions on the chosen reference fluid. Within the set of hydrocarbons, the heavier the hydrocarbon was, the better it predicted the water-rich phase density. However, the reference fluid was found not to play a significant role in phase equilibrium capture. The prediction of phase equilibrium properties was more influenced by the mixing rule used in the approach of calculating the scale factors. Based on these systematic assessments, a new ECS approach was developed, which preserved the advantages of the SPUNG EoS but eliminated the limitations. The proposed EoS accurately captures the phase equilibrium and densities of the $CO_2$ - water systems at wide set of conditions of pressure, temperature and composition. The new model is an ECS that uses Bender's 20-parameter MBWR as a reference equation, and SRK-HV as bases to the approach used to calculate the shape factors for scaling. The recommended reference fluids were $NH_3$, R23, and R503 with parameters of Polt. All the evaluations in the presented articles were compared to large covering set of experimental data. Since one major advantage of the ECS based approaches is the good capture of transport properties, future work should assess the new model accuracy for predicting the $CO_2$ - water

*Abstract*

transport properties.

# Contents

# Preface

This thesis is submitted in partial fulfillment of the requirements for the degree of Philosophiae Doctor (PhD) at the Norwegian University of Science and Technology (NTNU).
I have done this work at Department of Energy and Process Engineering. My supervisors have been Prof. Ivar S. Ertesvåg and Dr. Geir Skaugen.

I hereby declare that this thesis is entirely the result of my own work except where otherwise indicated. I have only used the resources given in the list of references.

# List of Publications

The main part of the work is the following manuscripts included at the end of the thesis;

**Paper 1:** Mohamed Ibrahim, Geir Skaugen, Ivar S. Ertesvåg. PVTx modeling of $CO_2$ pipeline depressurization using SPUNG equation of state (EoS) with a comparison to SRK EoS. Energy Procedia 2014; 63:2467-2474

**Paper 2:** Mohamed Ibrahim, Geir Skaugen, Ivar S. Ertesvåg. The impact of varying reference fluid on the predictability of the extended corresponding state equation SPUNG for modelling $CO_2$ - Water. Energy Procedia 2014; 51:353-362

**Paper 3:** Mohamed Ibrahim, Geir Skaugen, Ivar S. Ertesvåg, Tore Haug-Warberg. Modelling $CO_2$ - water mixture thermodynamics using various equations of state (EoS) with emphasis on the potential of the SPUNG EoS. Chemical Engineering Science 2014; 113:22-34

**Paper 4:** Mohamed Ibrahim, Geir Skaugen, Ivar S. Ertesvåg. An Extended Corresponding States Equation of State (EoS) for CCS Industry. Chemical Engineering Science 2015; 137:572-582

**Other articles (not included in this thesis)**   Mohamed Ibrahim, Geir Skaugen, Ivar S. Ertesvåg, Preliminary evaluation of the SPUNG equation of state for modelling the thermodynamic properties of $CO_2$– Water mixtures. Energy Procedia 2012; 26:90-97

**Author's contribution**   Ivar S. Ertesvåg and Geir Skaugen are my main supervisor and co-supervisor, respectively. Their contribution to the papers have been discussions, suggestions and critical review. For Paper 3, Tore Haug-Warberg played a similar role.

# Acknowledgments

First and foremost, all my gratitude and praises are due to Allah, Who gave me all what I have, and guided me all the way to the right path.

Then I would like to pay a deep gratitude to my family. I would like to thank my grandmother Esmat Yousef, who was my greatest teacher ever and who ignited my passion for acquiring knowledge and my curiosity for science, from the age of two and a half on. I would like to thank my father for continuously supporting and motivating me ever since I was a child, and especially during my academic career. I would like to thank my mother for her care, for always being there when we needed her, and for all the happy moments she brought into our lives. Without their continuous encouragement and support, I would not have achieved what I have done so far. It is a great honor to be their son. Also, I would like to express my deep gratitude to my beloved sister for everything she did to me. She was one-of-a-kind sister who cannot be thanked enough for all what she put up with and did for me. Indeed, I miss you too much. I would like to thank my cousin Hossam El-Sherif for his support and for the many times he replicated me in my absence. Big thank you to my supportive brothers and friends without whom I would not have kept it up during hard times, my good decisions that they contributed to, or for the life lessons I learned from them. Including but not exclusive; 'The Fazlijans' (Bledar, Arber and Dardan), Hesham Mahmoud, Nasser Morsy, Ayoub Hmaidi, Malek Chaabane, Altug Basol, Djamel Lakehal and many others.

I would like to thank all my teachers and professors who have taught me at; the schools I have attended, my undergraduate engineering school of HTI in Egypt, CSE school of TU Munich, ETH Zurich, and finally NTNU. Last but not least, I would like to thank all the hardships that have honed my skills and kept me challenged and sharp.

Trondheim, Norway.

# Part I

# Chapter 1

# Background and Introduction

Global warming, the term describing the continuous increase of the earth's average temperature, is one of the current era challenges. The term climate change is used interchangeably to describe the same challenge due to evidences that link global warming to significant changes in climate. Examples of climate changes are; higher frequencies and amplitudes of heat waves, oceans warming, glaciers melting, floods, heavy rains where it is not usual, etc. This can affect humanity and the globe regardless of who is responsible or where it happens, hence the challenge is global. The emissions of greenhouse gases (e.g. water vapor, $CO_2$, methane, nitrous oxides, etc.) are strongly linked to global warming since the gases trap and radiate heat within the atmosphere. The effects are natural and mandatory for human lives and activities. However, more than a century and half emission of greenhouse gases caused the effect to magnify resulting in an increase of the severity of climate changes. Since the challenge is global, countries under the umbrella of the united nations (UN) have formed the United Nations Framework Convention on Climate Change in 1992 [41]. The framework was established to limit the global warming and the consequences in climate changes. Since then, polices were made, rules were introduced and awareness was raised every year. In 1995 many countries adopted the Kyoto Protocol [1], an agreement that binds the developed countries more than others (Common but differentiated responsibilities) for emission reduction targets. Since the protocol entered into force in 2005, many countries made acts defining their targets. An example is the British Climate change act [7], which aims to reduce the greenhouse gas emissions by 2050 to 20% of the 1990 level. The targets are becoming stricter and aimed to be shifted forward. Most recently, the Norwegian parliament brought the neutrality goal forward to 2030 instead of 2050. The Kyoto protocol was followed by more global agreements, most recently the Paris agreement in 2015.

There are many greenhouse gases but $CO_2$ is regarded as the major contributor to global warming. Therefore, $CO_2$ Capture and Storage (CCS) industry grows rapidly. In conjunction, research undergoing on various aspects of these processes acquire much interest, and a global community has formed. Indeed, the $CO_2$ production and its effects on climate change are among the current era challenges. Therefore, the Carbon Capture and Storage (CCS) research and industry are de-

veloping very fast to cope with the challenge. There is a number of impurities in mixture with $CO_2$ that are relevant for the CCS industry. Among these are $H_2O$, $H_2S$, $CH_4$, $CO$, $O_2$, $NO_2$ and $N_2$. The availability of the thermodynamic and transport properties of these mixtures is vital for the design of various CCS processes. The experimental data are highly important. However, they are discrete in nature and local. Therefore, a generic and continuous solution is essential. Hence, modeling transport and thermodynamic properties of $CO_2$ with impurities is crucial for design, safety, efficiency and economy of the process.

It is possible to use empirically fitted models, but these models always have poor extendability and generality outside the fitted range. Moreover, they are not thermodynamically consistent over phases. A more appropriate and physically grounded approach is to use equations of state (EoSs). There are various categories of EoSs. Cubic EoSs like Soave-Redlich-Kwong (SRK) [37], SRK with Huron Vidal mixing rules (SRK-HV) [15] and Peng–Robinson (PR) [34] are amongst the lightest in computations. Consequently, they are the most widely used in industry. Among the heaviest in computation time are the full extended corresponding states (ECS) equations. A modern approach that is less computationally expensive than ECS, and offers generally good accuracy, is the multi parameters approach. Nevertheless, it is at least one order of magnitude higher than Cubic EoS in computation time [44]. Span–Wagner [38] for pure $CO_2$ and GERG (Groupe Européen de Recherches Gaziéres) [23] for mixtures that belong to this category. The Cubic-Plus-Association (CPA) [22] and the Statistical Associating Fluid Theory (SAFT) [4] EoSs are state-of-the-art approaches. The results of the CPA and Perturbed Chain SAFT (PC-SAFT) for modeling $CO_2$-water systems were presented by Tsivintzelis et al. [40] and Diamantonis and Economou [9], respectively. The two articles also included a literature survey on CPA and SAFT type developments and recent achievements. The level of sophistication and generality usually has a direct relation to accuracy and computational complexity and, consequently, a trade-off arises. While the accuracy of a model is of higher importance than the computational efficiency for the process analysis, the computational complexity has a significant effect on the cost and feasibility of a CFD simulation. Three other dimensions of the challenge of developing or selecting a model are the generality with respect to different fluids and mixtures, consistency, and numerical stability when using it in conjunction with CFD simulations. Hence, the work of this thesis is to introduce a compromise for these usually conflicting objectives to enable a CFD simulation of a high accuracy and feasible execution time.

Transport of $CO_2$ in pipelines is one of the important links in the chain of CCS. During shutdown or by a fracture, $CO_2$ is depressurized from very high pressures. This can result in large drops in temperatures. Very fast, non-controlled depressurization can cause dry ice formation and steel pipelines to become very brittle. This can reduce integrity of the pipe significantly. The dissipation of $CO_2$ during depressurization can form clouds, which raises safety concerns. Therefore, proper modeling and simulation of the depressurization process is very important for the safety and efficiency of a design. Process modeling consists of many components from fluid dynamics to thermodynamics of the multi-phase multicomponent phenomena. Therefore, Paper 1 of this work studied the effect of impurities on the predictions from the thermodynamics point of view. This was done by comparing

results of the same equation of state (EoS) when modeling pure $CO_2$ and mixtures with different compositions. Moreover, the sensitivity of predictions to the quality of the used EoS was also studied in the same article. This was done by comparing the results of two EoSs of different classes of sophistication and, subsequently, of accuracy. These are the SPUNG EoS and SRK. The predictions of thermodynamic properties were conducted over a PVTx of two sets of $CO_2$ depressurization experimental data [6], [8]. The results of SPUNG were compared to the cubic EoS SRK, which was chosen because of its popularity in industry and low computational cost. The SPUNG EoS was chosen as it was shown to be more accurate than SRK for $CO_2$ non-polar mixtures [44] and polar mixtures [16, 18]. SPUNG EoS [19] is not a well known ECS equation although it handles the trade-off between accuracy and computational complexity well.

The SPUNG EoS was first introduced for hydrocarbons. Recently, Wilhelmsen et al. [44] showed that SPUNG is a promising EoS for modeling $CO_2$ non-polar mixtures. However, we showed [16, 18] (Papers 2,4) that the SPUNG EoS qualities did not fully hold for modeling $CO_2$-water densities and phase equilibrium over a large range of conditions. This is mainly for water-rich phase density predictions and $CO_2$ solubilities at all tested pressures. We also investigated the effect of the reference fluid on the density predictions, and found that for the set of chosen hydrocarbons tested as reference fluids, the heavier the hydrocarbon the better it predicted the water-rich phase density. Moreover, the study recommended development of asymmetric or non-quadratic mixing rules for better modeling of phase equilibrium [17, 18] (Paper 3,4). Mollerup [30] earlier discussed generally the possibility of introducing non-quadratic mixing rules. However, he did not provide detailed derivations of specific mixing rule derivatives, nor did he present a concrete model results. Furthermore, his general suggestions were incompatible with the TP_Lib (the thermodynamics liberary used for this work) implementation of SPUNG using van der Waals quadratic mixing rule. Therefore, they were not followed here. A similar discussion is made by Michelsen and Mollerup [29].

Finally, we introduced a new original ECS EoS (Paper 4) that uses SRK EoS and HV mixing rules for the computation of the scale factors. The new equation uses the Bender Modified Benedict-Webb-Rubin (MBWR) EoS parameters by Polt [35] as the reference equation. The results using three alternative reference fluids that exhibited the best compromise for phase equilibrium and density predictions are demonstrated.

# Chapter 2

# Theory

## 2.1 Equations of state (EoS)

An EoS is a model that calculates for both the liquid and gas phases using the same expression. This enhances the continuity near the critical point. An EoS for an $N_c$ component mixture can be regarded as an expression for pressure $P$ as a function of the vector of mole fractions $n$ , the temperature $T$ and the volume $V$. Given this expression, the Helmholtz residual function $A_\mathrm{m}^{\mathrm{res}}[V, T, n]$, or generally any departure function can be computed. Here, $n$ is the vector of mole fractions of the components of the mixture and subscript m stands for mixture. The thermodynamic properties can then be computed from the derivatives of the departure function as explained by Jørstad [19] or most thermodynamics textbooks concerned with EoSs. In the following section a brief discussion of all the EoSs used in this PhD work is outlined.

### 2.1.1 The standard SRK

The classical Soave-Redlich-Kwong (SRK) model with Van der Waals mixing rules [37] is a cubic EoS that is written for a mixture as:

$$P = \frac{RTn}{V - bn} - \frac{an^2}{V^2 - bnV} \tag{2.1}$$

$$a = \sum_i \sum_j x_i x_j \sqrt{a_i a_j}(1 - K_{ij}), b = \sum_i x_i b_i \tag{2.2}$$

$$a_i = \alpha_i \frac{0.42748 R^2 T_{c,i}^2}{P_{c,i}}, b_i = \frac{0.08664 R T_{c,i}}{P_{c,i}} \tag{2.3}$$

Here, $T_{c,i}$, $P_{c,i}$ are the critical temperature and pressure of component $i$ and $R$ is the gas constant. In order to close the system, an expression for $\alpha_i$ should be provided and a lot of varieties already exist.

### 2.1.2 The SRK model with Huron Vidal mixing rules

The SRK model with Huron Vidal mixing rules (SRK-HV), suggested by Huron and Vidal [15], is an improvement to the classical SRK, as it derives a definition for the mixing rules from the excess Gibbs energy at infinite pressure, $G_\infty^E$.

### 2.1.3 The GERG

The state-of-the-art GERG (Groupe Européen de Recherches Gaziéres) EoS presented by Kunz et al. [23] is a multi-parameter approximation. In this approach, the Helmholtz energy for a mixture $A_m(T, V, x)$ is described in terms of two contributions as follow;

$$A_m(T, V, x) = A_m^o(T, V, x) + A_m^r(T, V, x). \tag{2.4}$$

The first term $A_m^o(T, V, x)$ describes the ideal gas contribution of the pure fluids composing the mixture. This term is calculated with linear mixing at the physical temperature and volume of all components. This term in normalized form can be further expanded to :

$$a_m^o(T, V, x) = \sum_{i=1}^{NC} x_i[a_i^o(T, V) + \ln x_i], \tag{2.5}$$

where $a_i^o$ is the component $i$ normalized Helmholtz energy calculated at the physical temperature and volume.

The second term $A_m^r(T, V, x)$ is used to represent the residual mixture contribution. This term by its turn is composed of two components. In a normalized form the two components are:

- $\sum_{i=1}^{NC} x_i a_i^r(T_R, V_R)$, this part of the residual (here, superscript $r$ denotes residual) is a linear mixing of the normalized Helmholtz energy calculated at the reduced temperature and volume (here, subscript $R$ denotes reduced).

- $\Delta a_m^r(T_R, V_R, x)$ is the term used to describe deviations from the corresponding states approach for binary mixtures with particularly good data.

Thus, one can expand Eq. 2.4 and write it in a normalized form as

$$a_m(T, V, x) = \sum_{i=1}^{NC} x_i[a_i^o(T, V) + \ln x_i] + \sum_{i=1}^{NC} x_i a_i^r(T_R, V_R) + \Delta a_m^r(T_R, V_R, x). \tag{2.6}$$

The challenge with such formulations in addition to the high computational cost is that a reference EoS for each of the involved components should exist and be valid over an appropriate range of conditions.

## 2.2 The corresponding states principle

The principle of corresponding states assumes that all substances exhibit the same behavior at a reduced state. Consequently, a departure function (here Helmholtz residual) can be described for a pure component in terms of its reduced values as

$$\frac{A_i{}^{\text{res}}[V,T]}{n \cdot R \cdot T} = \frac{A_{\text{Ref}}{}^{\text{res}}[V_{\text{Ref}}, T_{\text{Ref}}]}{n \cdot R \cdot T_{\text{Ref}}}, \tag{2.7}$$

or for a mixture as

$$\frac{A_{\text{m}}{}^{\text{res}}[V,T,x]}{n \cdot R \cdot T} = \frac{A_{\text{Ref}}{}^{\text{res}}[V_{\text{Ref}}, T_{\text{Ref}}]}{n \cdot R \cdot T_{\text{Ref}}}, \tag{2.8}$$

where index $i$ denotes component, subscript m stands for mixture and superscript res means residual.

A corresponding state EoS typically has one or more reference components described very accurately by a reference EoS. In the corresponding states approach, the reference fluid volume $V_{\text{Ref}}$ and temperature $T_{\text{Ref}}$ are the reduced volume and temperature, $V_{\text{R}}$ and $T_{\text{R}}$, of the fluid or the mixture investigated. Here, subscripts R and Ref stand for reduced and reference, respectively.

## 2.3 The extended corresponding states principle

### 2.3.1 Basic concept

In the extended corresponding states principle, the same principle of corresponding states is assumed. However, the mapping between the investigated fluid or mixture $T$ and $V$ and the reference fluid $V_{\text{Ref}}$ and $T_{\text{Ref}}$ is done via the scale factors $f_{\text{n}}$ and $h_{\text{n}}$ as

$$T_{\text{Ref}} = \frac{n \cdot T}{f_{\text{n}}}, \tag{2.9}$$

$$V_{\text{Ref}} = \frac{V}{h_{\text{n}}}. \tag{2.10}$$

These scale factors take into account how the fluid or the mixture in consideration differs from the reference fluid. As explained in Sect. 2.1, the thermodynamic properties are computed from the derivatives of the $F$ function. Therefore, from the definition of $F$, formulations for $f_{\text{n}}$ and $h_{\text{n}}$ and their derivatives are needed. The scale factors, $f_{\text{n}}$ and $h_{\text{n}}$, can be computed via scale factor functions, using semi-empirical functions, an accurate reference equation for each component, or using a simpler EoS. The work on shape factor functions was started by Leach et al. [24]. Subsequently, many contributions were made. Examples are the work by Fisher and Leland [12] and of Ely [10], who has introduced the first exact shape factor concept. In addition, a substantial work on shape factor functions was conducted by [11]. The computation of exact shape functions is computationally very expensive because they are implicit functions of the reference fluid $V_{\text{Ref}}$ and $T_{\text{Ref}}$. This is why the concept was left behind and thought to be impractical for use with numerical simulations. However, several implementations of the concept of extended corresponding states use simpler equations of state to compute shape factors and formulations that are independent of $V_{\text{Ref}}$ and $T_{\text{Ref}}$, which showed a good compromise between accuracy and computation time. Among these are the SPUNG EoS, which uses SRK EoS for the computation of the shape factor. The SRK EoS used

in SPUNG EoS uses Soave's formulation for the computation of $\alpha(T)$ that appears in the equation of computing the $a_i$ parameter of pure components,

$$a_i = a_i^{\mathrm{C}} \cdot \alpha(T). \tag{2.11}$$

Here, $a_i^{\mathrm{C}}$ is the parameter $a$ for the pure component $i$ at critical temperature.

Using SRK EoS with Soave's formulation for $\alpha(T)$, Jørstad [19] showed that $f_{\mathrm{n}}$ and $h_{\mathrm{n}}$ can be defined, respectively, as

$$f_{\mathrm{n}} = \left( \frac{\sqrt{\frac{a_{\mathrm{n}}}{a_{\mathrm{Ref}}^{\mathrm{C}} \cdot h_{\mathrm{n}}}} + m_{\mathrm{Ref}} \cdot \sqrt{\frac{n \cdot T}{T_{\mathrm{Ref}}^{\mathrm{C}}}}}{1 + m_{\mathrm{Ref}}} \right)^2 \tag{2.12}$$

and

$$h_{\mathrm{n}} = \frac{b_{\mathrm{n}}}{b_{\mathrm{Ref}}}, \tag{2.13}$$

where

$$m_{\mathrm{Ref}} = \lambda + \beta \cdot \omega_{\mathrm{Ref}} - \gamma \cdot \omega_{\mathrm{Ref}}^2 \tag{2.14}$$

and $\lambda$ , $\beta$ and $\gamma$ are constants that vary with the type of cubic EoS (e.g. 0.480, 1.574, and 0.176, respectively, for SRK). $\omega_{\mathrm{Ref}}$ is the acentric factor of the reference component. The superscript $C$ means at critical conditions, and the subscript n means molar based. A similar discussion is made by Mollerup [30] and Michelsen and Mollerup [29].

From Eq. 2.12 it is clear that to compute the derivatives of $f_{\mathrm{n}}$ and $h_{\mathrm{n}}$, a closure mixing rule formulation for the parameter $a_{\mathrm{n}}$ and its derivatives is needed. The mixing rule to be selected or developed must be thermodynamically consistent.

### 2.3.2 The new EoS

In the new EoS that we introduce here for the first time, the Bender Modified Benedict-Webb-Rubin (Bender-MBWR)EoS with 20 parameters of Polt [35] was used for the reference fluid. The reference fluids recommended here are R23, R503 and $NH_3$. R23 is $CHF_3$, and R503 is a mixture of R23 and R13 ($CClF_3$). The reference fluids are recommended after investigating several reference fluids including $O_2$, $N_2$, water, $CO_2$, C1 to C9, and a set of refrigerants. Moreover, the cubic SRK-HV EoS was used to calculate the $a$ parameter in the scale factors. The parameter $a$ using Huron-Vidal mixing rules [15] is defined as

$$a = b \left( \sum_{i=1}^{N_c} \left( x_i \frac{a_i}{b_i} \right) - \frac{G_\infty^{\mathrm{E}}}{\ln(2)} \right), \tag{2.15}$$

where $b$ is the co-volume parameter defined as

$$b = \sum_{i=1}^{N_c} x_i \cdot b_i. \tag{2.16}$$

$G_\infty^{\mathrm{E}}$ is the excess Gibbs free energy at infinite pressure,

$$\frac{G_\infty^{\mathrm{E}}}{RT} = \sum_{i=1}^{N_c} x_i \; \cdot \; \frac{\sum_{j=1}^{N_c} \tau_{ji} b_j x_j C_{ji}}{\sum_{k=1}^{N_c} b_k x_k C_{ki}}, \tag{2.17}$$

where

$$\tau_{ji} = \frac{g_{ji} - g_{ii}}{RT}, \tag{2.18}$$

$$g_{ji} - g_{ii} = \Delta g_{ji} \tag{2.19}$$

and

$$C_{ji} = \exp(-\alpha_{ji}\tau_{ji}). \tag{2.20}$$

For a second order Huron-Vidal, $\Delta g_{ji}$ can be written as

$$\Delta g_{ji} = (d_{ji} + e_{ji} \; \cdot \; T + f_{ji} \; \cdot \; T^2) \; \cdot \; R \tag{2.21}$$

where $\alpha_{ji}$ in Eq. 2.20 and $d_{ji}$, $e_{ii}$, and $f_{ji}$ in Eq. 2.21 are binary parameters to be fitted to experimental data. The used $d$, $e$, and $f$ for $CO_2$-water are listed in Table 2.1.[1]

A general discussion was made by Kontogeorgis and Coutsikos [21], who reviewed 30 years development of the activity coefficient models that are incorporated for cubic EoSs.

Table 2.1: The $d$, $e$, and $f$ values used for this study, where component $i$ is $CO_2$ and $j$ is water (Table 1, Paper 4)

| $d_{ji}$ [K] | $e_{ji}$ [-] | $f_{ji}$ [K$^{-1}$] | $d_{ij}$[K] | $e_{ij}$ [-] | $f_{ij}$ [K$^{-1}$] | $\alpha_{ji}$ [-] |
|---|---|---|---|---|---|---|
| $-1035.17623$ | $17.07660$ | $0.03200$ | $5887.42379$ | $1.75852$ | $-0.01513$ | $0.03$ |

Here, for the ease of analysis and consistency with the work of Jørstad [19], the molar based parameter $a_{\mathrm{n}} = a \; \cdot \; n^2$ is used instead, defined as

$$a_{\mathrm{n}} = b_{\mathrm{n}} \left( \sum_{i=1}^{N_c} \left( n_i \frac{a_i}{b_i} \right) - \frac{G_{\infty\mathrm{n}}^{\mathrm{E}}}{\ln(2)} \right), \tag{2.22}$$

where $b_{\mathrm{n}} = b \; \cdot \; n$ is defined as

$$b_{\mathrm{n}} = \sum_{i=1}^{N_c} n_i \; \cdot \; b_i, \tag{2.23}$$

and $G_{\infty\mathrm{n}}^{\mathrm{E}} = G_\infty^{\mathrm{E}} \; \cdot \; n$.

---

[1]Dimensions of the parameters are missing in Paper 4.

Subsequently, the derivatives of $a_{\mathrm{n}}$ needed to calculate the scale factors can be easily derived as follows:

$$\frac{\partial a_{\mathrm{n}}}{\partial n_i} = b_i \ \cdot \ \frac{a_{\mathrm{n}}}{b_{\mathrm{n}}} + b_{\mathrm{n}} \left( \frac{a_i}{b_i} \ - \ \frac{1}{\ln(2)} \ \cdot \ \frac{\partial G_{\infty \mathrm{n}}^{\mathrm{E}}}{\partial n_i} \right) \tag{2.24}$$

$$\frac{\partial^2 a_{\mathrm{n}}}{\partial n_j \partial n_i} = b_i \cdot \left( \frac{a_j}{b_j} \ - \ \frac{1}{\ln(2)} \ \cdot \ \frac{\partial G_{\infty \mathrm{n}}^{\mathrm{E}}}{\partial n_j} \right) + b_j \cdot \left( \frac{a_i}{b_i} \ - \ \frac{1}{\ln(2)} \ \cdot \ \frac{\partial G_{\infty \mathrm{n}}^{\mathrm{E}}}{\partial n_i} \right)$$
$$- \, b_{\mathrm{n}} \ \cdot \ \frac{1}{\ln(2)} \ \cdot \ \frac{\partial^2 G_{\infty \mathrm{n}}^{\mathrm{E}}}{\partial n_j \partial n_i} \tag{2.25}$$

$$\frac{\partial a_{\mathrm{n}}}{\partial T} = b_{\mathrm{n}} \left( \sum_{i=1}^{N_c} \left( \frac{n_i}{b_i} \cdot \frac{\partial a_i}{\partial T} \right) \ - \ \frac{1}{\ln(2)} \ \cdot \ \frac{\partial G_{\infty \mathrm{n}}^{\mathrm{E}}}{\partial T} \right) \tag{2.26}$$

$$\frac{\partial^2 a_{\mathrm{n}}}{\partial T \partial n_i} = b_i \left( \sum_{i=1}^{N_c} \left( \frac{n_i}{b_i} \cdot \frac{\partial a_i}{\partial T} \right) - \frac{1}{\ln(2)} \ \cdot \ \frac{\partial G_{\infty \mathrm{n}}^{\mathrm{E}}}{\partial T} \right)$$
$$+ \frac{b_{\mathrm{n}}}{b_i} \cdot \frac{\partial a_i}{\partial T} \ - \ \frac{b_{\mathrm{n}}}{\ln(2)} \ \cdot \ \frac{\partial^2 G_{\infty \mathrm{n}}^{\mathrm{E}}}{\partial T \partial n_i} \tag{2.27}$$

$$\frac{\partial^2 a_{\mathrm{n}}}{\partial T^2} = b_{\mathrm{n}} \left( \sum_{i=1}^{N_c} \left( \frac{n_i}{b_i} \cdot \frac{\partial^2 a_i}{\partial T^2} \right) \ - \ \frac{1}{\ln(2)} \ \cdot \ \frac{\partial^2 G_{\infty \mathrm{n}}^{\mathrm{E}}}{\partial T^2} \right) \tag{2.28}$$

Once the $a_{\mathrm{n}}$ and its derivatives are computed, the $f_{\mathrm{n}}$ and $h_{\mathrm{n}}$ and their derivatives can be computed.

# Chapter 3

# Methodology

## 3.1  Numerical tools

The NTNU-Sintef in-house thermodynamic library was mainly used for the studies presented. The new model was integrated to the library framework. The library is a tool for predicting the thermodynamic properties using various approaches that range in level of sophistication and underlying theory. The library already had SPUNG EoS and Bender reference EoS implemented before the course of this PhD started. Numerical tolerance used for this study was $10^{-4}$ for both the multi-phase flash algorithm and the compressibility factor calculations. The GERG results presented used the NIST REFPROP library by Lemmon et al. [25].

## 3.2  Setup

This section describes briefly the numerical setup of each paper.

### 3.2.1  Setup of Paper 1

The first setup investigated in Paper 1 was the depressurization of a 50 km long 24 inches $CO_2$ pipeline by Clausen et al. [6]. The article provided temperature and pressure profiles over time at the first end and second end of the pipeline during the process. There, we computed the densities and speeds of sound for the pairs of pressure and temperature obtained from the graphs of Clausen et al. [6] at different time steps of the first end. We conducted the numerical simulations for three compositions using SPUNG and SRK. The first was a pure $CO_2$ case. The second was a mixture of 99.14% of $CO_2$, 0.22% of $N_2$, 0.63% of $CH_4$ and 0.01% of water and is what we refer to as real mixture. The third was a mixture of 98%$CO_2$ and 2% of water. The second setup was of the conditions tested by de Koeijer et al. [8] for pure $CO_2$ at 139 m downstream.

### 3.2.2 Setup of Paper 2

**Single phase density**

In addition to the standard SPUNG equation using C3 as the reference fluid, the four alternative reference fluids $N_2$, C1, C2 and NC4 were used for density prediction. For this preliminary study, data at elevated pressures (from 10 up to 100 MPa) and at a temperature of 400 °C were used. Four concentrations of 20, 40, 60 and 80% of $CO_2$ were investigated. The pressures, temperature and mole fractions were chosen to allow a comparison with the set of experimental data of Seitz and Blencoe [36].

**Vapour-liquid equilibrium**

The ECS concept using $N_2$, C1, C2, C3, and NC4 was used for the prediction of the mutual solubilities of $CO_2$ and $H_2O$. A set of experimental data by Bamberger et al. [2] was used in the comparison providing data over moderate pressures that ranged between 4 and 14 MPa at a temperature of 50 °C.

### 3.2.3 Setup of Paper 3

**Single phase density predictions, low to moderate pressures**

The four EoSs were evaluated at a set of low to moderate pressures (up to 100 bars), which ensured a single phase at given temperatures and water concentrations in the mixture. The pressures, levels of temperature and water concentrations were chosen to enable comparison with the experimental work of [32]. Four concentrations of 98, 90, 75 and 50% $H_2O$ were evaluated. The concentration of 98% was evaluated at the temperatures of 225, 200, 100 and 50 °C. The 90% concentration was evaluated at 200, 100 and 71 °C, the 75% was evaluated at 225, 200, and 100 °C, and finally the 50% was evaluated at 225, 200 and 125 °C, respectively. It was clear that, as the $H_2O$ concentration increased in the mixture, it was not possible to go to some low temperatures while maintaining the mixture in gaseous phase conditions. This explains the differences in the lower limit of the evaluated temperatures at the four studied concentrations.

**Single phase density predictions, high pressures**

A more challenging set of conditions at elevated pressures over a wider range of concentrations was evaluated. The set of concentrations ranged from $CO_2$ dominant (90%) to $H_2O$ dominant (90%). The pressures varied from 10 to 100 MPa. All experiments were conducted at a temperature of 400 °C. The evaluated conditions were chosen to enable comparisons with the experimental data of [36].

**Dew line prediction**

The dew lines were evaluated at five different concentrations of 2, 5, 10, 25 and 50% $H_2O$. The pressures were chosen to comply with the work done by Patel et al. [33], and the dew temperatures were then computed dependently.

**Rich phases density predictions**

The EoSs were evaluated at four sets of data provided by King et al. [20], Chiquet et al. [5], Hebach et al. [13] and the validated predictions by Bikkina et al. [3]. King et al. [20] provided only water-rich liquid-phase densities between 6 to 24 MPa at three temperatures of 15, 20, and 25 °C co-existing with $CO_2$-rich liquid phase. The 15 and 25 °C test sets were chosen for the analysis here. Chiquet et al. [5] provided densities of both water-rich and $CO_2$-rich phases when $CO_2$ was at supercritical conditions. The set of data covered pressures from 5 to 45 MPa, and the selected sets of temperatures were about 35, 50, 90 and 110 °C. The work done by Hebach et al. [13] was used for comparisons of water-rich liquid phase densities co-existing with $CO_2$-rich gas phase. The selected cases were at temperatures of 19, 29, 39 and 49 °C and pressures less than 5 MPa to ensure a gaseous $CO_2$-rich phase. The results of Chiquet et al. [5] and Hebach et al. [13] were measured at temperatures slightly around the listed values, although precisely fixed for each point. The simulations conducted here use the exact measurement temperatures. The group of Bikkina et al. [3] provided validated predictions that cover the missing rich phases density of $CO_2$-rich liquid and the co-existing water-rich liquid densities and $CO_2$-rich gaseous phase. The selected Liquid Liquid Equilibrium (LLE) data of Bikkina et al. [3] went over pressures between 8 to 21 MPa at one temperature of 25 °C. Finally, the Vapour Liquid Equilibrium (VLE) data went over pressures between 1 to 6 MPa at four temperatures of 25, 40, 50 and 60 °C.

**Solubilities**

The accuracy of the SPUNG and SRKs EoS in predicting the mutual solubilities of $CO_2$ and $H_2O$ was validated. Three experimental studies covering a wide range of pressures in CCS industry were used in the comparison. These are by Takenouchi and Kennedy [39], Bamberger et al. [2] and Valtz et al. [42]. The first study done by Takenouchi and Kennedy [39] provided very high pressure solubilities ranging between 10 and 70 MPa at a temperature of 110 °C. The second study conducted by Bamberger et al. [2] provided data over moderate pressures between 4 and 14 MPa at three temperatures of 50, 60 and 80 °C. The last set of experimental data used in the solubility study was the one by Valtz et al. [42], which covered very low pressures at three temperatures of approximately 5, 25, and 45 °C. For the low temperature of 5 °C, the pressures ranged approximately between 0.5 and 1 MPa, the range went wider as the temperature increased reaching approximately the range of 0.1 to 7 MPa at the temperature of 45 °C.

**Sensitivity to the interaction parameter $K_{ij}$**

The SPUNG EoS uses the SRK EoS for computing the shape factors and SRK EoS uses the symmetric interaction parameter $K_{ij}$ for computing the mixing coefficients. Therefore, we performed a simple sensitivity study on the effects of tuning $K_{ij}$ on the results. The tuning was done by matching the $CO_2$ solubilities as good as possible and letting the density and $H_2O$ solubility be computed accordingly. The results of the tuning for the evaluated cases are plotted and labeled as *SPUNG-Reg $K_{ij}$* in the following.

**Reference fluid sensitivity**

An examination was conducted for the impact of using other reference fluids on the density predictions of the water-rich liquid phase. $N_2$, $O_2$, ethane (C1), methane (C2), iso-butane (IC4) and normal-butane (NC4) were used as reference fluids for this study as an alternative to the originally used propane (C3). The aim of this part of the analysis was to find a criterion of selection or to search for the proper reference fluid to model $CO_2$-water mixtures.

### 3.2.4   Setup of Paper 4

The setup of Paper 4 for the newly proposed model was similar to the one of Paper 3 except for that the comparisons were made between the model and SPUNG EoS and to the experimental data only. Furthermore, there were no $K_{ij}$ sensitivity studies as the HV mixing rules does not have $K_{ij}$ parameters in formulation. A large number of reference fluids assessed and the three reference fluids in the results and discussions were recommended.

## 3.3   Error definitions

The errors of an EoS are measured here by the Relative Error (RE) and the Average of Absolute Deviation (AAD) defined for an arbitrary variable $C$ as

$$RE(C_r, \%) = \frac{|C_{s,r} - C_{\exp,r}|}{C_{\exp,r}} \times 100 \tag{3.1}$$

and

$$AAD(C, \%) = \frac{100}{N} \times \sum_{r=1}^{N} \frac{|C_{s,r} - C_{\exp,r}|}{C_{\exp,r}}. \tag{3.2}$$

Here, $N$ is the total number of points, subscripts s and exp refer to simulation data and experimental data, respectively, and $r$ is a point index.

# Chapter 4

# Summary of Results and Conclusions

This chapter is a summary of the results of the author's contributions. However, it is not a substitute of reading the articles for better understanding and more details of the results and findings.

## 4.1 SPUNG equation of state

During the thesis work we have assessed the results of the PVTx modeling of $CO_2$ pipeline at depressurization conditions. Looking into the density predictions of the three tested compositions, we found that the $CO_2$ -water mixture density predictions are higher than that of pure $CO_2$ until it turned to gas phase. This difference was due to the existence of only 2% of water. The realistic mixture (Section 3.2.1) went through two phase region between 1.5 and 2.5 hours for SPUNG EoS and at 1.5 to 2.0 hours for SRK, which led to less steep drop of density. The AAD of the $CO_2$ - water case from the pure one was 69.2% and 40.5% for SPUNG EoS and SRK, respectively. The AAD of the realistic mixture was 9.8% and 13.7% for SPUNG EoS and SRK, respectively. Moreover, the comparison between the density predictions of SRK and SPUNG EoS for the pure $CO_2$ case taking SPUNG as reference, showed that the AAD over all the predictions was 8.1% with a maximum deviation of 18.5%. We took SPUNG EoS as reference since Wilhelmsen et al. [44] and [16–18] showed that SPUNG EoS was superior in predictions to SRK over the predicted conditions. The predictions of the speed of sound for the pure $CO_2$ case using both EoSs dropped as instantaneous as the mixtures changes from the heavy to the light phase. The AAD of SRK to SPUNG EoS was 6.7%, with a maximum deviation of 14.9%. The comparison between SRK and SPUNG EoS density predictions for the realistic mixture showed that the AAD of SRK to SPUNG EoS as a reference was 13.5%, with a maximum deviation of 29.7%. The AADs between SRK and SPUNG EoS density predictions for the $CO_2$ - water mixture was 13.8%, with a maximum deviation of 21.4%. Finally, the comparison between SRK and SPUNG EoS density predictions for the pure-$CO_2$ for the case of de Koeijer et al. [8] showed that the AAD was 10.3%, with a maximum deviation of 12.8%.

This showed that the inclusion of impurities is very important for such a process design, but using an accurate EoS is also very crucial for the accuracy of the

simulation. Therefore, a study and evaluation of various EoSs for modeling $CO_2$ – water was conducted as part of the PhD work. We found that the standard SRK and its modification with Huron Vidal mixing rules are behaving almost the same in the single phase for this polar mixture. This shows no advantage of using SRK-HV instead of the standard formulation for both liquid and gas phase calculations. The SPUNG error in the liquid phase is one-fifth of the cubic equation models and very close to the GERG results with less than 2% AAD, while it is much less expensive compared to the GERG complexity. Although SPUNG was developed for better prediction of hydrocarbon behavior, it showed a great potential in capturing $CO_2$ -water in the cases where VLE is not of interest.

For low-pressure density calculations presented, the comparison of the densities showed that the errors over the investigated intervals were on average very small for all the tested EoSs.

From the results of the high-pressure single-phase density calculations, the comparisons showed an increase of the errors as the pressure increased and as the $H_2O$ content increased. While at low pressure the increase and the relative error values were small, the errors jumped to an order of magnitude higher at the combination of the upper-bounds of both intervals. The results also showed clearly that the errors behavior of SPUNG is much better than that of SRK and SRK-HV and, considering the computational expenses study by Wilhelmsen et al. [44], it can be concluded that it is a good compromise of an EoS.

Although the errors of SPUNG reached 20% at the extreme of the investigated conditions, the method has a possible high potential for improvement via using other reference fluids, while the SRKs do not have the same potential. The inaccuracies of the used cubic EoS are due to the simple structure of the models, which have very few parameters to tune. A study similar to the presented work but for other mixtures was made by Li and Yan [27], who reported the same inaccuracies using SRK and other cubic equations for mixtures of $CH_4$, $H_2S$, $N_2$ and Ar. Furthermore, Li et al. [26] reviewed several studies testing cubic equations for gas and liquid density predictions for other mixtures. In our investigation, the errors reached approximately 25% at the extreme conditions using cubic EoS. This was higher than in the studies of other mixtures, emphasizing how challenging this particular mixture is for cubic EoS compared to the other mixtures. In addition, this showed the need for a more predictive concept when dealing with $CO_2$-water mixture.

On the other hand, the SPUNG EoS superiority in density computations was inherited from the use of the 32-parameter MBWR reference equation, which is very accurate for propane. However, the errors of the SPUNG EoS came from the incapability of propane to achieve the high density of the $CO_2$ - water liquid phase.

The dew line predictions of SPUNG EoS, SRK and SRK-HV for three of the datasets from Patel et al. [33] were tested. For another two datasets, 25% and 50% $H_2O$, the computed results matched the experimental data as good as for 10%, or better. At the compositions of 10% and 25% $H_2O$, all the EoSs predicted pseudo critical pressures that were lower than the highest pressure of the experiments. SRK-HV predicted 8.045, and 9.394 MPa pseudo critical pressures respectively. SRK predicted 8.161, and 9.55 MPa respectively. Since SPUNG uses the SRK to calculate for the pseudo critical quantities, it predicted the same pseudo critical

pressures as of SRK.

The densities of the Supercritical Liquid Equilibrium (SGLE) of the $CO_2$-rich phase co-existing with a liquid water-rich phase were modeled, and the results are presented in comparison to the experimental data of Chiquet et al. [5] in Table 1, Paper 3.

There were two experimental points that seemed to be anomalous: at 110 °C, 25 MPa and 90 °C, 7 MPa. These points deviated from the trend of each dataset, and the model errors jumped significantly. For the discussion, the AADs were recalculated without these two points in Table 1, Paper 3.

Model computations of the liquid $CO_2$-rich phase were compared with the predicted data of Bikkina et al. [3] and the corresponding AADs are included in Table 1, Paper 3.

For the gaseous $CO_2$-rich phase predictions, errors were very small with all models. However, the values of the binary interaction parameter $K_{ij}$ used to get the proper $CO_2$ solubility decreased with increasing temperature. The used values were $-1.44$, $-0.130$, $-0.115$ and $-0.107$, respectively, for 25, 40, 50 and 60 °C. The AADs for the entire used dataset are included in Table 1, Paper 3. For gaseous phase, the AADs reported were temperature averaged.

The density predictions of the liquid water-rich phase are presented in Table 2, Paper 3, which contains a summary of the results in terms of temperature averaged AADs.

The density predictions of the liquid water-rich phase co-existing with a supercritical $CO_2$-rich phase were compared to the experimental data of Chiquet et al. [5]. The results for the temperatures of 50, 90 and 110 °C were very similar in trend. However, the $K_{ij}$ values used to get the proper $CO_2$ solubility decreased with temperature increase, where the used values were $-0.132$, $-0.118$, $-0.068$, $-0.045$, respectively, for the temperatures from 35 to 110 °C.

The results showed that the errors of all the evaluated EoSs were considerable especially when compared to the results of Tsivintzelis et al. [40] and Diamantonis and Economou [9] for CPA and PC-SAFT, respectively. The errors were not very sensitive to temperature and pressure. This caused the RE profiles to be rather flat and made the AAD a very representative measure.

As mentioned in Sect. 2.3, propane was chosen as the reference fluid in the SPUNG EoS. Table 3, Paper 3 shows the results from the reference fluid sensitivity study. The AADs are averaged over temperature. The difference in AADs is around 7% between using $N_2$ and $NC4$ as a reference fluid.

The behavior of SPUNG, SRK and SRK-HV at low pressures and low temperatures were evaluated, and results in comparison to experimental data are summarized in Paper 3.

The results in Table 8, Paper 3 show that the predictability of SRK-HV for the solubility of $CO_2$ in water was much better than those of SRK and SPUNG EoSs and of low errors. The predictions by SPUNG and SRK were poor. On the other hand, the prediction of the $H_2O$ solubility by SRK-HV was much worse than that of SRK and SPUNG, where all the models were inaccurate. Since SRK uses a symmetric interaction parameter $K_{ij}$ between $CO_2$ and $H_2O$ in the van der Waals geometric mean-based mixing rules, it was expected that the SRK predictability of one of the mutual solubilities will be quite low due to the polar nature of the

mixture. The results suggested that SPUNG EoS inherits this shortcomings from SRK since it uses SRK to compute the shape factors.

The comparison with Wiebe [43] at high pressures and low temperatures showed very low predictability of all the EoSs with very deviating results using both SPUNG and SRK EoSs. There were no improvements for SPUNG and SRK EoSs achieved by the regression.

The solubilities at moderate pressures, chosen in consistency to the experimental work conducted by Bamberger et al. [2], were predicted by the three models. The results presented in terms of AADs in Table 6, Paper 3 showed that the errors in predicting $CO_2$ solubility became more severe than those at very high pressures for SPUNG and SRK EoSs. This highlighted the superior behavior of SRK-HV even more. Furthermore, the errors of SPUNG and SRK were reduced as the temperature increased, which suggested a need for correlating the interaction parameter $K_{ij}$ to temperature in addition to a more general mixing rule. This analysis was confirmed by the $K_{ij}$ sensitivity study conducted here. The predictability of SPUNG and SRK improved for $H_2O$ solubilities, while that of SRK-HV improved for both mutual solubilities and behaved much better than those of SPUNG and SRK.

The comparison to the set of data of Hou et al. [14] showed the same behavior as the one with Bamberger et al. [2] at similar temperatures. However, the errors of all the EoSs were reduced significantly as the temperature increased.

For low pressures, the AADs in Table 4, Paper 4 showed the same trend in comparison with the experimental data of Bamberger et al. [2], except that SRK-HV did not behave equally well.

For the low pressures and high temperatures, the results showed good and improved predictability as the temperature increased.

In general, the predictions of all the EoSs improved with temperatures increase at all pressures.

For this work we concluded that the three tested EoSs predicted the dew temperature with high quality and precision, but predicted low pseudo-critical pressures for two tested data sets.

For single phase, at low pressure gas phase, SPUNG EoS exhibits a better behavior to SRK and SRK-HV cubic EoSs. However, the relative errors are low for all models. The role of SPUNG becomes significant as high pressures are of concern, where the error become considerable.

SPUNG has a superior behavior in predicting the rich phase densities of the $CO_2$ -water system compared to the evaluated cubic EoSs. Although $CO_2$ solubility prediction of SPUNG is very low at moderate pressures and low temperatures, the impact on density calculations for the $H_2O$-rich phase is not pronounceable. Improving the $CO_2$ solubility on the benefits of that of $H_2O$, leads to severe mis-prediction in the density of the $CO_2$-rich phase. The impact on the overall density prediction of the system will depend on the feed composition. Therefore, for the cases where water is an impurity, the impact of $CO_2$ solubility mis-prediction will have much less impact on the overall density prediction.

The effect of varying the reference fluids was investigated, and the errors span between the lightest and the heaviest reference fluid was large. This implies a significant impact of the reference fluid on the properties prediction. Nevertheless, the

heaviest evaluated hydrocarbon was not heavy enough (not sufficiently long chain) to give a significant improvement. However, the observed trend and highlighted criterion of the search for a reference fluid raises the expectations in the SPUNG EoS potential for improving the water-rich phase density prediction, if a proper reference fluid is found, while the cubic EoSs do not have a similar potential.

SRK-HV EoS predicted the mutual solubilities for the binary polar mixture with high accuracy. Nevertheless, it showed much poorer predictability of the density of the $CO_2$-water system in general and compared to SPUNG in particular.

SRK EoS with van der Waals mixing rules combines the shortcommings of both SPUNG and SRK-HV EoS. Therefore, it is not recommended for this system, unless low-pressure gas-phase densities are the only interests.

The study showed that the SPUNG EoS predictability of mutual solubilities is limited by the EoS used for the computation of the shape factors, which here was SRK. However, the predictability of the density depends more on the choice of the reference fluid and the reference equation used. Since one of the powerful features of the concept is to allow a free choice of the EoS for the shape factors, the reference fluid, and the reference equation (given that the reference fluid coefficients exist for this reference equation), a promising alternative is to use an asymmetric quadratic mixing rule. It is also possible to use SRK-HV, which showed a very high success for solubility predictions of $CO_2$-water system. The work shows that the mixing rule has to have parameters fitted at each temperature for $CO_2$-water system.

The sensitivity of the prediction accuracy of SPUNG EoS to reference fluid is significant. Within the set of hydrocarbons as a reference fluid, the heavier the reference fluid, the larger the range of densities the EoS can represent. In this case, within the set of hydrocarbons, the heavier the reference fluid was, the better the method predicted the densities. This implies that the SPUNG EoS has a potential for improving the density predictions by using other reference fluids than propane. Further work is being undertaken to investigate the best reference fluid and reference equation for this system. The results also showed that the choice of reference fluid had small impact on the predictions of the VLE solubilities. For VLE, how the interaction between $CO_2$ and water is described (mixing rules) plays a more significant role than the choice of the reference fluid. Further development of SPUNG mixing rules for this system is required.

## 4.2 The new equation of state

In the light of the potential, capabilities and limitations of the SPUNG EoS, the author with his co-workers have developed a new extended EoS described earlier.

The results of the proposed model for single phase density showed very good matching and an improvement compared to SPUNG and SRKs EoSs results presented by Ibrahim et al. [18], especially as the pressure went up to 99.93 MPa. The mixing rules do not play a significant role, especially for single phase, because they influence only the $a$ parameter calculations. Hence, improvement is argued to be mainly due to the use of the Bender-type 20 parameters MBWR EoS of Polt [35] with the reference fluids R23, R503 and $NH_3$.

The $CO_2$-rich phase density accuracy using the new EoS is presented in comparison to SPUNG and with the experimental data of Chiquet et al. [5] in terms of AADs in Table 2, Paper 4.

The density predictions using the new EoS of the liquid water-rich phase are presented in comparison with the experimental data of Chiquet et al. [5] , King et al. [20] and Hebach et al. [13] in Table 3, Paper 4.

Using the new EoS, the results for the $CO_2$-rich phase are slightly overshooting. However, the water-rich phase density predictions became very accurate. This can be attributed to the use of the reference fluids R23, R503 and $NH_3$. The results imply that R23 is the best compromise when $CO_2$-water is of concern.

We assessed the proposed EoS by comparing the predictions to SPUNG EoS and with the experimental works. Table 4, Paper 4 gives the associated AADs in comparison to Valtz et al. [42].

Table 5, Paper 4 shows the AADs in comparison to Mueller et al. [31] for the three assessed temperatures.

For moderate pressures we chose the conditions to model according to Bamberger et al. [2], where Table 6, Paper 4 presents the AADs of the comparison.

Table 8, Paper 4 summarizes AADs with respect to Hou et al. [14], while Table 9, Paper 4 compares our results with those of Wiebe [43] experiments.

The proposed EoS was used to predict the mutual solubilities of $CO_2$ and $H_2O$ at very high pressures. The conditions are consistent with the work of Takenouchi and Kennedy [39], namely between 10 MPa and 70 MPa, in conjunction with a temperature of 110 °C. Table 10, Paper 4 shows our results and errors (in terms of AADs), respectively, with reference to the work of Takenouchi and Kennedy [39].

## 4.3    General discussion

The new EoS predicted the phase equilibrium very accurately. The comparison to SPUNG EoS showed large improvements. This is because the HV mixing rules have the advantage of handling asymmetric polar mixtures like $CO_2$-water, contrary to the symmetric quadratic mixing rule of van der Waals used in SPUNG EoS. We chose to derive the HV mixing rule for the shape factors calculation as it has the advantage of being a consistent mixing rule unlike the other asymmetric mixing rules, which suffers from the Michelsen-Kistenmacher syndrome [28]. Moreover, in combination with the usage of the Bender-MBWR EoS parameters of Polt [35] and the tested reference fluids, the new EoS predicted both densities and phase equilibrium for the polar mixture of $CO_2$-water accurately using the same set of parameters.

Wilhelmsen et al. [44] showed that for the calculations of density, enthalpy and entropy over a 10 000 random conditions in different phase regions, and for three component $CO_2$ mixtures, SPUNG run time was only 4 times higher than SRK. The new EoS is of the same order of computational complexity as the SPUNG EoS. Therefore, the new ECS EoS is a superior compromise between computational time and accuracy. These achievements make the new EoS readily usable for CFD computations that already use EoSs like SRK. This is because the new EoS is of the same order of computational time. However, it offers a much greater accuracy

in the capture of phase equilibrium, and thermodynamical properties. Therefore, I strongly recommend it for process design in CCS industry for its high accuracy and reasonable computational time. This will lead to more robust designs and accurate predictions and estimations of behaviors at different scenarios at affordable cost.

Since the new EoS is of ECS type, I anticipate that it inherits the qualities that qualify it for good capture of transport properties like good prediction of derivatives. If this is proven true, it will give the new EoS superiority to CPA approach. However, there is no formal work done to prove this. Therefore, I recommend such a work for future investigation. A coupling to a CFD tool to investigate stability robustness of the approach is also highly recommend for future work.

## 4.4 Conclusions

A thermodynamically consistent extended corresponding states (ECS) EoS was developed for CCS industry. The new EoS can handle the phase equilibrium of the polar mixtures of $CO_2$-water with high accuracy. The high accuracy when compared with experimental data is achieved over a wide range of pressures and temperatures. This achievement is due to the proposed development of a Huron-Vidal mixing rules based approach of computing the scale factors. The usage of R23, R503 and $NH_3$ as reference fluids allowed simultaneous accurate predictions of the density of the $CO_2$-water systems. This is achieved for single phase at high pressures, supercritical-liquid, liquid-liquid and vapor-liquid equilibrium.

# References

[1] Kyoto Protocol, 1995. Kyoto Protocol, `http://unfccc.int/essential_background/kyoto_protocol/items/6034.php`,(visited 10th june 2016).

[2] Bamberger, A., Sieder, G., Maurer, G., 2000. High-pressure (vapor+liquid) equilibrium in binary mixtures of (carbon dioxide+water or acetic acid) at temperatures from 313 to 353 K. J. Supercrit. Fluids, 17(2), 97 – 110.

[3] Bikkina, P.K., Shoham, O., Uppaluri, R., 2011. Equilibrated interfacial tension data of the CO2-water system at high pressures and moderate temperatures. J. Chem. Eng. Data, 56(10), 3725–3733.

[4] Chapman, W.G., Gubbins, K.E., Jackson, G., Radosz, M., 1990. New reference equation of state for associating liquids. Ind. Eng. Chem. Res., 29(8), 1709–1721.

[5] Chiquet, P., Daridon, J.L., Broseta, D., Thibeau, S., 2007. $CO_2$/water interfacial tensions under pressure and temperature conditions of $CO_2$ geological storage. Energy Convers. Manage., 48(3), 736 – 744.

[6] Clausen, S., Oosterkamp, A., Strøm, K., 2012. Depressurization of a 50 km long 24 inches co2 pipeline. Energy Procedia, 23, 256–265.

[7] Climate Change Act, 2008. Department of Energy and Climate Change, `http://www.legislation.gov.uk/ukpga/2008/27/contents`,(visited 29 may 2013).

[8] de Koeijer, G., Borch, J., Jakobsen, J., Drescher, M., 2009. Experiments and modeling of two-phase transient flow during co2 pipeline depressurization. Energy Procedia, 1(1), 1683–1689.

[9] Diamantonis, N.I., Economou, I.G., 2012. Modeling the phase equilibria of a $H_2O$-$CO_2$ mixture with PC-SAFT and tPC-PSAFT equations of state. Mol. Phys., 110(11-12), 1205–1212.

[10] Ely, J.F., 1990. A predictive, exact shape factor extended corresponding states model for mixtures. Adv. Cryog. Eng., 35, 1511–1520.

[11] Estela-Uribe, J.F., Trusler, J.P.M., 1998. Shape factors for the light hydrocarbons. Fluid Phase Equilib., 150-151, 225 – 234.

[12] Fisher, G.D., Leland, T.W., 1970. Corresponding states principle using shape factors. Ind. Eng. Chem. Fundam., 9(4), 537–544.

[13] Hebach, A., Oberhof, A., Dahmen, N., 2004. Density of water + carbon dioxide at elevated pressures: measurements and correlation. J. Chem. Eng. Data, 49(4), 950–953.

[14] Hou, S.X., Maitland, G.C., Trusler, J.M., 2013. Measurement and modeling of the phase behavior of the (carbon dioxide + water) mixture at temperatures from 298.15 K to 448.15 K. J. Supercrit. Fluids, 73, 87–96.

[15] Huron, M.J., Vidal, J., 1979. New mixing rules in simple equations of state for representing vapour-liquid equilibria of strongly non-ideal mixtures. Fluid Phase Equilib., 3(4), 255 – 271.

[16] Ibrahim, M., Skaugen, G., Ertesvåg, I.S., 2012. Preliminary evaluation of the SPUNG equation of state for modelling the thermodynamic properties of $CO_2$-water mixtures. Energy Procedia, 26, 90 – 97.

[17] Ibrahim, M., Skaugen, G., Ertesvåg, I.S., 2014. Modelling $CO_2$ – water thermodynamics using spung equation of state (EoS) concept with various reference fluids. Energy Procedia, In press.

[18] Ibrahim, M., Skaugen, G., Ertesvåg, I.S., Haug-Warberg, T., 2014. Modelling $CO_2$ - water mixture thermodynamics using various equations of state (EoS) with emphasis on the potential of the SPUNG EoS. Chem. Eng. Sci., 113, 22 – 34.

[19] Jørstad, O., 1993. Equations of state for hydrocarbon mixtures. Dr. Ing. thesis No. NTH 1993:92. Norwegian Inistitute of Technology, Trondheim, Norway.

[20] King, M.B., Mubarak, A., Kim, J.D., Bott, T.R., 1992. The mutual solubilities of water with supercritical and liquid carbon dioxides. J. Supercrit. Fluids, 5(4), 296 – 302.

[21] Kontogeorgis, G.M., Coutsikos, P., 2012. Thirty years with eos/ge models—what have we learned? Ind. Eng. Chem. Res., 51(11), 4119–4142.

[22] Kontogeorgis, G.M., Voutsas, E.C., Yakoumis, I.V., Tassios, D.P., 1996. An equation of state for associating fluids. Ind. Eng. Chem. Res., 35(11), 4310–4318.

[23] Kunz, O., Klimeck, R., Wagner, W., Jaeschke, M., 2007. The GERG-2004 Wide-Range Equation of State for Natural Gases and Other Mixtures. GERG TM15, VDI Verlag, Düsseldorf, Germany.

[24] Leach, J.W., Chappelear, P.S., Leland, T.W., 1968. Use of molecular shape factors in vapor-liquid equilibrium calculations with the corresponding states principle. AIChE J., 14(4), 568–576.

[25] Lemmon, E.W., Huber, M.L., McLinden, M.O., 2010. NIST Standard Reference Database 23: Reference Fluid Thermodynamic and Transport Properties - REFPROP, version 9.0. National Institute of Standards and Technology, Standard Reference Data Program, Gaithersburg, Maryland.

[26] Li, H., Jakobsen, J.P., Wilhelmsen, Ø., Yan, J., 2011. PVTxy properties of CO2 mixtures relevant for CO2 capture, transport and storage: Review of available experimental data and theoretical models. Appl. Energy, 88(11), 3567 – 3579.

[27] Li, H., Yan, J., 2009. Impacts of equations of state (EOS) and impurities on the volume calculation of CO2 mixtures in the applications of CO2 capture and storage (CCS) processes. Appl. Energy, 86(12), 2760 – 2770.

[28] Michelsen, M.L., Kistenmacher, H., 1990. On composition-dependent interaction coefficeints. Fluid Phase Equilib., 58(1–2), 229 – 230.

[29] Michelsen, M., Mollerup, J., 2007. Thermodynamic Models: Fundamentals & Computational Aspects. Tie-Line Publications.

[30] Mollerup, J., 1998. Unification of the two-parameter equation of state and the principle of corresponding states. Fluid Phase Equilib., 148(1-2), 1–19.

[31] Mueller, G., Bender, E., Maurer, G., 1988. Das Dampf-fluessigkeitsgleichgewicht des ternaeren Systems Ammonik-Kohlendioxid-Wasser bei hohn Wassergehalten im Bereich zwischen 373 und 473 Kelvin. Ber. Bunsenges. Phys. Chem., 92, 148–160.

[32] Patel, M.R., Eubank, P.T., 1988. Experimental densities and derived thermodynamic properties for carbon dioxide-water mixtures. J. Chem. Eng. Data, 33(2), 185–193.

[33] Patel, M.R., Holste, J.C., Hall, K.R., Eubank, P.T., 1987. Thermophysical properties of gaseous carbon dioxide-water mixtures. Fluid Phase Equilib., 36, 279 – 299.

[34] Peng, D.Y., Robinson, D.B., 1976. A new two-constant equation of state. Ind. Eng. Chem. Fundam., 15(1), 59–64.

[35] Polt, A., 1987. Zur beschreibung der thermodynamischen eigenschaften reiner fluide mit "Erweiterten BWR-Gleichungen". Dissertation.

[36] Seitz, J.C., Blencoe, J.G., 1999. The CO2-H2O system. I. Experimental determination of volumetric properties at 400°C, 10-100 MPa. Geochim. Cosmochim. Acta, 63(10), 1559 – 1569.

[37] Soave, G., 1972. Equilibrium constants from a modified Redlich-Kwong equation of state. Chem. Eng. Sci., 27(6), 1197 – 1203.

[38] Span, R., Wagner, W., 1996. A new equation of state for carbon dioxide covering the fluid region from the tripple-point temperature to 1100 K at pressures up to 800 MPa. J. Phys. Chem. Ref. Data, 25(6), 1509–1596.

27

[39] Takenouchi, S., Kennedy, G.C., 1964. The binary system $H_2O$-$CO_2$ at high temperatures and pressures. Am. J. Sci., 262(9), 1055–1074.

[40] Tsivintzelis, I., Kontogeorgis, G.M., Michelsen, M.L., Stenby, E.H., 2011. Modeling phase equilibria for acid gas mixtures using the CPA equation of state. Part II: Binary mixtures with $CO_2$. Fluid Phase Equilib., 306(1), 38–56.

[41] UNFCC, 1992. United Nations Framework Convention on Climate, http://unfccc.int/essential_background/items/6031.php,(visited 10th june 2016).

[42] Valtz, A., Chapoy, A., Coquelet, C., Paricaud, P., Richon, D., 2004. Vapour-liquid equilibria in the carbon dioxide-water system, measurement and modelling from 278.2 to 318.2 K. Fluid Phase Equilib., 226, 333 – 344.

[43] Wiebe, R., 1941. The binary system carbon dioxide-water under pressure. J. Am. Chem. Soc., 29(3), 475–481.

[44] Wilhelmsen, Ø., Skaugen, G., Jørstad, O., Li, H., 2012. Evaluation of SPUNG and other equations of state for use in carbon capture and storage modelling. Energy Procedia, 23, 236 – 245.

# Part II: Papers

# PAPER I

GHGT-12

# PVTx Modeling of $CO_2$ Pipeline at Depressurization Conditions Using SPUNG Equation of State (EoS) with a Comparison to SRK

Mohamed Ibrahim[a]*, Ivar S. Ertesvåg[a]

*[a]Department of Energy and Process Engineering, Norwegian University of Science and Technology, Kolbjørn Hejes veg 1B, NO-7491 Trondheim, Norway.*

## Abstract

The proper modeling of $CO_2$ depressurization is very important for the design for safety of a pipeline. One key element of the modeling process is the thermodynamics and transport properties modeling. In this work, an analysis of the error in thermodynamics for modeling $CO_2$ at depressurization conditions was conducted. For the study presented here, the sophisticated equation of state (EoS) SPUNG was used. The results were compared to an EoS of a different level of complexity and, consequently, accuracy. This EoS is the cubic equation Soave–Redlich–Kwong (SRK) with van der Waal's mixing rules. The results show the significance of the thermodynamics modeling at a set of pressures, temperatures and compositions PVTx over time steps complying with two sets of experimental data.

## 1. Introduction

The $CO_2$ production and its effects on the climate change are among the current era challenges. Therefore, the Carbon Capture and Storage (CCS) research and industry are developing very fast to cope with the challenge. Transport of $CO_2$ in pipelines is one of the important links in the chain. During shutdown or by a fracture, the $CO_2$ is depressurized from very high pressures. This can result in large drop in temperatures. Very fast, non-controlled depressurization can cause dry ice formation and the steel of the pipelines to become very brittle. This can reduce

---

* Corresponding author. Tel.: +4773593841; fax: +4773593580.
  *E-mail address:* mohamed.ibrahim@ntnu.no

integrity of the pipe significantly. The dissipation of $CO_2$ during depressurization can form clouds, which raise safety concerns. Therefore, the proper modeling and simulation of the depressurization process is very important for the safety and for efficiency of a design. The process modeling consists of many components from fluid dynamics to thermodynamics of the multi-phase multicomponent phenomena.

---

**Nomenclature**

| | |
|---|---|
| $a, b$ | Gas parameters in SRK [J m$^3$ mol$^{-2}$], [m$^3$ mol$^{-1}$] |
| $C$ | Arbitrary variable [-] |
| $f$ | Function of [-] |
| $k$ | Binary interaction parameter |
| $N$ | Total number of points |
| $n$ | Amount of substance [mol] |
| NC | Number of components in a mixture |
| $P$ | Pressure [Pa] |
| $R$ | Universal gas constant [J K$^{-1}$ mol$^{-1}$] |
| $T$ | Temperature [K] |
| $V$ | Volume [m$^3$] |
| $x$ | Mole fraction [-] |
| Z | Compressibility factor [-] |
| $\theta$ | Shape factor [-] |
| $\varphi$ | Shape factor [-] |
| $\omega$ | Acentric factor [-] |

**Subscripts/Superscripts**

| | |
|---|---|
| c | Critical state |
| $i, j$ | Component i, j |
| M | Mixture |
| R | Reduced variable |
| Ref | Reference fluid |
| s | Simulation |

---

A number of publications have studied the sensitivity of modeling transient pipeline flows to multiphase, friction, heat transfer and shock models. Other studied the effect of stream impurities on the overall results. Here, we studied the effect of impurities on the predictions from the thermodynamics point of view. This was done by comparing results of the same equation of state (EoS) when modeling pure $CO_2$ and mixtures with different compositions. Moreover, we studied the sensitivity of predictions to the quality of the EoS. This was done by comparing the results of two EoS of different classes of sophistication and, subsequently, of accuracy. There are a number of EoS classes available in literature. Among the most known and widely used in industry are the cubic EoSs like Soave-Redlich-Kwong (SRK) [1], SRK with Huron-Vidal mixing rules (SRK-HV) [2] and Peng-Robinson (PR) [3]. They are mainly used for their reasonable accuracy and low computation time. Among the highest in computation time are the full extended corresponding states (ECS) equations like the models implemented in the REFPROP library of the National Institute of Standards and Technology (NIST) [4], which are mainly used for transport properties. A modern approach that is less computationally expensive than ECS and offers generally good accuracy is the multi parameters approach. Nevertheless, it is at least one order of magnitude higher than Cubic EoS in computation time. Span-Wagner [5] for pure $CO_2$ and GERG (Groupe Européen de Recherches Gaziéres) [6] for mixtures belong to this category. The Cubic-Plus-Association (CPA) [7] and the Statistical Associating Fluid Theory (SAFT) [8] EoSs are state-of-the-art approaches. Results of the CPA and Perturbed Chain SAFT (PC-SAFT) for modeling $CO_2$-water were presented in [9] and [10], respectively. The two articles also provided a literature survey on CPA and SAFT type developments and recent achievements. Here, we used the Extended Corresponding States (ECS) EoS SPUNG for the prediction of

thermodynamic properties over a PVTx of two sets of $CO_2$ depressurization experimental data [11], [12]. The results were compared to the cubic EoS SRK, which was chosen because of its popularity in industry and low computational cost. The SPUNG EoS was chosen as it was shown to be more accurate than SRK for $CO_2$ non-polar mixtures [13] and polar mixtures [14, 15, and 16]. Furthermore, the relatively higher accuracy of SPUNG EoS comes on relatively low cost compared to other sophisticated concepts. This is because SPUNG EoS is only about five times more expensive than SRK. The concept captures the phase equilibrium very accurately and maintain the other properties accuracy very high, unlike cubic equations. The use of the standard ECS for long-pipeline Computational Fluid Dynamics (CFD) simulations was infeasible, and cubic EoS, or even simpler forms, are mainly used by industry due to the computational cost. However, SPUNG EoS is a class of ECS that with the usage of SRK for computing shape factors, computational cost of the ECS approach was significantly reduced, while the accuracy remained generally high. This might make the coupling to a flow solver and running a multi-component and multi-phase simulations feasible. In this study only thermodynamics was regarded, and the sets of PT pairs over which the predictions were conducted, were taken at different time steps from real experimental depressurization conditions [11], [12].

## 2. Theory

An EoS is a model that calculates for both the liquid and gas phase using the same expression, which enhances the continuity near the critical point. An EoS for an NC component mixture is an expression for pressure as a function of the mole fractions, the temperature and the volume. Given this expression, it can be manipulated to calculate the fugacity of each component. In the following subsection, a brief description of the EoS used in the work will be given together with further references.

### 2.1. The standard SRK

The classical SRK model with van der Waal's mixing rules [1] is a cubic EoS that is written for a mixture as

$$P = \frac{RTn}{V - bn} - \frac{an^2}{V^2 + bn\,V} \tag{1}$$

$$a = \sum_i \sum_j x_i x_j \sqrt{a_i\,a_j}\,(1 - k_{ij}), \qquad b = \sum_i x_i b_i \tag{2}$$

$$b_i = \frac{0.08664\,RT_{c,i}}{P_{c,i}} \tag{3}$$

Here, $T_{c,i}$, $P_{c,i}$ are the critical temperature and pressure of component $i$.

### 2.2. The corresponding states principle

The principle of corresponding states assumes that all substances exhibit the same behavior at a reduced state. A corresponding states EoS typically has one or more reference components described very accurately by a reference EoS. Therefore, the compressibility of the investigated fluids or mixtures can be evaluated as

$$Z = f\big(V_{Ref}, T_{Ref}, \omega, ....\big)_{Ref} \tag{4}$$

In the corresponding states approach the $V_{Ref}$ and $T_{Ref}$ of the reference fluid are the reduced volume and temperature $V_R$, and $T_R$ of the fluid or the mixture investigated.

### 2.3. The extended corresponding states principle

In the extended corresponding states concept, the mapping between the investigated fluid or mixture $T$ and $V$ and the reference fluid $V_{Ref}$, $T_{Ref}$ is done via the shape factors $\varphi$ and $\theta$. These shape factors take into account how the fluids or the mixture in consideration differs from the reference fluid.

$$T_{Ref} = \frac{T}{\theta} \qquad\qquad (5)$$

$$V_{Ref} = \frac{V}{\varphi} \qquad\qquad (6)$$

where the shape factors $\varphi$ and $\theta$ are function of $T_{Ref}$ and $V_{Ref}$. This implicit formulation make it very computationally expensive to calculate them using an accurate EoS. However, they can be computed analytically, or by using simpler forms of EoS.

### 2.4. The SPUNG EoS

The SPUNG EoS investigated here, is an extended corresponding state approach that uses the SRK cubic EoS to calculate the shape factors and propane as a reference fluid. The SPUNG EoS uses the accurate modified Benedict-Webb-Rubin (MBWR) [17] EoS for the reference fluid. The SPUNG EoS was introduced in the doctoral thesis of Jørstad in 1993 [18] for low temperature hydrocarbon mixtures, which was enlightened by the work of Mollerup (1980) [19]. Propane was chosen as the reference fluid to ensure that the reduced temperature of the considered mixtures would be above the reduced triple point of the reference fluid in order to avoid extrapolation of the reference equation.

## 3. Methodology

### 3.1. The numerical tools

The NTNU-SINTEF in-house thermodynamic library was used for the study presented. The library is a tool for predicting the thermodynamic properties using various approaches that ranges in level of sophistication and underlying theory. The library was used with a tolerance of $10^{-4}$ for both the multi-phase flash algorithm and the compressibility factor calculations.

### 3.2. Setup

The first setup investigated here was the depressurization of a 50 km long 24 inches $CO_2$ pipeline by Clausen et al. [11]. The article provided temperature and pressure profiles over time at the first end and second end of the pipeline during the process. Here, we computed the densities and speed of sound for the pairs of pressure and temperature obtained from the graphs of [11] at different time steps of the first end. We conducted the numerical simulations for three compositions using SPUNG and SRK. The first was a pure $CO_2$ case. The second was a mixture of 99.14 % of $CO_2$, 0.22% of $N_2$, 0.63% of $CH_4$ and 0.01% of water and is what we refer to as real. The third was a mixture of 98%$CO_2$ and 2% of water.

The second setup was of the conditions tested by de Koeijer et al. [12] for pure $CO_2$ at 139 m downstream.

### 3.3. Error definition

Since the cited literature did not provide experimental density data, but only measurements of temperature and pressure over time and at different locations, we used the SPUNG EoS as a reference when computing the deviation of SRK. We considered this as a valid strategy since SPUNG EoS had proven to be a way more accurate than SRK [13, 14, 15, 16]. The deviations of predictions was measured here by the Average of Absolute Deviation (AAD) defined for an arbitrary variable $C$ as:

$$AAD(C, \%) = \frac{100}{N} \sum_{r=1}^{N} \frac{(C_{datum} - C\ )}{C_{datum}} \qquad\qquad (7)$$

Where subscript datum denotes the dataset towards which the deviations is calculated (e.g. SPUNG EoS results).

## 4. Results and discussion

The results of the density predictions of the three tested compositions are plotted in Fig. 1. The Real mixture refers to the $CO_2$, $N_2$, $CH_4$ and water case described in the setup section. The results show that the $CO_2$-water mixture density predictions are higher than that of pure $CO_2$ until it turned to gas phase. This difference was due to the existence of only 2% of water. The realistic mixture went through the two phase region between 1.5 and 2.5 hours for SPUNG EoS and at 1.5 to 2.0 hours for SRK, which led to the less steep drop of density seen in Fig. 1. The AAD of the $CO_2$-water case from the pure one was 69.2% and 40.5% for SPUNG EoS and SRK, respectively. The AAD of the realistic mixture was 9.8% and 13.7% for SPUNG EoS and SRK, respectively.
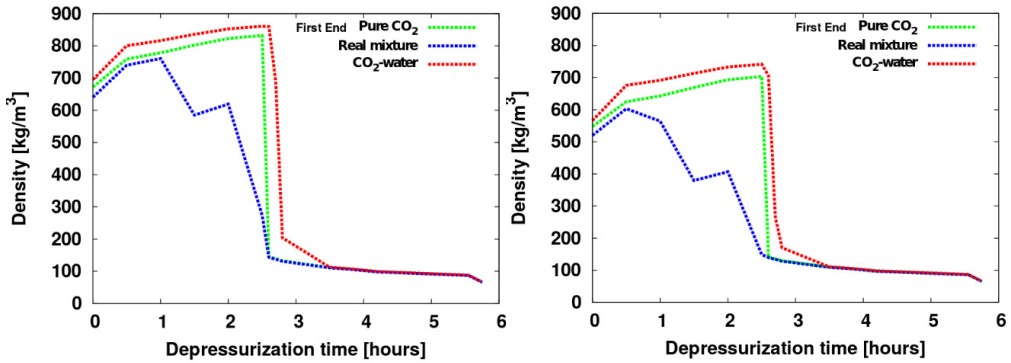


Fig. 1. Predictions of the first end density over time using (left) SPUNG EoS; (right) SRK EoS.

The comparison between the density predictions of SRK and SPUNG EoS for the pure $CO_2$ case is plotted in Fig. 2. The main difference lies in the heavy phase predictions, where [13, 14, 15, and 16] showed that SPUNG EoS was superior in predictions to SRK. Therefore, taking SPUNG EoS as a reference, the AAD of all the predictions was 8.1% with a maximum deviation of 18.5%.
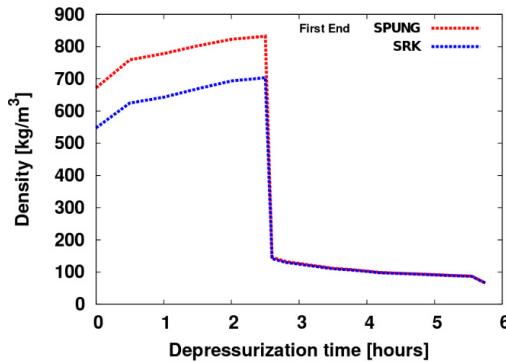


Fig. 2. Pure $CO_2$ density predictions over time using SPUNG and SRK EoS.

The predictions of the speed of sound for the pure $CO_2$ case are plotted in Fig. 3. The speed of sound using both EoSs drops as instantaneous as the mixtures changes from the heavy to the light phase. The AAD of SRK to SPUNG EoS was 6.7%, with a maximum deviation of 14.9%.
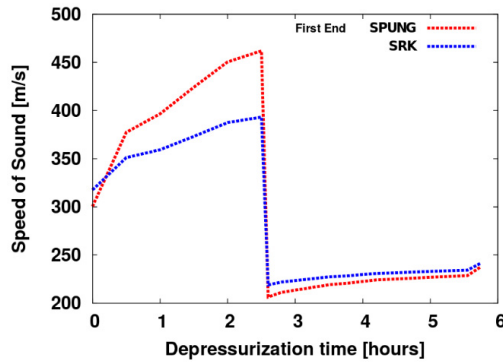


Fig. 3. Pure $CO_2$ speed of sound predictions over time using SPUNG and SRK EoSs.

Figure 4 shows the comparison between SRK and SPUNG EoS density predictions for the realistic mixture. The AAD of SRK to SPUNG EoS as a reference was 13.5%, with a maximum deviation of 29.7%.
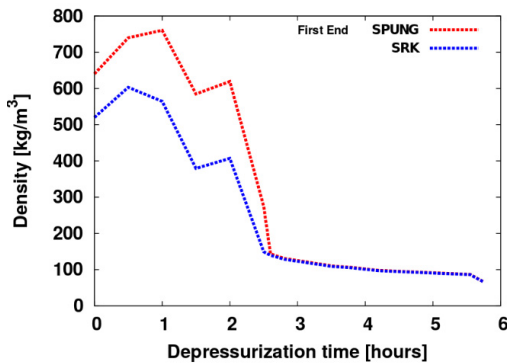


Fig. 4. The density predictions of the realistic mixture of $CO_2$, $N_2$, $CH_4$ and water over time using SPUNG and SRK EoSs.

The comparison between SRK and SPUNG EoS density predictions for the $CO_2$-water mixture is shown in Fig. 5. The AAD for this case was 13.8%, with a maximum deviation of 21.4%.
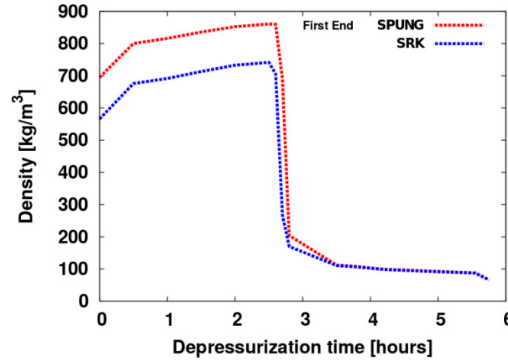
Fig. 5. The 98% $CO_2$ - 20% water density predictions over time using SPUNG and SRK EoSs.
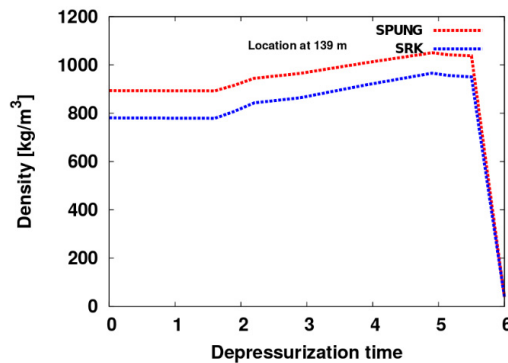


Fig. 6. The density predictions at de Koeijer et al. [12] temperature and pressure pairs.

Figure 6 shows the comparison between SRK and SPUNG EoS density predictions for the pure-$CO_2$ case of de Koeijer et al. [12]. The AAD was 10.3%, with a maximum deviation of 12.8%.

A 1-D flow solver will always include models that are fitted to recover pipeline measurements, which would increase or decrease the relevance of thermodynamics depend on how new the investigated setup is. Therefore, this work was conducted to isolate this model fitting effects on the relevance of EoSs and impurities. The results showed how the density and speed of sound profiles look like for a set of real depressurization conditions taken from experiments. This density reflects on the mass fractions, pumping power, etc. The speed of sound will influence the pressure wave propagation for a full simulation. Consequently, the crack propagation speed in a case of fracture. The results showed that including impurities is important from the thermodynamics behavior point of view. Moreover, the results also showed that the accuracy of an EoS is as important as the inclusion of impurities and can have a strong impact on the final dynamic simulation results. A coupling to a 2-D flow solver is planned for future work.

## 5. Conclusions

The SPUNG EoS was used for prediction of thermodynamics properties over a real depressurization TP conditions. The phase fraction and composition was computed using TP-flash routines. The results were compared to SRK. We conclude that the inclusion of impurities is very important, but using an accurate EoS is also very crucial for the accuracy of the simulation.

**Acknowledgements**

This work was financed through the CO2 Dynamics project. The authors acknowledge the support from the Research Council of Norway (189978), Gassco AS, Statoil Petroleum AS and Vattenfall AB.

**References**

[1] Soave, G. Equilibrium constants from a modified Redlich-Kwong equation of state. Chem. Eng. Sci. 1972;27(6): 1197 – 1203.

[2] Huron, M.J., Vidal, J. New mixing rules in simple equations of state for representing vapour-liquid equilibria of strongly non-ideal mixtures. Fluid Phase Equilib. 1979; 3(4): 255 – 271.

[3] Peng, D.Y., Robinson, D.B.. A new two-constant equation of state. Ind. Eng. Chem. Fundam. 197 ; 15 (1), 59–64

[4] Lemmon, E.W., Huber, M.L., McLinden, M.O. NIST Standard Reference Database 23: reference fluid thermodynamic and transport properties REFPROP. 2010; Version 9.0. National Institute of Standards and Technology, Standard Reference Data Program, Gaithersburg, Maryland.

[5] Span, R., Wagner, W. A new equation of state for carbon dioxide covering the fluid region from the triple-point temperature to 1100 K at pressures up to 800 MPa. J. Phys. Chem. Ref. Data. 1996;25(6): 1509–1596.

[6] Kunz, O., Klimeck, R., Wagner, W., Jaeschke, M. The GERG-2004 wide-range equation of state for natural gases and other mixtures, 2007. GERG TMIS, VDI Verlag, Düsseldorf, Germany.

[7] Kontogeorgis, G.M., Voutsas, E.C., Yakoumis, I.V., Tassios, D.P. An equation of state for associating fluids. Ind. Eng. Chem. Res. 1996 ; 35 (11), 4310–4318.

[8] Chapman, W.G., Gubbins, K.E., Jackbson, G., Radosz, M. New reference equation of state for associating liquids. Ind. Eng. Chem. Res. 1990; 29(8): 1709–1721.

[9] Tsivintzelis, I., Kontogeorgis, G.M., Michelsen, M.L., Stenby, E.H.. Modeling phase equilibria for acid gas mixtures using the CPA equation of state. Part II: Binary mixtures with CO 2 . Fluid Phase Equilib. 2011; 306 (1), 38–56.

[10] Diamantonis, N.I., Economou, I.G.. Modeling the phase equilibria of a H2O-CO2 mixture with PC-SAFT and tPC-PSAFT equations of state. Mol. Phys. 2012 ; 110 (11–12), 1205–1212.

[11] Clausen, S., Oosterkamp, A., Strøm, K.L. Depressurization of a 50 km long 24 inches CO2 pipeline. Energy Procedia, 2012; 23, 256-265.

[12] de Koeijer, G., Borch, J.K., Jakobsen, J., Drescher, M. Experiments and modeling of two-phase transient flow during CO2 pipeline depressurization. Energy Procedia, 2009; 1(1), 1683-1689.

[13] Wilhelmsen, Ø., Skaugen,G., Jørstad, O., Li, H. Evaluation of SPUNG and other equations of state for use in carbon capture and storage modeling, Energy Procedia, 2012; 23: 236 - 45.

[14] Ibrahim, M., Skaugen, G., Ertesvåg, I.S. Preliminary evaluation of the SPUNG equation of state for modeling the thermodynamic properties of CO₂-water mixtures. Energy Procedia. 2012; 26: 90-97

[15] Ibrahim, M., Skaugen, G., Ertesvåg, I.S. Modeling CO2-water thermodynamics using SPUNG equation of state (EoS) concept with various reference fluids, Energy Procedia. 2014; 51:353-362.

[16] Ibrahim, M., Skaugen, G., Ertesvåg, I.S., Warberg, T.H. Modeling mixture thermodynamics using various equations of state (EoSs) with emphasis on the potential of the SPUNG EoS, Chemical Engineering Science. 2014; 113: Pages 22-34.

[17] Younglove, B.A., Ely, J.F. Thermophysical properties of fluids: II. Methane, ethane, propane, isobutane, and normal butane. J. Phys. Chem. Ref. Data. 1987; 16(4): 577–798.

[18] Jørstad, O. Equations of state for hydrocarbon mixtures. Dr. Ing. Thesis No. NTH 1993:92. Norwegian Institute of Technology, Trondheim, Norway. 1993.

[19]  Mollerup, J., Thermodynamic properties from corresponding states theory, Fluid Phase Equilibria. 1980; 4(1-2): 11-34.

# PAPER II

7th Trondheim CCS Conference, TCCS-7, June 5-6 2013, Trondheim, Norway

# Modelling CO₂ –Water Thermodynamics Using SPUNG Equation of State (EoS) concept with Various Reference Fluids

Mohamed Ibrahim[a], Geir Skaugen[b], Ivar S. Ertesvåg [a]

*[a]NTNU, Kolbjørn Hejes veg 1A, N-7465Trondheim, Norway*
*[b]Sintef Energy Research, Kolbjørn Hejes veg 1A, N-7465Trondheim, Norway*

**Abstract**

Due to the continuous increase of $CO_2$ emission to environment, the Carbon Capture and Storage (CCS) processes gained a very high importance in the last decades. One common $CO_2$ impurity during various CCS processes is water. Therefore, the calculation of CO–water thermodynamic properties is a vital issue. This work preliminary investigates the accuracy of the extended corresponding states equation of state SPUNG using various reference fluids for the density and vapour liquid equilibrium (VLE) calculations of the $CO_2$ - water system. The evaluation is done by comparing the numerical prediction with experimental data. The study is conducted at different mixture concentrations, and covering a broad range of conditions. The study is conducted using $N_2$, $O_2$, C1, C2, C3, and C4 as reference fluids. The results show an impact on density prediction. On the other hand, the VLE calculations exhibited very low sensitivity to varying reference fluids.

*Keywords:* Coressponding States, Extended Corresponding States, Reference Equation of State, MBWR, CCS, VLE

---

| | |
|---|---|
| **Nomenclature** | |
| **Symbols** | |
| $C$ | Arbitrary variable [-] |
| $N$ | Total number of points |
| $P$ | Pressure [Pa] |

| $T$ | Temperature [K] |
| --- | --- |
| $V$ | Volume [m$^3$] |
| $x$ | Mole fraction [-] |
| Z | Compressibility factor [-] |
| $\theta$ | Shape factor [-] |
| $\varphi$ | Shape factor [-] |
| $\omega$ | Acentric factor [-] |
| **Subscripts/Superscripts** | |
| c | Critical state |
| exp | Experimental |
| $i$ | Component i |
| R | Reduced variable |
| $r$ | Point index |
| Ref | Reference fluid co-ordinate |
| s | Simulation |

## 1. Introduction

One important aspect for the analysis and simulations of Carbon Capture and Storage (CCS) processes is the modeling of the thermodynamic properties for pure $CO_2$ and $CO_2$ mixtures. Indeed, the choice of model may have a great impact on efficiency, economy and safety. One such model is the SPUNG EoS. It is an extended corresponding state model that uses one reference fluid to calculate the behavior for mixtures of interest. The SPUNG EoS is a consistent approach that was developed for hydrocarbons systems and it showed a good compromise in accuracy and computational efficiency [1]. A later work [2] showed the same results for non-polar binary and ternary $CO_2$-rich mixtures. In an on-going research, this approach also shows a superiority in density predictions of the $CO_2$-water system at low pressures compared to the cubic equation Soave-Redlich-Kwong (SRK) [3], and SRK with Huron Vidal mixing rules (SRK-HV) [4]. The value of the error using the standard SPUNG equation was still high compared to experimental data, reaching above 20% at extreme conditions. Furthermore, the work by Ibrahim et al. [5] showed that the VLE predictions of SPUNG and SRK were poor. The standard SPUNG model, used in the previous studies, uses propane (C3) as the reference fluid. Therefore, this work will preliminarily investigate the impact of using various reference fluids on the predictions of $CO_2$–water thermodynamics. The aim was to get guidance or criterions of how to select the reference fluid and what are the limitations and constraints in order to improve the density and VLE prediction using the SPUNG EoS or similar concepts.

Here, an evaluation is done by comparing the behavior of the SPUNG EoS using alternative reference fluids like N$_2$, methane (C1), and ethane (C2). The first investigations suggested the use of heavier hydrocarbons. Therefore, the normal-butane (NC4) was implemented for comparisons as well.

## 2. Theory

### 2.1. Equations of state

An EoS is a model that calculates for both the liquid and gas phases using the same expression, which enhances the continuity near the critical point. An EoS for a mixture with a given number of components is an expression for pressure as a function of the mole fraction $x_i$, the temperature $T$, and the volume $V$;

$$P = P(x_i, T, V) \qquad (1)$$

Given this expression, it can be manipulated to calculate the fugacity of each component. In the following subsection, a brief description of the EoS used in the work will be given together with references for further reading.

There is a variety of EoS that have different structure complexity. One of the simplest structure set of EoS is the cubic EoS, examples are SRK[2], SRK-HV[3], and Peng—Robinson (PR) [6]. A more complicated structure is the set of multi-parameter approaches like GERG [7] and Span—Wagner [8] EoS. The Extended Corresponding States (ECS) is also one of the advanced modelling concepts and will be discussed in the following subsection as the base theory for the SPUNG EoS investigated. The most sophisticated concept is the SAFT approach [9].

### 2.2. The corresponding states principle

The principle of corresponding states assumes that all substances exhibit the same behavior at reduced states, ($V/V_c$ and $T/T_c$). A corresponding states EoS typically has one or more reference components described very accurately by a reference EoS. Therefore, the compressibility of the investigated fluids or mixtures can be evaluated as

$$Z = Z(V_{Ref}, T_{Ref}, \omega, \dots.)_{Ref} \qquad (2)$$

In the corresponding states approach the reference fluid $V_{Ref}$ and $T_{Ref}$ are the reduced volume and temperature $V_R$ and $T_R$ of the fluid or the mixture investigated.

### 2.3. The extended corresponding states principle (ECS)

In the ECS concept, the mapping between the investigated fluid or mixture $T$ and $V$ and the reference fluid $V_{Ref}$ $T_{Ref}$ is done via the shape factors $\varphi$, $\theta$. These shape factors take into account how the fluids or the mixture in consideration differs from the reference fluid.

$$T_{Ref} = \frac{T}{\theta} \qquad (3)$$
$$V_{Ref} = \frac{V}{\varphi} \qquad (4)$$

The shape factors $\varphi$ and $\theta$ can be computed analytically, using an accurate EoS, or using simpler forms of EoS.

### 2.4. The SPUNG EoS

SPUNG EoS is an ECS type of EoS that uses propane as a reference fluid, the modified Benedict-Webb-Rubin (MBWR) [10] as a reference EoS, and SRK EoS to evaluate the shape factors. The SPUNG EoS was developed by Jørstad in 1993[1] as part of his doctoral work. Propane was chosen as reference fluid to guarantee that the reduced triple point of the reference fluid is always below the reduced triple point temperature of any hydrocarbon mixture since propane has the lowest reduced triple point among all hydrocarbons.

## 3. Methodology

### 3.1. Numerical Tools

For the numerical prediction of the density and VLE properties, the NTNU-SINTEF in-house thermodynamic library TP_Lib was used for the study presented.

### 3.2. Setup

#### 3.2.1. Single phase density

In addition to the standard SPUNG equation using C3 as the reference fluid, the four additions reference fluids N2, C1, C2 and NC4 were used for density prediction. For this preliminary study data at elevated pressures (from 10 up to 100 MPa) and at a temperature of 400 °C were used. Four concentrations of 20, 40, 60 and 80% of $CO_2$ were investigated. The pressures, temperature and mole fractions were chosen to allow a comparison with the set of experimental data of Seitz and Blencoe [11]. A more detailed study are on-going to cover a wider range of CCS applications.

#### 3.2.2. Vapour Liquid Equilibrium

The ECS concept using N2, C1, C2, C3, and NC4 was used for the prediction of the mutual solubilities of $CO_2$ and $H_2O$. A set of experimental data by Bamberger et al. [12] was used in the comparison that provided data over moderate pressures that ranged between 4 and 14 MPa at a temperature of 50 °C.

### 3.3. Error definition

The prediction error compared with experimental data sets is described by the Relative Error (RE) and the Average of Absolute Deviation (AAD) defined for an arbitrary variable $C$ as:

$$RE(C,r) = \frac{|C_{s,r} - C_{exp,r}|}{C_{exp,r}} \tag{5}$$

$$AAD(C) = \sum_{r=1}^{N} \frac{|C_{s,r} - C_{exp,r}|}{C_{exp,r}} \tag{6}$$

## 4. Results and discussion

### 4.1. Single phase density prediction

The single phase density predictions using SPUNG and the similar ECS-based EoS that only differ in using $N_2$, C1, C2 as a reference fluid are plotted in Fig. 1. The predications were compared with experimental data by Seitz and Blencoe [11] over moderate to elevated pressures that varied from approximately 10 to 100 MPa. The REs of the predictions compared with experimental data are plotted in Fig. 2. The comparison was done over a broad band of concentrations from 20 to 80% of $CO_2$. The results showed that the error of all the used reference fluids grew as the pressure and $H_2O$ mole fraction increased. The error using propane, which is the reference fluid used by SPUNG EoS was the lowest out of all the tested reference fluids. Nevertheless, Figs. 1 and 2 show a clear trend that within the hydrocarbons, the heavier the reference fluid is the better it predicts the heavy phase density. The comparison with $O_2$ showed an overlap with C1 results, and was omitted for clarity of the figure. In order to confirm this observation, NC4 set of coefficients by Younglove et al. [10] was implemented. The new results
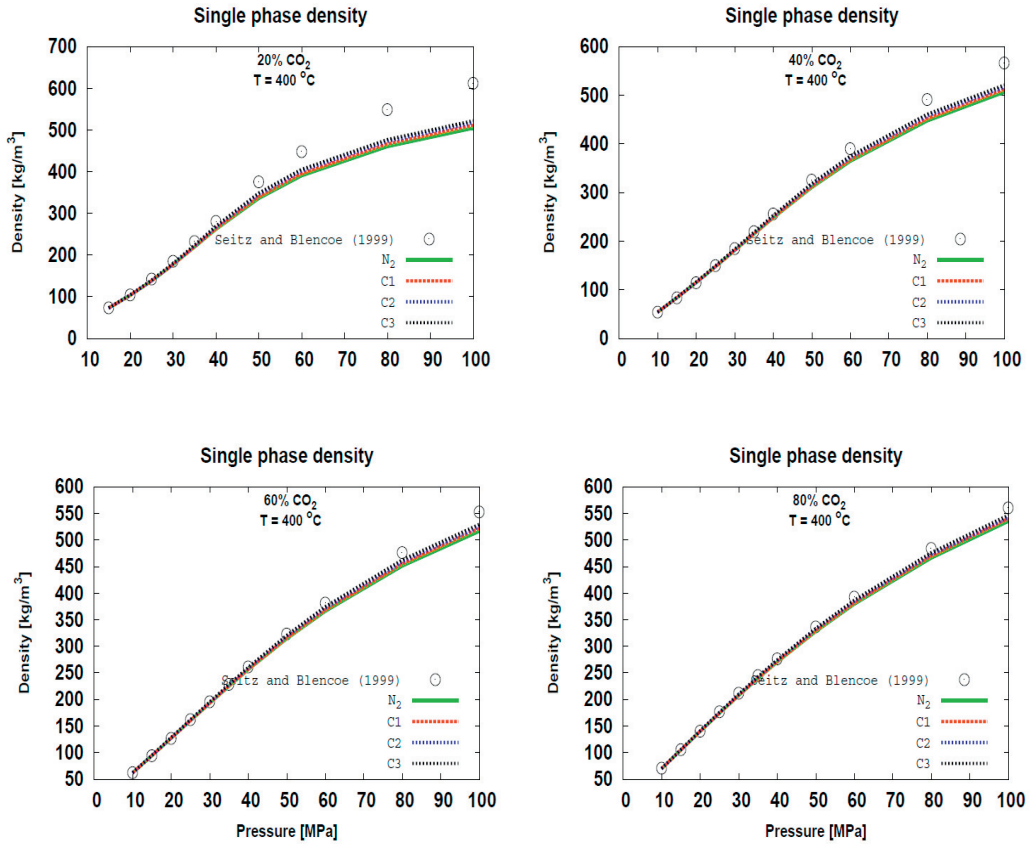
Figure 1: Density predictions using $N_2$, C1, C2, and C3 in comparison with experimental data set of Seitz and Blencoe (1999) [10] over pressure, at mole fractions of 20, 40, 60, and 80% of $CO_2$, and a temperature of 400 ºC.

together with C3, the heaviest among the initially tested reference fluids, are shown in Fig. 3 in comparison with the experimental data. The REs of propane and normal butane are compared in Fig. 4. Except for the case of 80% $CO_2$, the results show the same behavior, where that normal butane as a heavier reference fluid predicted the density of the $CO_2$ mixture better than propane did. However, the improvement was very small, which did not suggest butane as an ultimate alternative to propane in solving the investigated problem. Therefore, a more comprehensive study in the guidance of the trend observed from the results need to be conducted to find the optimal reference fluid for modeling $CO_2$-water using ECS.
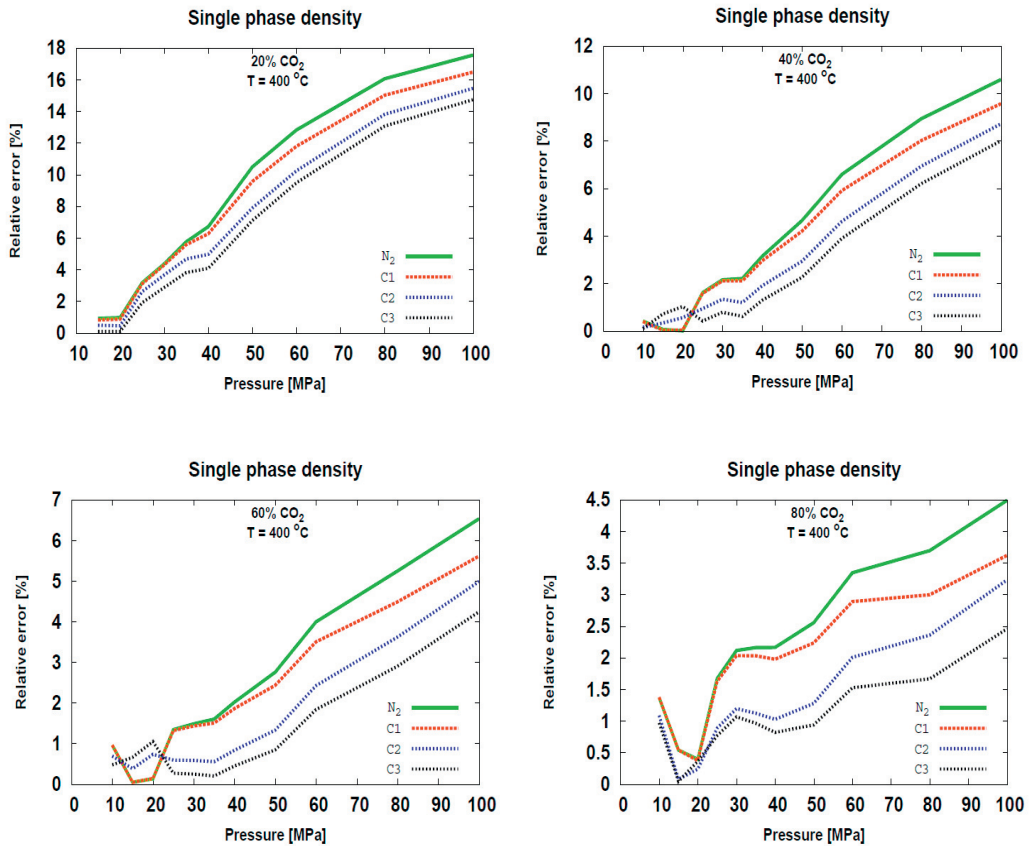
Figure 2: The relative error in density predictions using $N_2$, C1, C2, and C3 over pressure, at mole fractions of 20, 40, 60 and 80% of $CO_2$, and a temperature of 400 °C.

#### 4.1.1. Vapour Liquid Equilibrium predictions

The predictions of the $CO_2$-water mutual solubility at moderate pressures were computed using $N_2$, C1, C2, C3 and NC4 as reference fluid. The solubility predictions compared with experimental data of Bamberger et al. [12] are plotted in Fig. 5. Top right and left are the $H_2O$ and $CO_2$ solubilities, respectively. Below each solubility plot, the corresponding REs are plotted in the same Fig. 5.

From the results in Fig. 5 it was observed that there was no certain trend according to how heavy the reference fluids is in similarity to the density calculations. The improvement and deterioration between a reference fluid and the other might have come from the accuracy of the reference equation with respect to each of them. Besides the non-trendy behavior, the errors were extremely high which imply that the overcome of this VLE inaccuracy problem will require a different type of solution. Nevertheless, these results imply the need for parameter regression of binary interaction coefficients specifically for the choice of reference fluid. As the impact of the reference fluid is excluded, the VLE error is thought to be mainly due to the use of the SRK geometric averaging mixing rule for the shape
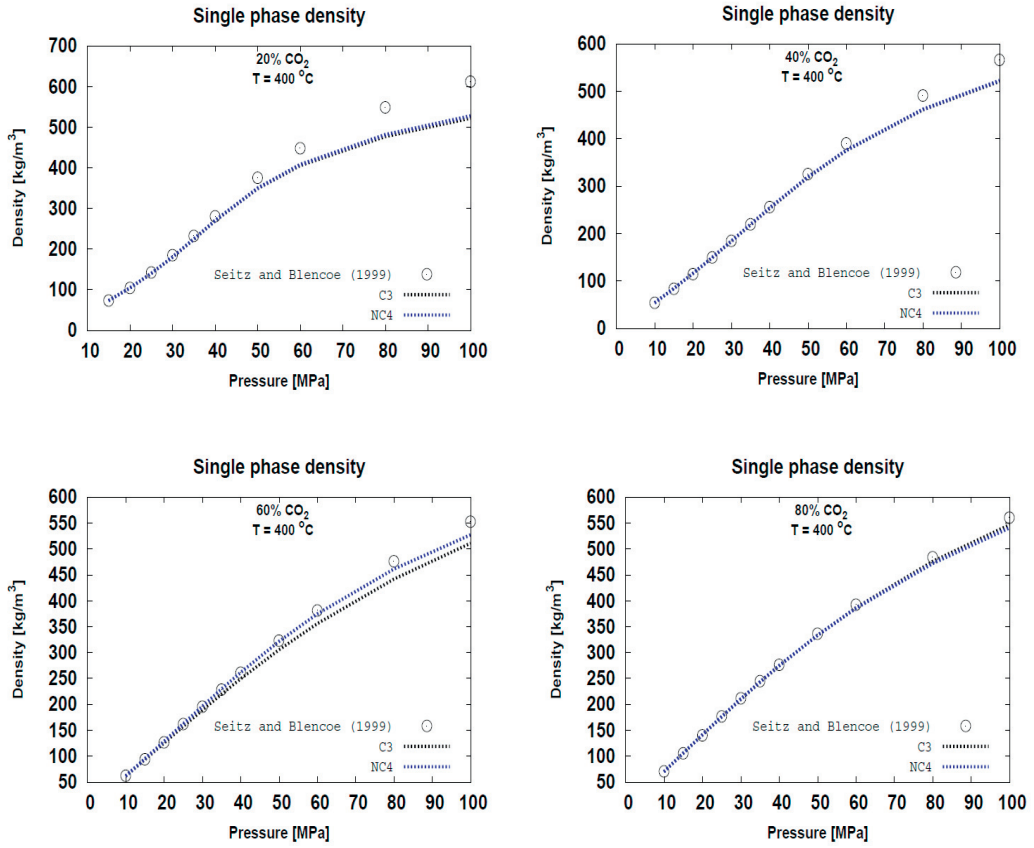
Figure 3: Density predictions using C3, and NC4 in comparison with experimental data set of Seitz and Blencoe (1999) [11] over pressure, at mole fractions of 20, 40, 60 and 80% of $CO_2$, and a temperature of 400 ºC.

factors computations. Therefore doing the shape factor scaling with a mixing rule more adequate of dealing with polar mixtures could improve the VLE predictions.
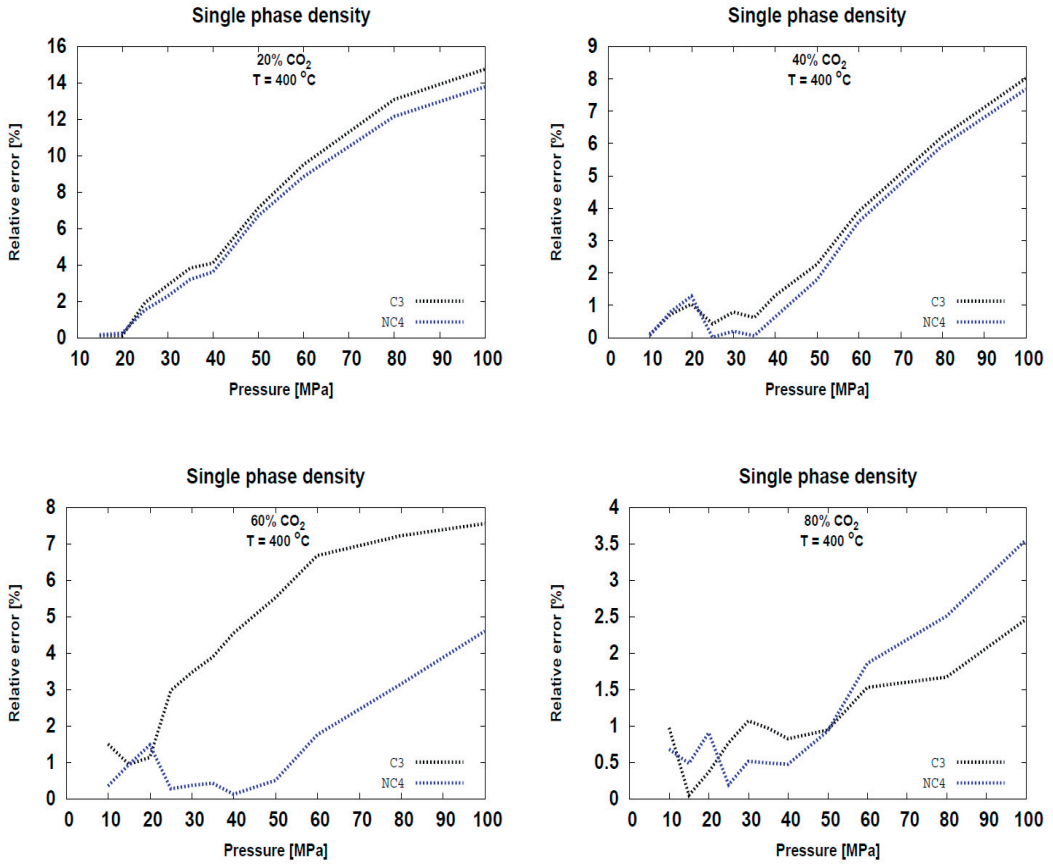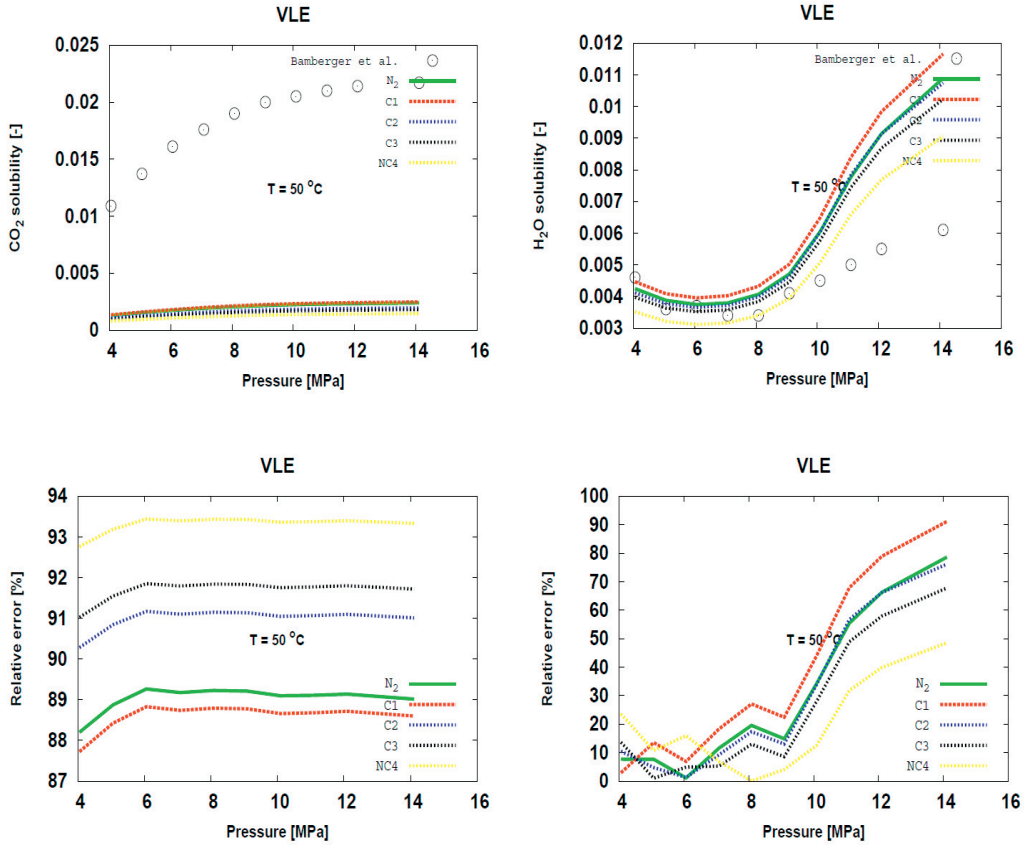
Figure 4: The relative error in density predictions using C3, and NC4 over pressure, at mole fractions of 20, 40, 60 and 80% of $CO_2$, and a temperature of 400 ºC

Figure 5: The solubility predictions and relative errors using $N_2$, C1, C2, C3 and NC4 over pressure, at a temperature of 50 °C. Top left and right are the $CO_2$ and $H_2O$ solubility respectively, in comparison with the experimental data of Bamberger et al. [12]. Bottom is the corresponding relative errors.

## 5. Conclusions

In this work the sensitivity of the density and VLE predictions to the choice of reference fluid used for modelling $CO_2/H_2O$ systems using the SPUNG EoS was studied.

The results showed that the heavier the reference fluid was, the larger the range of densities the EoS can represent. In this case, within the set of hydrocarbons, the heavier the reference fluid was, the better the method predicted the densities. This implies that the SPUNG Eos has a potential for improving the density predictions by using other reference fluids than propane. Further work is undergoing investigating the best reference fluid and reference

equation for this system.

The results also showed that the choice of reference fluid had small impact on the predictions of the VLE solubilities. For VLE, how the interaction between $CO_2$ and water is described (mixing rules) plays a more significant rule that the choice of reference fluid. Further development of SPUNG mixing rules for this system is required.

**Acknowledgements**

**References**

[1] Jørstad, O. Equations of state for hydrocarbon mixtures. Dr. Ing. Thesis No. NTH 1993:92. Norwegian Institute of Technology, Trondheim, Norway. 1993.
[2] Wilhelmsen, Ø., Skaugen,G., Jørstad, O., Li, H. Evaluation of SPUNG and Other Equations of State for Use in Carbon Capture and Storage Modelling, Energy Procedia*, 2012; 23: 236 - 45.
[3] Soave, G. Equilibrium constants from a modified Redlich-Kwong equation of state. Chem. Eng. Sci.  1972;27(6): 1197 – 1203.
[4] Huron, M.J., Vidal, J. New mixing rules in simple equations of state for representing vapour-liquid equilibria of strongly non-ideal mixtures. Fluid Phase Equilib. 1979; 3(4): 255 – 271.
[5] Ibrahim, M., Skaugen, G., Ertesvåg, I.S. Preliminary Evaluation of the SPUNG Equation of State for Modelling the Thermodynamic Properties of $CO_2$-Water Mixtures. Energy Procedia. 2012; 26: 90-97
[6] Peng, D.Y., Robinson, D.B. A new two-constant equation of state. Ind. Eng. Chem. Fundam. 1976;15(1): 59–64.
[7] Kunz, O., Klimeck, R., Wagner, W., Jaeschke, M. The GERG-2004 Wide-Range Equation of State for Natural Gases and Other Mixtures, 2007. GERG TMIS, VDI Verlag, Düsseldorf, Germany.
[8] Span, R., Wagner, W. A new equation of state for carbon dioxide covering the fluid region from the tripple-point temperature to 1100 K at pressures up to 800 MPa. J. Phys. Chem. Ref. Data. 1996;25(6): 1509–1596.
[9] Chapman, W.G., Gubbins, K.E., Jackson, G., Radosz, M. New reference equation of state for associating liquids. Ind. Eng. Chem. Res. 1990; 29(8): 1709–1721.
[10] Younglove, B.A., Ely, J.F. Thermophysical properties of fluids: II. Methane, ethane, propane, isobutane, and normal butane. J. Phys. Chem. Ref. Data. 1987; 16(4): 577–798.
[11] Seitz, J.C., Blencoe, J.G. The $CO_2$-$H_2O$ system. I. Experimental determination of volumetric properties at 400ºC, 10-100 MPa. Geochim. Cosmochim. Acta. 1999; 63(10): 1559 – 1569.
[12] Bamberger, A., Sieder, G., Maurer, G. High-pressure (vapor+liquid) equilibrium in binary mixtures of (carbon dioxide+water or acetic acid) at temperatures from 313 to 353 K. J. Supercrit. Fluids. 2000; 17(2): 97 – 110.

# PAPER III

CHEMICAL
ENGINEERING
SCIENCE

CrossMark

# Modeling CO₂–water mixture thermodynamics using various equations of state (EoSs) with emphasis on the potential of the SPUNG EoS

Mohamed Ibrahim [a,*], Geir Skaugen [b], Ivar S. Ertesvåg [a], Tore Haug-Warberg [c]

[a] Department of Energy and Process Engineering, Norwegian University of Science and Technology, Kolbjørn Hejes veg 1B, NO-7491 Trondheim, Norway
[b] SINTEF Energy Research, Trondheim, Norway
[c] Department of Chemical Engineering, Norwegian University of Science and Technology, Trondheim, Norway

## HIGHLIGHTS

- SPUNG equation of state (EoS) was evaluated for modeling CO₂–water thermodynamics.
- The evaluation is done by comparing with experimental data and to two other EoS.
- The single and two phase density, saturation line, and mutual solubility were modeled.
- The density results showed high accuracy using SPUNG in general.
- Yet the accuracy of SPUNG was low for some conditions, and potential for improvement was investigated.

## ARTICLE INFO

## ABSTRACT

CO₂–water is a very important mixture in the Carbon Capture and Storage (CCS) industry. The mixture can have a broad range of concentrations, from water as an impurity in CO₂ transport to high water concentrations in sequestration processes. CO₂–water mixture is challenging due to the polar nature that induces difficulties describing the interaction between CO₂ and water when modeling the behavior. The work focuses on the evaluation of the predictability of the extended corresponding state equation SPUNG in dealing with CO₂–water thermodynamics. The evaluation is done by comparing the behavior of SPUNG equation of state (EoS) to experimental data, and two other EoSs of a different class. The two other EoSs are the cubic equation Soave–Redlich–Kwong (SRK) with van der Waals mixing rules, and SRK with Huron–Vidal mixing rules.

The predictability of the single and liquid rich phase densities, two-phase solubilities and dew line is investigated over a wide range of pressures, temperatures and mixture compositions. The results show better density prediction using SPUNG EoS over all the evaluated conditions compared to SRKs with a potential of improvements by changing the reference fluid. However, the CO₂ solubility prediction using SPUNG requires the use of other mixing rules that can account for the polar nature of the system.

© 2014 Elsevier Ltd. All rights reserved.

## 1. Introduction

Through the various CCS processes, CO₂ exists in mixtures with various impurities like CH₄, CO, H₂O, H₂S, N₂, NO₂ and O₂. Therefore, the knowledge of the thermophysical properties of those mixtures is a key challenge for accurate design of efficient and secure processes. Hendriks et al. (2010) pointed out the need for accurate thermophysical properties.

Even in the cases where experimental data exist for a mixture, they are discrete and local in nature, and more continuous and generic solutions are rather practical. Consequently, the modeling of the thermodynamic properties for pure CO₂ and CO₂ mixtures is a very important aspect for the analysis and detailed simulation of CCS processes. Indeed, the choice of models may have a great impact on the decisions about process design, energy efficiency, economy and safety.

A computationally cheap modeling strategy is to empirically fit experimental data. This solution has a poor generality to different mixtures and for different phases and intervals outside the fitted range. A more physically profound and rather general and continuous approach is the use of Equations of State (EoSs), which will

be discussed more in detail in the following section. There is a large variety of EoSs at various levels of sophistication. Cubic EoSs like Soave–Redlich–Kwong (SRK) (Soave, 1972), SRK with Huron Vidal mixing rules (SRK-HV) (Huron and Vidal, 1979) and Peng–Robinson (PR) (Peng and Robinson, 1976) are among the simplest. Multi-parameter approaches like Span–Wagner (Span and Wagner, 1996) for pure $CO_2$ and GERG (Groupe Européen de Recherches Gaziéres) (Kunz et al., 2007) for mixtures are at least one order of magnitude higher in computational time. The full methods of extended corresponding states like those implemented in the REFPROP library of the National Institute of Standards and Technology (NIST) (Lemmon et al., 2010) are even more expensive than the multi-parameter approaches. Among the state-of-the-art approaches are the Cubic-Plus-Association (CPA) (Kontogeorgis et al., 1996) and the Statistical Associating Fluid Theory (SAFT) (Chapman et al., 1990) EoSs. Tsivintzelis et al. (2011) and Diamantonis and Economou (2012) demonstrated the success of the CPA and Perturbed Chain SAFT (PC-SAFT), respectively, in modeling the polar mixtures including $CO_2$–water. The two mentioned articles included reviews of the development of CPA and SAFT, and their different modifications and combinations.

The level of sophistication and generality usually has a direct relation to accuracy and computational complexity and, consequently, a trade-off arises. While the accuracy of a model is of higher importance than the computational efficiency for the process analysis, the computational complexity has a significant effect on the cost and feasibility of a CFD simulation. Three other dimensions of the challenge of developing or selecting a model are the generality with respect to different fluids and mixtures, consistency, and numerical stability when using it in conjunction with CFD simulations.

A consistent approach that is not well known but has shown a very good compromise in accuracy and computation time for hydrocarbons is the SPUNG EoS (Jørstad, 1993). The SPUNG EoS was not published outside Jørstad thesis before the work of Wilhelmsen et al. (2012). The latter demonstrated that SPUNG is a very good compromise for $CO_2$ with some non-polar binary and ternary impurities. They showed that for the calculations of density, enthalpy and entropy over a 10 000 random conditions in different phase regions, and for three component $CO_2$ mixtures, SPUNG run time was 4 times and GERG was 40 times to that of SRK. The work also showed that the SPUNG EoS accuracy was generally high and close to GERG and Span–Wagner for pure species as references. These results of computational time were only for single phase including critical and near critical conditions, since flash results would strongly depend on algorithmic implementation.

Since generality is a critical aspect when selecting a model to be used for CFD, this work aims to study the behavior of the SPUNG EoS for the polar mixture of $CO_2$ and water. The study of the SPUNG EoS generality with respect to $CO_2$–water mixtures is of particular importance because these mixtures exist commonly in the range of processes in CCS industry. Moreover, they are very challenging mixtures due to the polar nature. A preliminary study was conducted by Ibrahim et al. (2012) that covered a few conditions that exist in CCS. The study presented here is to extend the evaluation over a wide range of conditions, compositions, temperatures, pressures that might occur in various CCS processes. Consequently, this study can be used as a comprehensive visualized analysis of the behavior and the errors of each EoS at this wide range of conditions.

The study aims mainly to investigate the shortcoming and capabilities of SPUNG EoS when dealing with $CO_2$–water. Furthermore, the work investigates the impact of the EoS used for the shape factors scaling, and the choice of the reference fluid on the predictability and limitations of the method. In addition, the study

aims to investigate the potential and possibilities of improvement for SPUNG EoSs.

Here, an evaluation is done by comparing the behavior of SPUNG to two other EoSs and with experimental data. The two EoSs are the cubic equations SRK with the van der Waals mixing rule (Soave, 1972) and SRK-HV (Huron and Vidal, 1979).

The SRK-HV was used because it showed very good results for the solubility predictions for the investigated mixtures as reported by Austegard et al. (2006). Furthermore, the classical SRK was chosen because SPUNG uses it for computing the shape factors and because it is a simple model and is commonly used in industry.

In this work, the predictability of single phase densities, dew lines, mixture solubilities in two-phase, and rich densities will be evaluated.

## 2. Theory

### 2.1. Equations of state

An EoS is a model that calculates for both the liquid and the gas phase using the same expression. This enhances the continuity near the critical point. An EoS for an $N_c$ component mixture can be regarded as an expression for pressure $P$ as a function of the mole fractions $x_i$, the temperature $T$ and the volume $V$. Given this expression, it can be manipulated to calculate the fugacity of each component. In the following subsections, a brief description of the equations of state used in the work will be given together with references for further discussions.

### 2.2. The SRKs EoSs

The classical SRK model used here (Soave, 1972) is a cubic EoS that uses van der Waals mixing rules.

The SRK-HV model, proposed by Huron and Vidal (1979), is an improvement from the classical SRK, as it derives a definition for the mixing rules from the excess Gibbs energy at infinite pressure. A detailed description of that model has been given by Solbraa (2002). The SRK-HV implementation used in this work has parameters regressed over a wide range of $CO_2$–water data, and the regression work is described in detail by Austegard et al. (2006). The SRK-HV evaluated in this work uses the Twu–Bluck–Cunningham (TBC) (Twu et al., 1991) formulation for computing the alpha parameter.

### 2.3. The corresponding states principle

The principle of corresponding states assumes that all substances exhibit the same behavior at a reduced state. A corresponding state EoS typically has one or more reference components described very accurately by a reference EoS. Therefore, the compressibility of the investigated fluids or mixtures can be evaluated as $Z = Z(V_{Ref}, T_{Ref}, \omega, \ldots)$. In the corresponding states approach, the reference fluid volume $V_{Ref}$ and temperature $T_{Ref}$ are, respectively, the reduced volume and temperature, $V_R$ and $T_R$, of the fluid or the mixture investigated.

### 2.4. The extended corresponding states principle

#### 2.4.1. Basic concept

In the extended corresponding states concept, the mapping between the investigated fluid or mixture $T$ and $V$ and the reference fluid $V_{Ref}$ and $T_{Ref}$ is done via the shape factors $\theta$ and $\phi$. These shape factors take into account how the fluids or the mixture in consideration differ from the reference fluid, where $T_{Ref} = T/\theta$ and $V_{Ref} = V/\phi$. The shape factors $\theta$ and $\phi$ can be

computed via shape factor functions, using semi-empirical functions, an accurate reference equation for each component, or using a simpler EoS. The work on shape factor functions started as early as 1968 by Leach et al. (1968). Subsequently, many contributions were made, examples are the work by Fisher and Leland (1970) and of Ely (1990). The Latter has introduced the first exact shape factor concept. One of the most recent works on shape factor functions was conducted by Estela-Uribe and Trusler (1998). The computation of exact shape functions is computationally very expensive, which is why the concept was left behind and thought to be impractical for use with numerical simulations. However, several implementations of the concept of extended corresponding states use simpler equations of state to compute shape factors, which show a good compromise between accuracy and computation time.

### 2.4.2. The SPUNG EoS

The SPUNG EoS investigated here is an instance of the extended corresponding states approach, which was enlightened by the work of Mollerup (1980) and developed first for hydrocarbons. The SPUNG EoS uses the cubic SRK EoS to calculate the shape factors and propane as a reference fluid. Furthermore, it uses the accurate modified Benedict–Webb–Rubin (MBWR) (Younglove and Ely, 1987) EoS for the reference fluid. The SPUNG EoS is described more in detail in the doctoral thesis by Jørstad (1993). It was developed for low temperature hydrocarbon mixtures, and it has improved density and enthalpy prediction while maintaining a good compromise in computational expenses. Propane was chosen as the reference fluid to ensure that the reduced temperature of the considered mixtures would always be above the reduced triple point of the reference fluid in order to avoid extrapolation of the reference equation. For $CO_2$ mixtures the choice of a different reference fluid and equation should be considered, but in this work only the original SPUNG EoS formulation was used.

## 3. Methodology

### 3.1. Numerical tools

The NTNU-SINTEF in-house thermodynamic library was mainly used for the study presented. The library is a tool for predicting the thermodynamic properties using various approaches that ranges in level of sophistication and underlying theory. The SRK-HV model used here was the one described by Austegard et al. (2006) and with the regressed coefficients listed there. The library uses a tolerance of $10^{-4}$ for both the multi-phase flash algorithm and the compressibility factor calculations.

### 3.2. Setup of the investigation

### 3.2.1. Single phase density predictions, low to moderate pressures

The three EoSs were evaluated at a set of low to moderate pressures (up to 100 bars) that ensured a single phase at given temperatures and water concentrations in the mixture. The pressures, levels of temperature and water concentrations were chosen to enable comparison with the experimental work of Patel and Eubank (1988). Four concentrations of 98, 90, 75 and 50% $H_2O$ were evaluated. The concentration of 98% was evaluated at the temperatures of 225, 200, 100 and 50 °C. The 90% was evaluated at 200, 100 and 71 °C, the 75% was evaluated at 225, 200, and 100 °C, and finally the 50% was evaluated at 225, 200 and 125 °C. It was clear that, as the $H_2O$ concentration increased in the mixture, it was not possible to go to some low temperatures while maintaining the mixture in gaseous phase conditions. This explains the

differences in the lower bound of the evaluated temperatures at the four studied concentrations.

### 3.2.2. Single phase density predictions, high pressures

A more challenging set of conditions at elevated pressures over a wider range of concentrations was evaluated. The set of concentrations ranged from $CO_2$ dominant (90%) to $H_2O$ dominant (90%). The pressures varied from 10 to 100 MPa. All experiments were conducted at a temperature of 400 °C. The evaluated conditions were chosen to enable comparisons with the experimental data of Seitz and Blencoe (1999).

### 3.2.3. Dew line prediction

The dew lines were evaluated at five different concentrations of 2, 5, 10, 25 and 50% $H_2O$. The pressures were chosen to comply with the work done by Patel et al. (1987), and the dew temperatures were then computed dependently.

### 3.2.4. Rich phases density predictions

The EoSs were evaluated at four sets of data provided by King et al. (1992), Chiquet et al. (2007), Hebach et al. (2004) and the validated predictions by Bikkina et al. (2011). King et al. (1992) provided only water-rich liquid-phase densities between 6 and 24 MPa at three temperatures of 15, 20, and 25 °C co-existing with $CO_2$−rich liquid phase. The 15 and 25 °C test sets were chosen for the analysis here. Chiquet et al. (2007) provided densities of both water-rich and $CO_2$−rich phases when $CO_2$ were at supercritical conditions. The set of data covered pressures from 5 to 45 MPa, and the selected sets of temperatures were about 35, 50, 90 and 110 °C. The work done by Hebach et al. (2004) was used for comparisons of water-rich liquid phase densities co-existing with $CO_2$−rich gas phase. The selected cases were at temperatures of 19, 29, 39 and 49 °C and pressures less than 5 MPa to ensure a gaseous $CO_2$−rich phase. The results of Chiquet et al. (2007) and Hebach et al. (2004) were measured at temperatures slightly around the listed values, although precisely fixed for each point. The simulations conducted here use the exact measurements temperature nodes. The group of Bikkina et al. (2011) provided validated predictions that cover the missing rich phases density of $CO_2$−rich liquid and the co-existing water-rich liquid densities and $CO_2$−rich gaseous phase. The selected Liquid Liquid Equilibrium (LLE) data of Bikkina et al. (2011) went over pressures between 8 and 21 MPa at one temperature of 25 °C. Finally, the Vapor Liquid Equilibrium (VLE) data went over pressures between 1 and 6 MPa at four temperatures of 25, 40, 50 and 60 °C.

### 3.2.5. Solubilities

The accuracies of the SPUNG and SRKs EoSs in predicting the mutual solubilities of $CO_2$ and $H_2O$ were validated against experimental data. Pappa et al. (2009) reviewed the experimental data of $CO_2$–water system solubilities and recommended six sets of mutual solubilities experimental data for model regression and validations. The six sets were of Takenouchi and Kennedy (1964), Wiebe (1941), Bamberger et al. (2000), Valtz et al. (2004), Mueller et al. (1988), and King et al. (1992). For this work we replaced King et al. (1992) with the recent Hou et al. (2013), which covered the available intermediate pressures data available in the literature at various temperatures and filled in some gaps. The latter work also validated the new data against the available literature data and showed very good match. Takenouchi and Kennedy (1964) provided solubilities at very high pressures, ranging between 10 and 70 MPa at a temperature of 110 °C. The study of Wiebe (1941) covered pressures between 1 and 70 MPa and temperatures between 25 and 100 °C. Here, however, we present only the results at 50 and 75 °C since mutual solubilities were provided

only at these two temperatures. Bamberger et al. (2000) provided data over moderate pressures between 4 and 14 MPa at three temperatures of 50, 60 and 80 °C. The set of experimental data by Valtz et al. (2004) covered very low pressures at three temperatures of approximately 5, 25 and 45 °C. For the low temperature of 5 °C, the pressures ranged approximately between 0.5 and 1 MPa, the range went wider as the temperature increased reaching approximately the range of 0.1–7 MPa at the temperature of 45 °C. The set by Mueller et al. (1988) provided solubility data at low pressures and high temperatures between 100 and 200 °C. The last set of experimental data by Hou et al. (2013) covered a wide range of data for pressures around 1–17.5 MPa, and over temperature range of 25–175 °C.

### 3.2.6. Sensitivity to the interaction parameter $K_{ij}$

The SPUNG EoS uses the SRK EoS for computing the shape factors and SRK EoS uses the symmetric interaction parameter $K_{ij}$ for computing the mixing coefficients. Therefore, we performed a simple sensitivity study on the effects of tuning $K_{ij}$ on the results. The tuning was done by matching the $CO_2$ solubilities as good as possible and letting the density and $H_2O$ solubility be computed accordingly. The results of the tuning for the evaluated cases are plotted and labeled as *SPUNG-Reg $K_{ij}$* in the following.

### 3.2.7. Reference fluid sensitivity

An examination was conducted for the impact of using other reference fluids on the density predictions of the water-rich liquid phase. $N_2$, $O_2$, ethane (C1), methane (C2), iso-butane (IC4) and normal-butane (NC4) were used as a reference fluid for this study as an alternative to the originally used propane (C3). The aim of this part of the analysis was to find a criterion of selection or to search for the proper reference fluid to model $CO_2$–water mixtures.

### 3.3. Error definition

The errors of an EoS are measured here by the Relative Error (RE) and the Average of Absolute Deviation (AAD) defined for an arbitrary variable $C$ as

$$RE(C_r, \%) = \frac{|C_{s,r} - C_{\exp,r}|}{C_{\exp,r}} \times 100 \qquad (1)$$

and

$$AAD(C, \%) = \frac{100}{N} \times \sum_{r=1}^{N} \frac{|C_{s,r} - C_{\exp,r}|}{C_{\exp,r}} \qquad (2)$$

Here, $N$ is the total number of points, subscripts s and exp refer to simulation data and experimental data, respectively, and $r$ is a point index.

## 4. Results

### 4.1. Single phase density, high pressures

The comparisons among the three EoSs for the high-pressure data sets of Seitz and Blencoe (1999) are plotted in Figs. 1 and 2. The former shows the density changes over pressures for various $CO_2$ contents in the mixture, while the latter is an interesting re-plot of the data as density changes over molar fraction of $CO_2$ for the various pressures.

### 4.2. Single phase density, low to moderate pressures

A comparison among the three EoSs for the low pressure data sets of Patel and Eubank (1988) are plotted in Fig. 3 for 2% $H_2O$ and a temperature of 225 °C. Results for the three other temperatures of 50, 100 and 200 °C were virtually similar to those shown for 225 °C. Furthermore, the models were compared to experimental data for the concentrations of 10% $H_2O$ at temperatures 71, 100, 200 and 225 °C, for 25% $H_2O$ at 100, 200 and 225 °C and for 50% $H_2O$ at 125, 200 and 225 °C. For all these series of density variation with pressure, the errors were tiny and showed no significant dependency on temperature.

### 4.3. Dew line

The dew line predictions of SPUNG, SRK and SRK-HV are shown in Fig. 4 for three of the datasets from Patel et al. (1987). For another two datasets, 25% and 50% $H_2O$, the computed results matched the experimental data as good as for 10%, or better. At the compositions of 10% & 25% $H_2O$ all the EoSs predicted pseudo-critical pressures lower than the highest pressure of the experiments. SRK-HV predicted 8.045 and 9.394 MPa pseudo-critical pressures, and SRK predicted 8.161 and 9.55 MPa for the two compositions. Since SPUNG uses the SRK algorithm to calculate for the pseudo-critical quantities, it predicted the same pseudo-critical pressures as of SRK. Hence, the highest pressure point of the 10% $H_2O$ content from Patel et al. (1987) was not plotted. As seen in Fig. 4, the results showed an improvement of the EoSs predictions as the water content increased.

### 4.4. Rich phases density prediction

#### 4.4.1. $CO_2$-rich phases

The densities of the Supercritical Liquid Equilibrium (SGLE) of the $CO_2$−rich phase co-existing with a liquid water-rich phase were modeled, and the results are presented in comparison with the experimental data of Chiquet et al. (2007) in Fig. 5. The AADs
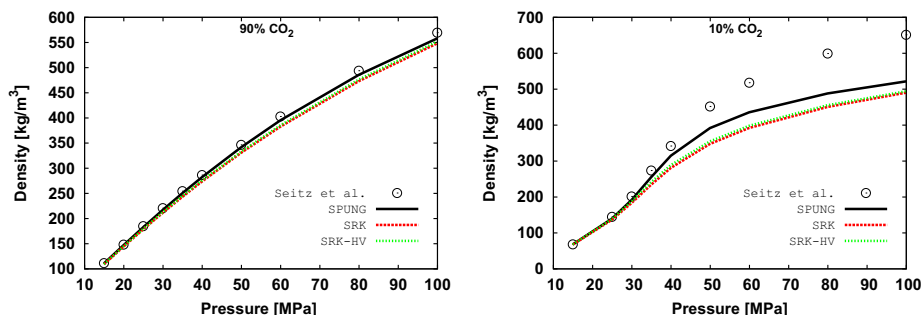


**Fig. 1.** Density computations in comparison with experimental data of Seitz and Blencoe (1999), over pressures up to 100 MPa at 90% and 10% $CO_2$ and a temperature of 400 °C.
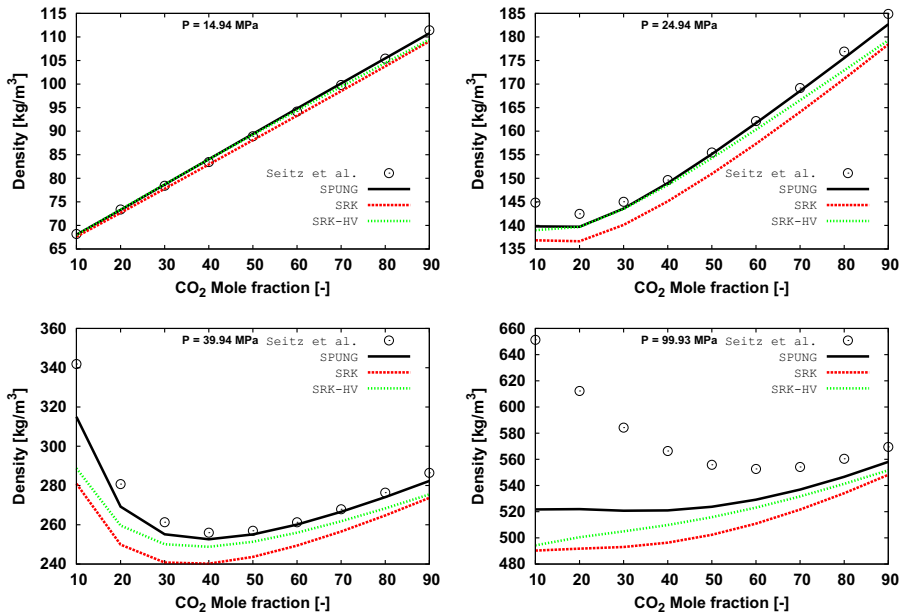
**Fig. 2.** Density computations in comparison with experimental data of Seitz and Blencoe (1999), over mole fractions of $CO_2$ at different pressures and a temperature of 400 °C.
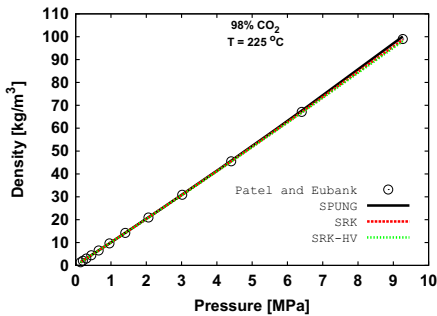


**Fig. 3.** Gas phase density calculations in comparison with experimental data of Patel and Eubank (1988) at 2% $H_2O$ and a temperature of 225 °C.

of the supercritical $CO_2$−rich phase density predictions are presented in Table 1.

From Fig. 5, two experimental points seemed to be anomalous: at 110 °C, 25 MPa and 90 °C, 7 MPa. These points deviated from the trend of each dataset, and the model errors jumped significantly. For the discussion, the AADs were recalculated without these two points in Table 1.

Model computations of the liquid $CO_2$−rich phase were compared with the predicted data of Bikkina et al. (2011) in Fig. 6. The corresponding AADs are included in Table 1.

For the gaseous $CO_2$−rich phase predictions (results are not plotted), errors compared with the data of Bikkina et al. (2011) were very small with all models and very similar to the single gas phase results. However, the values of the binary interaction parameter $K_{ij}$ used to get the proper $CO_2$ solubility decreased with increasing temperature. The used values were −1.44, −0.130, −0.115 and −0.107, respectively, for 25, 40, 50 and 60 °C. The AADs for the entire used dataset are included in Table 1. For the gaseous phase, the AADs reported were temperature averaged.

### 4.4.2. Water-rich liquid density prediction

The density predictions of the liquid water-rich phase co-existing with a supercritical $CO_2$−rich phase at a temperature of 35 °C are presented in comparison with the experimental data of Chiquet et al. (2007) in Fig. 7. The results for the temperatures of 50, 90 and 110 °C were very similar in trend. However, the $K_{ij}$ values used to get the proper $CO_2$ solubility decreased with temperature increase, where the used values were −0.132, −0.118, −0.068, −0.045 for the temperatures from 35 to 110 °C.

The results of the density predictions of the liquid water-rich phase co-existing with liquid $CO_2$−rich phase at a temperature of 25 °C are plotted in Fig. 8. The results of 15 °C behaved very similar to those at 25 °C and are not shown. The used $K_{ij}$ values were −0.15 and −0.14.

Density predictions of the liquid water-rich phase co-existing with gaseous $CO_2$−rich phase at a temperature of 29 °C are plotted in Fig. 9. The results of 19, 39 and 49 °C were very similar. The used $K_{ij}$ values were −0.154, −0.141, −0.129 and −0.118. Table 2 contains a summary of the results in terms of temperature averaged AADs.

As mentioned in Section 2.4.2, propane was chosen as the reference fluid in the SPUNG EoS. Table 3 shows the results from the reference fluid sensitivity study. The AADs are averaged over temperature. The C3 (propane) results were the same as shown for SPUNG in Fig. 9. Only one temperature out of the evaluated four was presented due to similarity in trends and uniformity of the errors. The curves of the REs showed almost equal slopes for the evaluated reference fluids (not shown). The difference in AADs is around 7% between using N2 and NC4 as a reference fluid.

### 4.5. Solubilities

The behavior of SPUNG, SRK and SRK-HV at low pressures and low temperatures was evaluated, and results in comparison to the work conducted by Valtz et al. (2004) are plotted in Fig. 10. The solubilities at 25.13 °C were also evaluated towards experimental
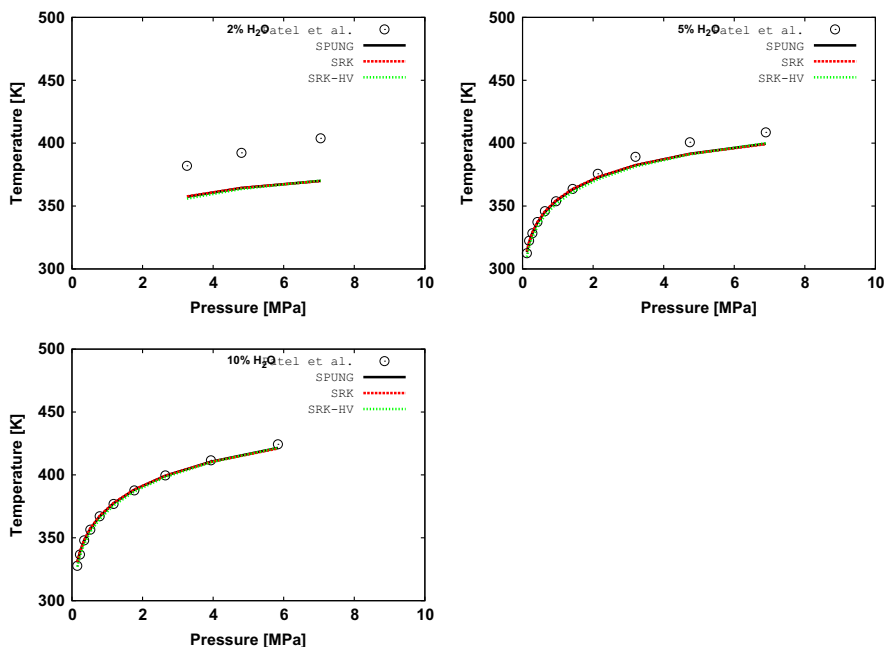
**Fig. 4.** Dew line temperature predictions in comparison with experimental data of Patel et al. (1987).
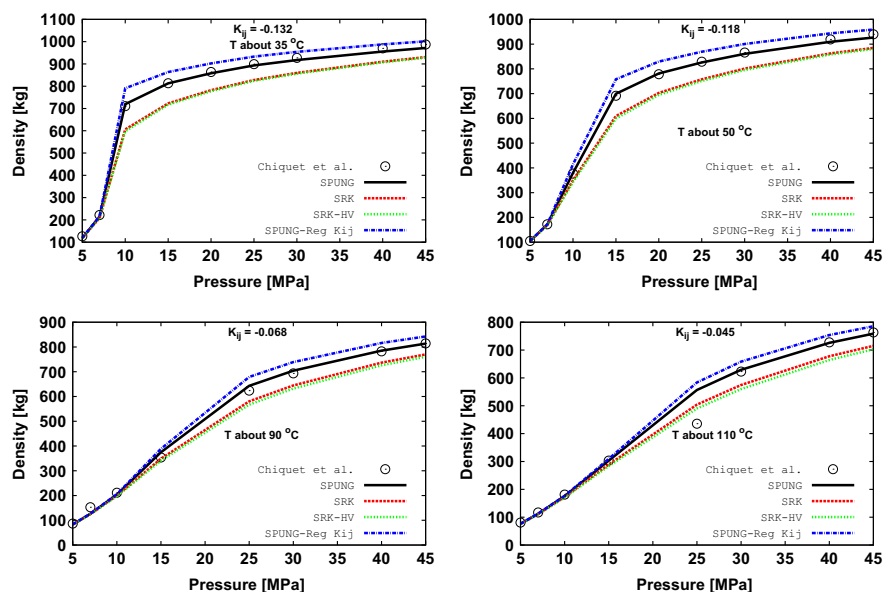


**Fig. 5.** SGLE $CO_2$−rich phase density predictions at temperatures of about 35, 50, 90 and 110 °C in comparison with Chiquet et al. (2007) experimental data.

data with results comparable to those shown. The AADs are presented in Table 4.

The results in comparison to the work conducted by Mueller et al. (1988) are plotted in Fig. 11. The results of the intermediate temperatures are not plotted, since the plotted ones are sufficient to show the trend. The AADs at 100, 140 and 200 °C are presented in Table 5.

The solubilities over moderate pressures were predicted by the three models at the temperatures of 50, 60 and 80 °C, which were chosen in consistency to the experimental work of Bamberger et al. (2000). Results are plotted in Figs. 12 and 13. The $CO_2$ solubility results at 50 and 60 °C turned out very similar to those shown at 80 °C. For $H_2O$ the 50 °C results were similar to those shown for 60 °C (Fig. 13), with some better match with

**Table 1**

AAD (%) of the $CO_2$−rich phases density calculations for the $CO_2$−water system at different $CO_2$ co-existing phases and temperatures.

| Data sets | Phase equilibrium | Temperature (°C) | SPUNG | SRK | SRK-HV | SPUNG-Reg $K_{ij}$ |
|---|---|---|---|---|---|---|
| Chiquet et al. (2007) | SGLE | 35 | 1.8 | 8.3 | 8.7 | 4.5 |
| | | 50 | 0.7 | 6.6 | 7.4 | 4.5 |
| | | 90 | 4.5 | 6.9 | 8.2 | 7.1 |
| | | 110 | 5.3 | 7.1 | 7.9 | 7.4 |
| | | 90[a] | 2.7 | 5.3 | 6.7 | 5.7 |
| | | 110[b] | 2.0 | 5.9 | 7.3 | 3.7 |
| Bikkina et al. (2011)[c] | LLE | 25 | 2.0 | 9.2 | 9.7 | 8.3 |
| Bikkina et al. (2011)[c] | VLE | | 0.6 | 0.3 | 0.3 | 0.7 |

[a] Without the anomalous point 7.5 MPa.
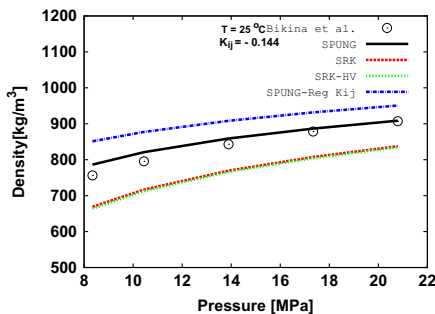[b] Without the anomalous point 25 MPa.
[c] Predicted data.



**Fig. 6.** LLE $CO_2$−rich phase densities prediction at a temperature of 25 °C in comparison to predictions of Bikkina et al. (2011).
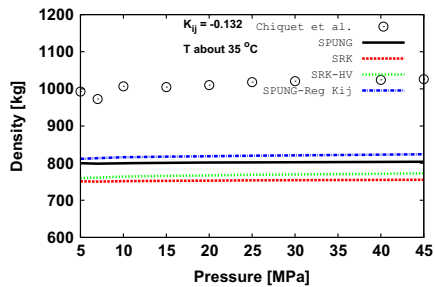


**Fig. 7.** Densities of the liquid water-rich phase co-existing with a supercritical $CO_2$−rich phase at a temperature about 35 °C in comparison with Chiquet et al. (2007) experimental data.

experimental data for SRK-HV. The AADs are presented in Table 6. A $K_{ij}$ sensitivity study was conducted over this set of conditions. The results showed that any improvement of $CO_2$ solubilities prediction causes a significant increase in the $H_2O$ solubility prediction errors for SRK and SPUNG EoSs.

The results of the comparisons to Hou et al. (2013) are plotted in Fig. 14. Graphs are included only at the lowest and highest temperatures, as these are sufficient to illustrate the trend.

The comparison with Wiebe (1941) is presented in Table 7. There were no compromise found for SPUNG EoS by tuning $K_{ij}$. The results showed that any improvement of $CO_2$ solubilities prediction causes a significant increase in the $H_2O$ solubility prediction errors for SRK, and SPUNG EoSs.
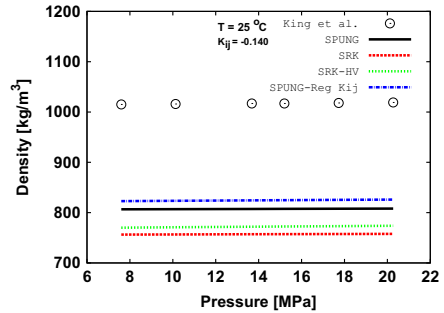


**Fig. 8.** LLE water-rich phase density predictions at a temperature 25 °C in comparison with King et al. (1992) experimental data.
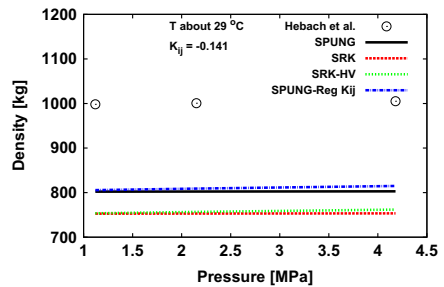


**Fig. 9.** Densities of the liquid water-rich phase co-existing with a gaseous $CO_2$−rich phase at a temperature about 29 °C in comparison with Hebach et al. (2004) experimental data.

**Table 2**

AAD (%) of water rich liquid phase densities averaged over the temperatures of each evaluated set of data.

| Data sets | Phase equilibrium | SPUNG | SRK | SRK-HV | SPUNG-Reg $K_{ij}$ |
|---|---|---|---|---|---|
| King et al. (1992) | LLE | 20.5 | 25.5 | 23.9 | 18.7 |
| Chiquet et al. (2007) | SGLE | 21.6 | 26.0 | 25.0 | 20.3 |
| Hebach et al. (2004) | VLE | 20.1 | 24.9 | 24.5 | 19.4 |

**Table 3**

AAD (%) of densities averaged over the temperatures of the comparison with Hebach et al. (2004) data using various reference fluids.

| Data set | Phase equilibrium | N2 | O2 | C1 | C2 | C3 | NC4 |
|---|---|---|---|---|---|---|---|
| Hebach et al. (2004) | VLE | 25.7 | 24.8 | 24.8 | 21.8 | 20.1 | 18.9 |

The evaluated EoSs were used to predict the mutual solubilities of $CO_2$ and $H_2O$ at very high pressures. The conditions were chosen in compliance with the work of Takenouchi and Kennedy (1964). Pressures from around 10 to 70 MPa were used for predictions at a temperature of 110 °C. The results are plotted in comparison with experimental data in Fig. 15. The errors are described in terms of AADs and presented in Table 8.

## 5. Discussion

### 5.1. Single phase and dew line prediction

Regarding dew line predictions or saturation conditions, Fig. 4 and results for higher $H_2O$ content showed that all the three EoSs
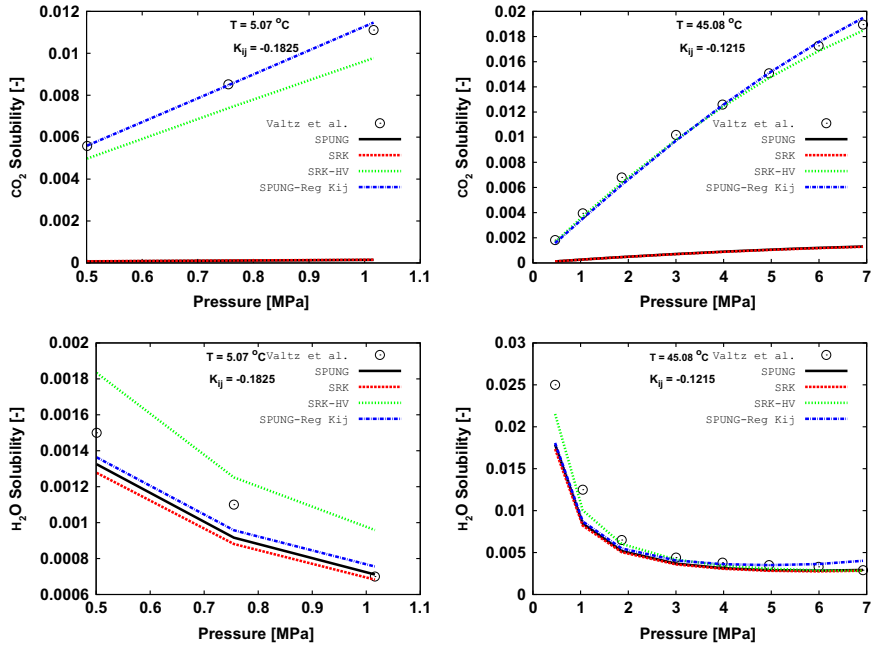
**Fig. 10.** $CO_2$ and $H_2O$ solubilities over low pressures and at temperatures of about 5 and 45 °C in comparison with Valtz et al. (2004) experimental data.

**Table 4**
AAD (%) of the solubility of $CO_2$ and $H_2O$ in comparison to Valtz et al. (2004).

| Component | Temperature (°C) | SPUNG | SRK | SRK-HV | SPUNG-Reg $K_{ij}$ |
|-----------|------------------|-------|------|--------|---------------------|
| $CO_2$ | 5.07 | 98.7 | 98.6 | 12.0 | 2.7 |
| | 25.13 | 96.8 | 96.7 | 8.8 | 5.5 |
| | 45.08 | 93.1 | 93.2 | 4.3 | 5.3 |
| $H_2O$ | 5.07 | 10.0 | 12.4 | 24.3 | 10.0 |
| | 25.13 | 17.8 | 20.8 | 8.3 | 17.0 |
| | 45.08 | 17.5 | 18.9 | 10.4 | 16.8 |

were behaving well in computing the saturation line. An exception is the case of 2% $H_2O$, which seems to be challenging for all the models. The simulations also showed that all the tested models predicted a low pseudo-critical pressure for the cases of 10% and 25% $H_2O$.

For low-pressure density calculations presented in Fig. 3, the densities comparison showed that the errors over the investigated intervals were on average very small for all the tested EoSs. Nevertheless, looking closely at the errors behavior, it was observed that the errors increased as the pressure increased and the mixture gradually departed from ideal behavior. The important observation was that the errors of SRK and SRK-HV grew steeply compared to that of the SPUNG EoS as the pressure went above a certain threshold in most of the cases. This behavior resulted in REs of SRK and SRK-HV that were multiples of that of SPUNG at the upper bound of the tested (pressure and $H_2O$) intervals. From the results of the high-pressure single-phase density calculations (Figs. 1 and 2), the comparisons showed an increase of the errors as the pressure increased and as the $H_2O$ content increased. While at low pressure the increase and the relative errors value were small, the errors jumped to an order of magnitude higher at the combination of the upper-bounds of both intervals.

The figures also show clearly that the errors behavior of SPUNG is much better than that of SRK and SRK-HV and, considering the computational expenses study by Wilhelmsen et al. (2012), it can be concluded that it is a good compromise between sophisticated and cubic EoSs.

Although the errors of SPUNG reached 20% at the extreme of the investigated conditions, the method has a possible high potential for improvement via using other reference fluids, while the SRKs do not have the same potential. Further research can evaluate this potential.

The inaccuracies of the used cubic EoSs are due to the simple structure of the models, which have very few parameters to tune. A study similar to the presented work but for other mixtures was made by Li and Yan (2009), who reported the same inaccuracies using SRK and other cubic equations for mixtures of $CH_4$, $H_2S$, $N_2$ and Ar. Furthermore, Li et al. (2011) reviewed several studies testing cubic equations for gas and liquid density predictions for other mixtures. In our investigation, the errors reached approximately 25% at the extreme conditions using cubic EoSs. This was higher than in the studies of other mixtures, emphasizing how challenging this particular mixture is for cubic EoSs compared to the other mixtures. In addition, this showed the need for a more predictive concept when dealing with $CO_2$–water mixture.

On the other hand, the SPUNG EoS superiority in density computations was inherited from the use of the 32-parameter MBWR reference equation, which is very accurate for propane. However, the errors of the SPUNG EoS came from the incapability of propane to achieve the high density of the $CO_2$–water liquid phase.

### 5.2. Rich phases density prediction

#### 5.2.1. $CO_2$–rich gas phase

The results of $CO_2$–rich gas phase showed that the accuracy of all the evaluated EoSs was very good. A high accuracy for gas
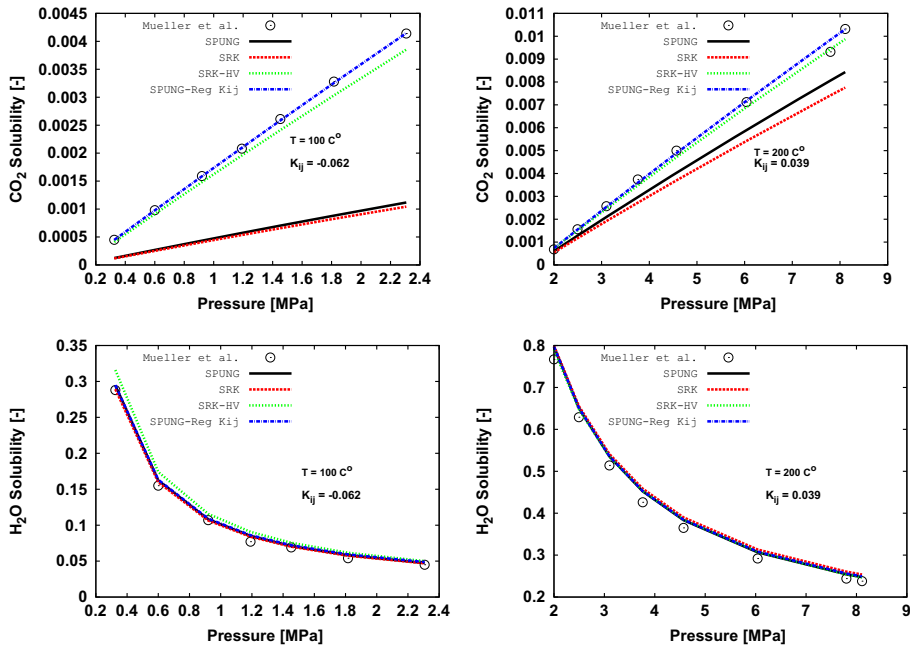
**Fig. 11.** $CO_2$ and $H_2O$ solubilities over low pressures and at temperatures of 100 and 200 °C in comparison with Mueller et al. (1988) experimental data.

**Table 5**
AAD (%) of the solubility of $CO_2$ and $H_2O$ in comparison to Mueller et al. (1988).

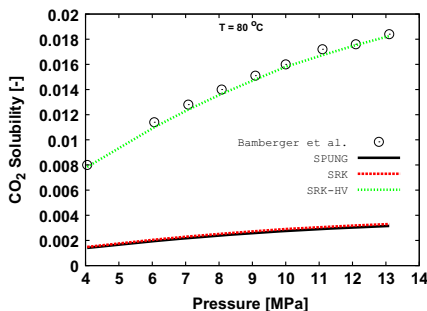| Component | Temperature (°C) | SPUNG | SRK | SRK-HV | SPUNG-Reg $K_{ij}$ |
|---|---|---|---|---|---|
| $CO_2$ | 100 | 72.8 | 74.5 | 7.2 | 0.5 |
| | 140 | 49.2 | 53.2 | 4.9 | 1.1 |
| | 200 | 17.0 | 24.2 | 4.5 | 2.8 |
| $H_2O$ | 100 | 4.9 | 3.6 | 11.8 | 6.3 |
| | 140 | 3.1 | 3.3 | 0.9 | 2.4 |
| | 200 | 4.5 | 6.1 | 4.4 | 4.9 |



**Fig. 12.** $CO_2$ solubilities over moderate pressures and at a temperature of 80 °C in comparison with Bamberger et al. (2000) experimental data.

phase density using cubic EoSs was reported in many studies that were listed in the review article of Li et al. (2011). Furthermore, the solubility of the $H_2O$ into $CO_2$−rich gas phase was too small to cause a challenge in modeling, as reported by Hebach et al. (2004).

*5.2.2. $CO_2$−rich liquid phase*
The results in Fig. 6 show that at the low pressure side, the errors of the SRKs were around 12% compared to 4% of SPUNG EoS. As the pressure went higher, the errors of all the EoSs became lower. However, the errors of SPUNG dropped to around 0.17 while the SRKs errors remained high at approximately 8%. This behavior was not revealed by the AADs in Table 1, which average the REs over the predicted interval to approximately 2% of SPUNG and 9% for SRKs.

*5.2.3. $CO_2$−rich supercritical phase*
As noted in Section 4.4.1, two measurement points (7 MPa, about 90 °C) and (25 MPa, about 110 °C) in Fig. 5 seemed to be anomalous. The deviation is seen for all the three evaluated models. Since the models are based on different theories, the anomaly suggested a measurement error. Alternatively, there might be a feature that is not captured by any of the models. At the two low evaluated temperatures, the predictions of SPUNG EoS were substantially better than those of the SRKs, especially in capturing the steep change in density over the pressures between 5 and 10 MPa at about 35 °C and between 5 and 15 MPa at about 50 °C, as observed in Fig. 5. In these two cases, the errors of SRKs jumped to around 15 and 13%, while the SPUNG errors were below 1.3%. Furthermore, the errors of the SRKs were reduced gradually as the density to pressure curve started saturating, while the errors of SPUNG remained low over the entire interval. Table 1 flattened out this behavior to AADs, which in their turns showed the high accuracy of SPUNG EoS prediction compared to SRKs EoSs. At the two evaluated high temperatures, the two mentioned points gave exceptional peaks in the error. Apart from this, the errors were similar to those of the lower temperatures, although the amplitude was much lower, and the RE distribution in general had a more flattened profile as the density increase with pressure
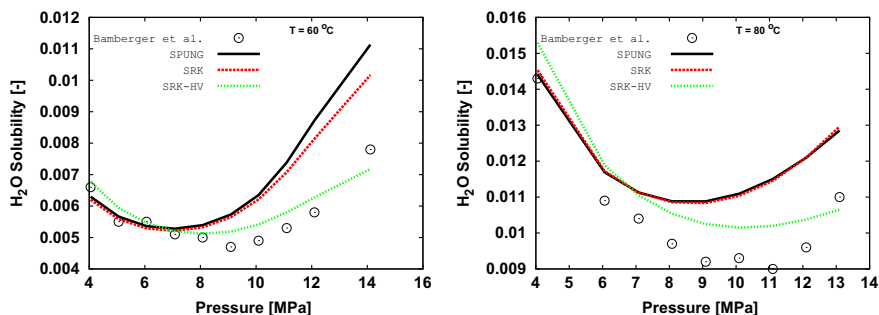
**Fig. 13.** $H_2O$ solubilities over moderate pressures and at temperatures of 60 and 80 °C in comparison with Bamberger et al. (2000) experimental data.

**Table 6**
AAD (%) of the solubility of $CO_2$ and $H_2O$ at different temperatures in comparison with Bamberger et al. (2000).

| Component | Temperature (°C) | SPUNG | SRK | SRK-HV |
|-----------|------------------|-------|------|--------|
| $CO_2$ | 50 | 91.8 | 91.7 | 2.1 |
|  | 60 | 88.9 | 89.2 | 1.3 |
|  | 80 | 82.8 | 81.9 | 2.0 |
| $H_2O$ | 50 | 18.2 | 24.9 | 4.2 |
|  | 60 | 20.5 | 17.1 | 6.2 |
|  | 80 | 15.0 | 15.1 | 8.4 |

was much more gradual at high temperatures than at the low temperature cases. The behavior of SPUNG remained superior, which can also be observed in the results summarized in terms of AADs in Table 1.

### 5.2.4. Water-rich liquid phase

The results in Fig. 7 and the results for other temperatures (not presented) showed that the errors of all the evaluated EoSs were considerable especially when compared to the results of Tsivintzelis et al. (2011) and Diamantonis and Economou (2012) for CPA and PC-SAFT, respectively. The errors were not very sensitive to temperature and pressure. This caused the RE profiles to be rather flat and made the AAD a very representative measure.

The capture of the temperature dependency was good. Furthermore, the insensitivity to both the pressure and co-existing phases was virtual as it was due to the incapability of all the EoSs to capture the high liquid-water density. This is regardless of how well the models capture the $CO_2$ solubility effect due to the increase in pressure. However, looking carefully to the SRK-HV slope in density-pressure behavior and the rather horizontal REs compared to the other evaluated EoSs, it could be observed that only SRK-HV captured the effect of $CO_2$ solubility as a function of pressure properly due to the superior prediction of $CO_2$ solubility using SRK-HV, which will be discussed below. This observation was supported by comparing the predictions of pure water at the same pressures and the one with $CO_2$ solubility, where SPUNG and SRK showed almost no difference in density predictions, whereas SRK-HV predicted the density difference accurately. This observation was not very clear from the first glance at the graphs, since the difference it made to capture the $CO_2$ solubility properly was of 1.5%, while the errors were above 20% for all the evaluated EoSs. Although SRK-HV predicted the deviation part correctly, SPUNG density prediction was superior to both SRKs, with a potential of improvement by using other reference fluids.

This discussion applies to the results of water-rich liquid phase co-existing with liquid and gaseous $CO_2$-rich phases in Figs. 8 and 9. Nevertheless, the difference in the case of water-rich liquid

co-existing with gaseous $CO_2$-rich phase was that the measured density had a slight increase with increased pressure, Fig. 9. This is due to the interfacial tension as reported by Hebach et al. (2004). The solubility was captured very good using SRK-HV. This can be observed in the inclination of the SRK-HV curve, which has the very similar slope as of the experimental data in the density results of Fig. 9.

An observation from Fig. 7 was that the point of 7 MPa seemed to deviate from the trend of the remaining points. Unless this was just an inaccuracy, the phenomenon was not captured by the models.

### 5.3. Solubilities

The results in Fig. 15 and Table 8 show that the predictability of SRK-HV for the solubility of $CO_2$ in water was much better than those of SRK and SPUNG EoSs and of low errors. The predictions by SPUNG and SRK were poor. On the other hand, the prediction of the $H_2O$ solubility by SRK-HV was much worse than that of SRK and SPUNG, where all the models were inaccurate. Since SRK uses a symmetric interaction parameter $K_{ij}$ between $CO_2$ and $H_2O$ in the van der Waals geometric mean-based mixing rules, it was expected that the SRK predictability of one of the mutual solubilities will be that low due to the polar nature of the mixture. The results suggested that SPUNG EoS inherits this impotence from SRK since it uses SRK to compute the shape factors.

The comparison with Wiebe (1941) at high pressures and low temperatures showed very low predictability of all the EoSs with very deviating results using both SPUNG and SRK EoSs. There were no improvement for SPUNG and SRK EoSs achieved by the regression.

The solubilities at moderate pressures, chosen in consistency to the experimental work conducted by Bamberger et al. (2000), were predicted by the three models. The results in Figs. 12 and 13 and AADs in Table 6 show that the errors in predicting $CO_2$ solubility became more severe than those at very high pressures for SPUNG and SRK EoSs. This highlighted the superior behavior of SRK-HV even more. Furthermore, the errors of SPUNG and SRK were reduced as the temperature increased, which suggested a need for correlating the interaction parameter $K_{ij}$ to temperature in addition to a more general mixing rule. This analysis was confirmed by the $K_{ij}$ sensitivity study conducted here (see Section 5.4). The predictability of SPUNG and SRK improved for $H_2O$ solubilities, while that of SRK-HV improved for both mutual solubilities and behaved much better than those of SPUNG and SRK.

The comparison to the set of data of Hou et al. (2013) showed the same behavior as of the one with Bamberger et al. (2000) at similar temperatures. However, the errors of all the EoSs were reduced significantly as the temperature increased.
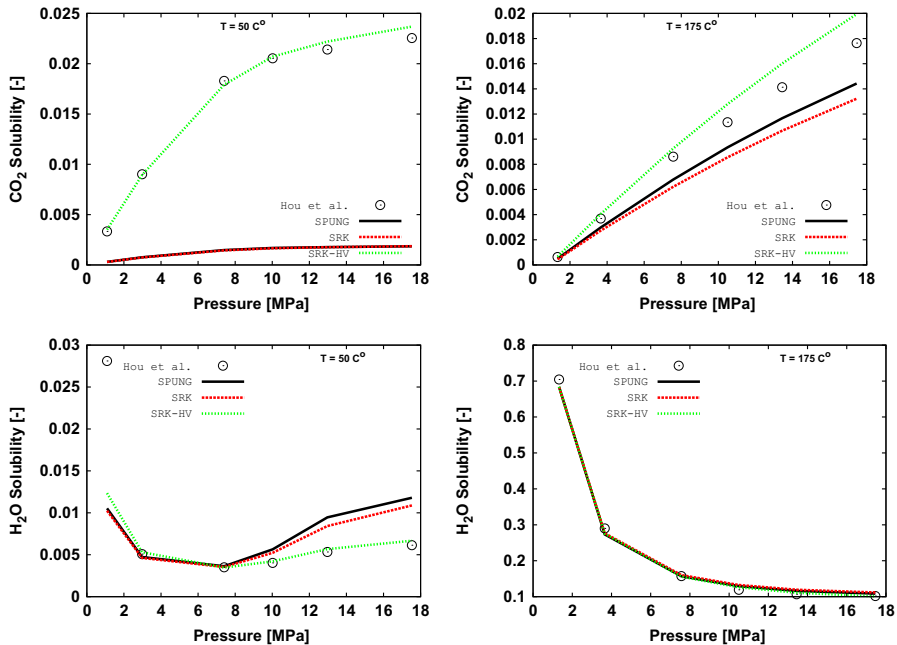
**Fig. 14.** $CO_2$ and $H_2O$ solubilities computations in comparison with experimental data of Hou et al. (2013).

**Table 7**
AAD (%) of the solubility of $CO_2$ and $H_2O$ at different temperatures in comparison with Wiebe (1941).

| Component | Temperature (°C) | SPUNG | SRK | SRK-HV |
|-----------|------------------|-------|-----|--------|
| $CO_2$ | 50 | 92.0 | 91.8 | 6.9 |
| | 75 | 84.3 | 84.3 | 2.01 |
| $H_2O$ | 50 | 167.9 | 157.9 | 33.1 |
| | 75 | 148.5 | 137.2 | 35.5 |

For low pressures, the results in Fig. 10 and the AADs in Table 4 showed the same trend in comparison with the experimental data of Bamberger et al. (2000), except that SRK-HV did not behave equally well.

For the low pressures and high temperatures in Fig. 11, the results showed good and improving predictability as the temperature increased.

In general, the predictions of all the EoSs improved with temperatures increase at all pressures.

### 5.4. Effects of the interaction parameter $K_{ij}$

Since the impotence of SPUNG in predicting the solubilities of $CO_2$–water was thought to be inherited from SRK due to the use of the symmetric interaction parameter $K_{ij}$, a simple sensitivity study on the effects of tuning $K_{ij}$ was conducted as explained in Section 3.2.6. The results of the tuning for the evaluated very high- and low-pressure cases are plotted in Figs. 10, 11, and 15. The AADs are presented in Tables 4, 5 and 8. These results showed that at these conditions there existed a $K_{ij}$ that could improve the mutual solubilities together, and which compromised the errors better than SRK-HV for the very high pressure, and for the low pressures-high temperatures cases. This implies a potential improvement by regression. Unfortunately, this behavior did not hold for the moderate pressures, and high pressures low temperatures cases. There, the $CO_2$ solubility errors could be improved, but causing the errors of $H_2O$ solubility to jump high with the expected counter effects due to the use of the geometric mean mixing rules. This behavior shows clearly that SPUNG EoS solubility prediction is limited to that of the EoS used to compute the shape factors.

The tuning of $K_{ij}$ influenced the rich-phase density predictions mainly through solubility. This was because $K_{ij}$ influences only the energy parameter $a$, and not the co-volume parameter $b$ in the cubic EoS formulations. In order to give a sense of the impact of each of the mutual solubility on the density predictions for $CO_2$–water system, a test was conducted at the conditions used for the density analysis discussed here. Since Chiquet et al. (2007), Hebach et al. (2004) and Bikkina et al. (2011) have not provided solubilities, the tuning was done by matching SRK-HV $CO_2$ solubility as good as possible. This was thought to be a valid step because SRK-HV showed a significantly good prediction of $CO_2$ solubility at similar pressure ranges in the work of Austegard et al. (2006). In addition, the comparison here, Figs. 12, 13 and Table 6, supported the same claim. The density predictions of the $K_{ij}$ tuned SPUNG EoS were included in the figures and summarized in the tables of the density predictions study. The results showed minor improvement on $H_2O$-rich phase density and major dis-improvement on $CO_2$−rich phase density due to the conjugate dis-improvement in $H_2O$ solubility prediction that was induced from the mixing rule.

It is important also to highlight the observation that the tuning showed a temperature-dependent behavior for $K_{ij}$ that was almost insensitive to the pressure and co-existing phases.

Since the solubilities are important for deciding co-existing phases, especially for small impurities of $H_2O$ in $CO_2$ or vice versa, and since SPUNG EoS has shown high potential, we are motivated under the guidance of this work for further developing the method to overcome this weakness. A more elaborated mixing rule that shall take into account the polar nature of the system, as
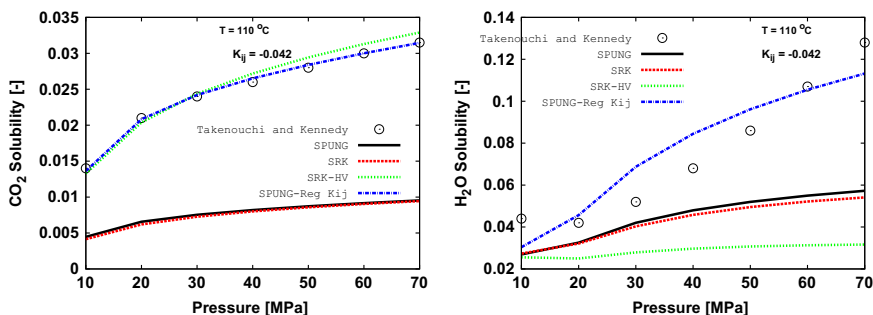
**Fig. 15.** $CO_2$ and $H_2O$ solubilities over very high pressures and a temperature of 110 °C in comparison with Takenouchi and Kennedy (1964) experimental data.

**Table 8**
AAD (%) of solubilities in comparison with Takenouchi and Kennedy (1964).

| Component | SPUNG | SRK | SRK-HV | SPUNG-Reg $K_{ij}$ |
|---|---|---|---|---|
| $CO_2$ | 68.9 | 69.9 | 4.0 | 1.1 |
| $H_2O$ | 36.2 | 38.3 | 56.5 | 17.3 |

well as the temperature dependency shown in this work, is needed.

### 5.5. Reference fluid sensitivity

The results in Table 3 showed clearly that the choice of reference fluid had a significant impact on the properties predictions and, in particular, on density predictions. Furthermore, the trend observed in the results was very interesting, where a heavier reference fluid within the set of hydrocarbons gave better predictions of the density compared to a lighter. Also within the set of $O_2$ and $N_2$ the same trend was seen. For all the reference fluids in Table 3, the curves of the REs showed almost equal slopes, which implied a low impact on solubility predictions.

### 6. Conclusions

The three tested EoSs predicted the dew temperature with high quality and precision, but predicted low pseudo-critical pressures for two tested data sets.

For single phase, at low pressure gas phase, SPUNG EoS exhibits a better behavior to SRK and SRK-HV cubic EoSs. However, the relative errors are low for all models. The role of SPUNG becomes significant as high pressures are of concern, where the error becomes considerable.

SPUNG has a superior behavior in predicting the rich phases density of the $CO_2$–water system compared to the evaluated cubic EoSs. Although $CO_2$ solubility prediction of SPUNG is very low at moderate pressures and low temperatures, the impact on density calculations for the $H_2O$-rich phase is not pronounceable. Improving the $CO_2$ solubility on the benefits of that of $H_2O$ leads to severe mis-prediction in the density of the $CO_2$−rich phase. The impact on the overall density prediction of the system will depend on the feed composition. Therefore, for the cases where water is an impurity, the impact of $CO_2$ solubility mis-prediction will have much less impact on the overall density prediction.

The effect of varying the reference fluids was investigated, and the errors span between the lightest and the heaviest reference fluid was large. This implies a significant impact of the reference fluid on the properties prediction. Nevertheless, the heaviest evaluated hydrocarbon was not heavy enough to give a significant

improvement. However, the observed trend and highlighted criterion of the search for a reference fluid rises the expectations in the SPUNG EoS potential for improving the water-rich phase density prediction, if a proper reference fluid is found, while the cubic EoSs do not have a similar potential.

SRK-HV EoS predicted the mutual solubilities for the binary polar mixture with high accuracy. Nevertheless, it showed much poorer predictability of the density of the $CO_2$–water system in general and compared to SPUNG in particular.

SRK EoS with van der Waals mixing rules combines the impotence of both SPUNG and SRK-HV EoS. Therefore, it is not recommended for this system, unless low-pressure gas-phase densities are the only interest.

The study showed that the SPUNG EoS predictability of the mutual solubilities is limited by the EoS used for the computation of the shape factors, which here, was SRK. However, the predictability of the density depends more on the choice of the reference fluid and the reference equation used. Since one of the powerful features of the concept is to allow a free choice of the EoS for the shape factors, the reference fluid, and the reference equation (given that the reference fluid coefficients exist for this reference equation), a promising alternative is to use an asymmetric quadratic mixing rule. It is also possible to use SRK-HV, which showed a very high success for solubility predictions of $CO_2$–water system. The work shows that the mixing rule has to have parameters fitted at each temperature for $CO_2$–water system.

### References

Austegard, A., Solbraa, E., deKoeijer, G., Mølnvik, M.J., 2006. Thermodynamic models for calculating mutual solubilities in $H_2O$–$CO_2$–$CH_4$ mixtures. Chem. Eng. Res. Des. 84 (9), 781–794.
Bamberger, A., Sieder, G., Maurer, G., 2000. High-pressure (vapor+liquid) equilibrium in binary mixtures of (carbon dioxide+water or acetic acid) at temperatures from 313 to 353 K. J. Supercrit. Fluids 17 (2), 97–110.
Bikkina, P.K., Shoham, O., Uppaluri, R., 2011. Equilibrated interfacial tension data of the $CO_2$–water system at high pressures and moderate temperatures. J. Chem. Eng. Data 56 (10), 3725–3733.
Chapman, W.G., Gubbins, K.E., Jackson, G., Radosz, M., 1990. New reference equation of state for associating liquids. Ind. Eng. Chem. Res. 29 (8), 1709–1721.
Chiquet, P., Daridon, J.L., Broseta, D., Thibeau, S., 2007. $CO_2$/water interfacial tensions under pressure and temperature conditions of $CO_2$ geological storage. Energy Convers. Manag. 48 (3), 736–744.

Diamantonis, N.I., Economou, I.G., 2012. Modeling the phase equilibria of a $H_2O$–$CO_2$ mixture with PC-SAFT and tPC-PSAFT equations of state. Mol. Phys. 110 (11–12), 1205–1212.

Ely, J.F., 1990. A predictive, exact shape factor extended corresponding states model for mixtures. Adv. Cryog. Eng. 35, 1511–1520.

Estela-Uribe, J.F., Trusler, J.P.M., 1998. Shape factors for the light hydrocarbons. Fluid Phase Equilib. 150–151, 225–234.

Fisher, G.D., Leland, T.W., 1970. Corresponding states principle using shape factors. Ind. Eng. Chem. Fundam. 9 (4), 537–544.

Hebach, A., Oberhof, A., Dahmen, N., 2004. Density of water + carbon dioxide at elevated pressures: measurements and correlation. J. Chem. Eng. Data 49 (4), 950–953.

Hendriks, E., Kontogeorgis, G.M., Dohrn, R., de Hemptinne, J.C., Economou, I.G., Zilnik, L.F., Vesovic, V., 2010. Industrial requirements for thermodynamics and transport properties. Ind. Eng. Chem. Res. 49 (22), 11131–11141.

Hou, S.X., Maitland, G.C., Trusler, J.M., 2013. Measurement and modeling of the phase behavior of the (carbon dioxide + water) mixture at temperatures from 298.15 K to 448.15 K. J. Supercrit. Fluids 73, 87–96.

Huron, M.J., Vidal, J., 1979. New mixing rules in simple equations of state for representing vapour–liquid equilibria of strongly non-ideal mixtures. Fluid Phase Equilib. 3 (4), 255–271.

Ibrahim, M., Skaugen, G., Ertesvåg, I.S., 2012. Preliminary evaluation of the SPUNG equation of state for modelling the thermodynamic properties of $CO_2$–water mixtures. Energy Procedia 26, 90–97.

Jørstad, O., 1993. Equations of State for Hydrocarbon Mixtures (Dr. Ing. thesis No. NTH 1993:92). Norwegian Institute of Technology, Trondheim, Norway.

King, M.B., Mubarak, A., Kim, J.D., Bott, T.R., 1992. The mutual solubilities of water with supercritical and liquid carbon dioxides. J. Supercrit. Fluids 5 (4), 296–302.

Kontogeorgis, G.M., Voutsas, E.C., Yakoumis, I.V., Tassios, D.P., 1996. An equation of state for associating fluids. Ind. Eng. Chem. Res. 35 (11), 4310–4318.

Kunz, O., Klimeck, R., Wagner, W., Jaeschke, M., 2007. The GERG-2004 Wide-Range Equation of State for Natural Gases and Other Mixtures. GERG TM15, VDI Verlag, Düsseldorf, Germany.

Leach, J.W., Chappelear, P.S., Leland, T.W., 1968. Use of molecular shape factors in vapor–liquid equilibrium calculations with the corresponding states principle. AIChE J. 14 (4), 568–576.

Lemmon, E.W., Huber, M.L., McLinden, M.O., 2010. NIST Standard Reference Database 23: Reference Fluid Thermodynamic and Transport Properties—REFPROP, Version 9.0. National Institute of Standards and Technology, Standard Reference Data Program, Gaithersburg, Maryland.

Li, H., Jakobsen, J.P., Wilhelmsen, Ø., Yan, J., 2011. PVTxy properties of $CO_2$ mixtures relevant for $CO_2$ capture, transport and storage: review of available experimental data and theoretical models. Appl. Energy 88 (11), 3567–3579.

Li, H., Yan, J., 2009. Impacts of equations of state (EOS) and impurities on the volume calculation of $CO_2$ mixtures in the applications of $CO_2$ capture and storage (CCS) processes. Appl. Energy 86 (12), 2760–2770.

Mollerup, J., 1980. Thermodynamic properties from corresponding states theory. Fluid Phase Equilib. 4 (1–2), 11–34.

Mueller, G., Bender, E., Maurer, G., 1988. Das Dampf-fluessigkeitsgleichgewicht des ternaeren Systems Ammonik-Kohlendioxid-Wasser bei hohn Wassergehalten im Bereich zwischen 373 und 473 Kelvin. Ber. Bunsenges. Phys. Chem. 92, 148–160.

Pappa, G.D., Perakis, C., Tsimpanogiannis, I.N., Voutsas, E.C., 2009. Thermodynamic modeling of the vapor–liquid equilibrium of the $CO_2/H_2O$ mixtures. Fluid Phase Equilib. 284 (1), 56–63.

Patel, M.R., Eubank, P.T., 1988. Experimental densities and derived thermodynamic properties for carbon dioxide-water mixtures. J. Chem. Eng. Data 33 (2), 185–193.

Patel, M.R., Holste, J.C., Hall, K.R., Eubank, P.T., 1987. Thermophysical properties of gaseous carbon dioxide–water mixtures. Fluid Phase Equilib. 36, 279–299.

Peng, D.Y., Robinson, D.B., 1976. A new two-constant equation of state. Ind. Eng. Chem. Fundam. 15 (1), 59–64.

Seitz, J.C., Blencoe, J.G., 1999. The $CO_2$–$H_2O$ system. I. Experimental determination of volumetric properties at 400 °C 10–100 MPa. Geochim. Cosmochim. Acta 63 (10), 1559–1569.

Soave, G., 1972. Equilibrium constants from a modified Redlich–Kwong equation of state. Chem. Eng. Sci. 27 (6), 1197–1203.

Solbraa, E., 2002. Equilibrium and Non-Equilibrium Thermodynamics of Natural Gas Processing (Dr. Ing. thesis No. 2002:146). Norwegian University of Science and Technology, Trondheim, Norway.

Span, R., Wagner, W., 1996. A new equation of state for carbon dioxide covering the fluid region from the triple-point temperature to 1100 K at pressures up to 800 MPa. J. Phys. Chem. Ref. Data 25 (6), 1509–1596.

Takenouchi, S., Kennedy, G.C., 1964. The binary system $H_2O$–$CO_2$ at high temperatures and pressures. Am. J. Sci. 262 (9), 1055–1074.

Tsivintzelis, I., Kontogeorgis, G.M., Michelsen, M.L., Stenby, E.H., 2011. Modeling phase equilibria for acid gas mixtures using the CPA equation of state. Part II: Binary mixtures with $CO_2$. Fluid Phase Equilib. 306 (1), 38–56.

Twu, C.H., Bluck, D., Cunningham, J.R., Coon, J.E., 1991. A cubic equation of state with a new alpha function and a new mixing rule. Fluid Phase Equilib. 69, 33–50.

Valtz, A., Chapoy, A., Coquelet, C., Paricaud, P., Richon, D., 2004. Vapour–liquid equilibria in the carbon dioxide-water system, measurement and modelling from 278.2 to 318.2 K. Fluid Phase Equilib. 226, 333–344.

Wiebe, R., 1941. The binary system carbon dioxide–water under pressure. J. Am. Chem. Soc. 29 (3), 475–481.

Wilhelmsen, Ø., Skaugen, G., Jørstad, O., Li, H., 2012. Evaluation of SPUNG and other equations of state for use in carbon capture and storage modelling. Energy Procedia 23, 236–245.

Younglove, B.A., Ely, J.F., 1987. Thermophysical properties of fluids: II. Methane, ethane, propane, isobutane, and normal butane. J. Phys. Chem. Ref. Data 16 (4), 577–798.

# PAPER IV
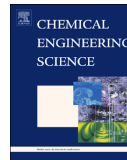
# An extended corresponding states equation of state (EoS) for CCS industry

Mohamed Ibrahim [a,*], Geir Skaugen [b], Ivar S. Ertesvåg [a]

[a] Department of Energy and Process Engineering, Norwegian University of Science and Technology, Kolbjørn Hejes veg 1B, NO-7491 Trondheim, Norway
[b] SINTEF Energy Research, Trondheim, Norway

## HIGHLIGHTS

- A new extended corresponding states equation of state (EoS) is proposed.
- The results are compared with experimental data and to another EoS of the same class.
- Three reference fluids (R23, R503, ammonia) were evaluated.
- The results showed very good capture of phase equilibrium over large PT conditions.
- The predictions of single and rich-phase densities were highly accurate.

## ARTICLE INFO

## ABSTRACT

For a good design of all the processes in Carbon Capture and Storage, the thermodynamics of the $CO_2$ and $CO_2$ mixtures should be accurately predicted. Among these mixtures are $CO_2$–water systems that are very difficult to deal with due to the polar nature. In this work we suggest a new extended corresponding states equation of state (EoS) that can handle polar mixtures. The new EoS uses the Bender Modified Benedict–Webb–Rubin EoS as a reference equation. $NH_3$, R23 and R503 are used as reference fluids with parameters from Polt. The EoS presented uses the Soave–Redlich–Kwong EoS with Huron Vidal mixing rules based approach to compute the scale factors. The evaluation of the new EoS is done over a large set of experimental data. The results show very high accuracy in predicting both phase equilibrium and densities.

© 2015 Elsevier Ltd. All rights reserved.

## 1. Introduction

There are a number of impurities in mixture with $CO_2$ that are relevant for the Carbon Capture and Storage (CCS) industry. Among these are $H_2O$, $H_2S$, $CH_4$, CO, $O_2$, $NO_2$ and $N_2$. The availability of the thermodynamic and transport properties of these mixtures is then vital for the design of various CCS processes. The experimental data are highly important. However, they are discrete in nature and local. Therefore, a generic and continuous solution is essential. Hence, modeling transport and thermodynamic properties of $CO_2$ with impurities is crucial for design, safety, efficiency and economy of the process.

It is possible to use empirically fitted models, but these models always have poor extendability and generality outside the fitted range. Moreover, they are not thermodynamically consistent over phases. A more appropriate and physically grounded approach is to use equations of state (EoSs). There are various categories of EoSs. Cubic EoSs like Soave–Redlich–Kwong (SRK) (Soave, 1972), SRK with Huron Vidal mixing rules (SRK-HV) (Huron and Vidal, 1979) and Peng–Robinson (PR) (Peng and Robinson, 1976) are amongst the lightest in computations. Consequently, they are the most widely used in industry. Among the heaviest in computation time are the full extended corresponding states (ECS) equations. A modern approach that is less computationally expensive than ECS, and offers generally good accuracy, is the multi-parameters approach. Nevertheless, it is at least one order of magnitude higher than cubic EoS in computation time (Wilhelmsen et al., 2012). Span–Wagner (Span and Wagner, 1996) for pure $CO_2$ and GERG (Groupe Européen de Recherches Gaziéres) (Kunz et al., 2007) for mixtures belong to this category. The Cubic-Plus-Association (CPA) (Kontogeorgis et al., 1996) and the Statistical Associating Fluid Theory (SAFT) (Chapman et al., 1990) EoSs are state-of-the-art approaches. The results of the CPA and Perturbed

* Corresponding author. Tel.: +47 735 93841.
E-mail addresses: mohamed.ibrahim@ntnu.no (M. Ibrahim),
Geir.Skaugen@sintef.no (G. Skaugen), ivar.s.ertesvag@ntnu.no (I.S. Ertesvåg).

Chain SAFT (PC-SAFT) for modeling CO₂–water systems were presented by Tsivintzelis et al. (2011) and Diamantonis and Economou (2012), respectively. The two articles also included a literature survey on CPA and SAFT type developments and recent achievements.

SPUNG EoS (Jørstad, 1993) is not a well known ECS equation although it handles the trade-off between accuracy and complexity well. The SPUNG EoS was first introduced for hydrocarbons. Recently Wilhelmsen et al. (2012) showed that SPUNG is a promising EoS for modeling $CO_2$ non-polar mixtures. However, we showed (Ibrahim et al., 2012, 2014b) that the SPUNG EoS qualities did not fully hold for modeling $CO_2$–water densities and phase equilibrium over a large range of conditions. This is mainly for water-rich phase density predictions and $CO_2$ solubilities at all tested pressures. We also investigated the effect of reference fluid on the density predictions, and found that for the set of tested hydrocarbons as reference fluids, the heavier the hydrocarbon, the better it predicted the water-rich phase density. Moreover, the study recommended development of asymmetric or non-quadratic mixing rules for better modeling of phase equilibrium (Ibrahim et al., 2014b, 2015). Mollerup (1998) earlier discussed generally the possibility of introducing non-quadratic mixing rules. However, he did not provide detailed derivations of specific mixing rule derivatives, or introduce a concrete model results. Furthermore, his general suggestions were incompatible with the implementation using van der Waals quadratic mixing rule. Therefore, they were not followed here. A similar discussion is made by Michelsen and Mollerup (2007).

**Table 1**
The $d$, $e$, $f$ and $\alpha$ values used for this study, where component $i$ is $CO_2$ and $j$ is water

| $d_{ji}$ | $e_{ji}$ | $f_{ji}$ | $d_{ij}$ | $e_{ij}$ | $f_{ij}$ | $\alpha_{ji}$ |
|---|---|---|---|---|---|---|
| − 1035.17623 | 17.07660 | 0.03200 | 5887.42379 | 1.75852 | − 0.01513 | 0.03 |

Here, we introduce a new original ECS EoS that uses SRK EoS and HV mixing rules for the computation of the scale factors. The new equation uses the Bender Modified Benedict–Webb–Rubin (MBWR) EoS parameters by Polt (1987) as the reference equation. The results using three alternative reference fluids that exhibited the best compromise for phase equilibrium and density predictions are demonstrated.

## 2. Theory

### 2.1. Equations of state

An EoS is a model that calculates for both the liquid and gas phases using the same expression. This enhances the continuity near the critical point. An EoS for an $N_c$ component mixture can be regarded as an expression for pressure $P$ as a function of the mole fractions $x_i$, the temperature $T$ and the volume $V$. Given this expression, the Helmholtz residual function $A_m^{res}[V, T, x]$, or the departure function $F = A_m^{res}[V, T, n]/(n_i RT)$, can be computed. Here, $n$ is the amount of substance, $R$ is the gas constant and subscript m stands for the mixture. The thermodynamic properties can then be computed from the derivatives of the departure function as explained by Jørstad (1993) or most thermodynamics textbooks concerned with EoSs.

### 2.2. The corresponding states principle

The principle of corresponding states assumes that all substances exhibit the same behavior at a reduced state. Consequently, the departure function can be written for a pure component as

$$\frac{A_i^{res}[V, T]}{n \cdot R \cdot T} = \frac{A_{Ref}^{res}[V_{Ref}, T_{Ref}]}{n \cdot R \cdot T_{Ref}}, \tag{1}$$
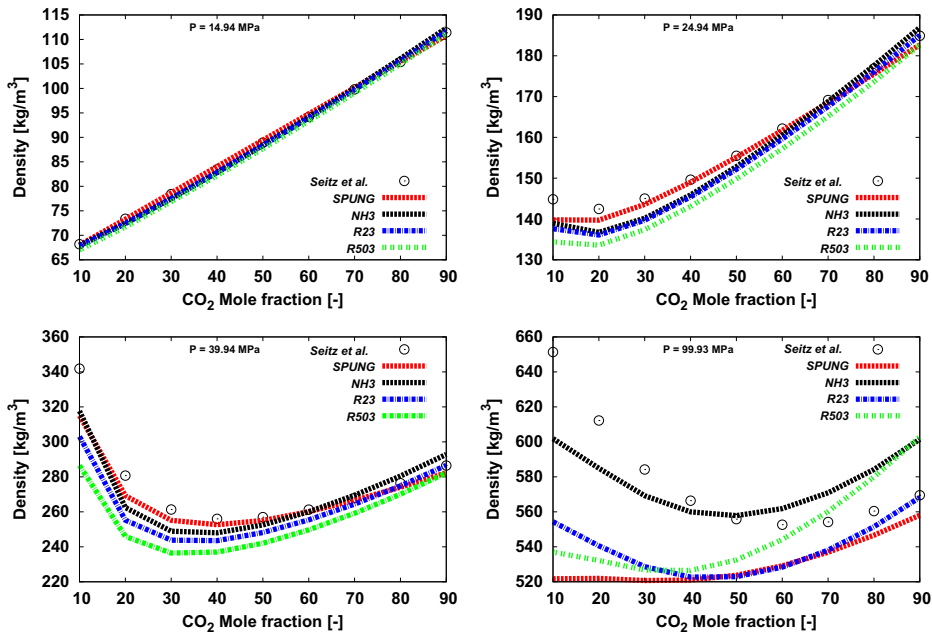


**Fig. 1.** Single phase density computations in comparison with experimental data of Seitz and Blencoe (1999), over mole fractions of $CO_2$ at different pressures and a temperature of 400 °C.
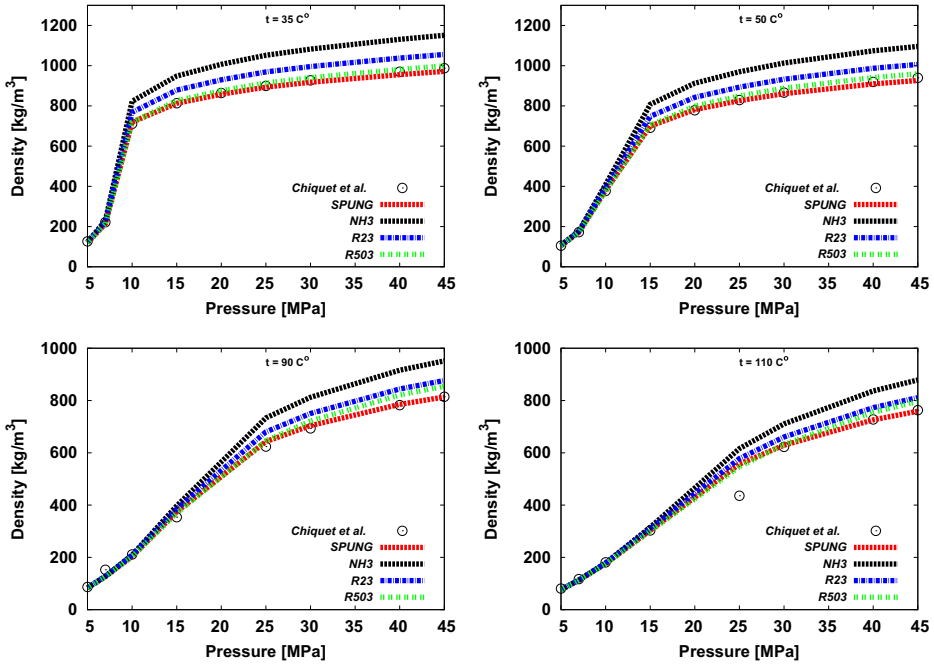
**Fig. 2.** SGLE $CO_2$-rich phase density predictions at temperatures about 35, 50, 90 and 110 °C in comparison with Chiquet et al. (2007) experimental data.

**Table 2**
AAD [%] of the $CO_2$-rich phases density calculations for the $CO_2$–water system at different temperatures.

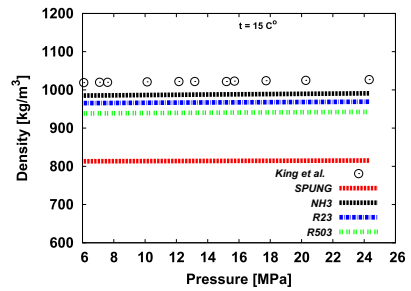| Data sets | Phase equilibrium | Temperature (°C) | SPUNG | NH3 | R23 | R503 |
|---|---|---|---|---|---|---|
| Chiquet et al. (2007) | SGLE | 35 | 1.8 | 13.5 | 6.3 | 2.1 |
| | | 50 | 0.7 | 12.8 | 6.0 | 1.7 |
| | | 70 | 2.0 | 13.0 | 6.9 | 3.2 |
| | | 90 | 4.5 | 12.7 | 7.9 | 5.9 |
| | | 110 | 5.3 | 12.4 | 7.9 | 6.2 |



**Fig. 4.** LLE water-rich phase density predictions at a temperature 15 °C in comparison with King et al. (1992) experimental data.
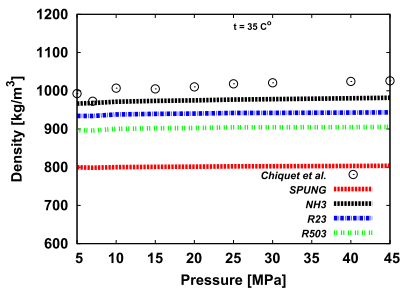


**Fig. 3.** Densities of the liquid water-rich phase co-existing with a supercritical $CO_2$-rich phase at a temperature about 35 °C in comparison with Chiquet et al. (2007) experimental data.
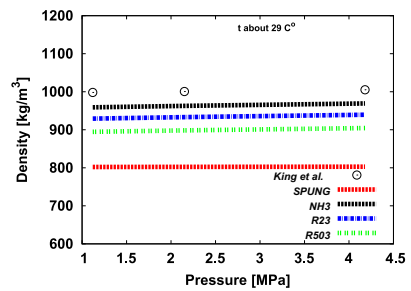


**Fig. 5.** Densities of the liquid water-rich phase co-existing with a gaseous $CO_2$-rich phase at a temperature about 29 °C in comparison with Hebach et al. (2004) experimental data.

or for a mixture as

$$\frac{A_m^{res}[V, T, x]}{n \cdot R \cdot T} = \frac{A_{Ref}^{res}[V_{Ref}, T_{Ref}]}{n \cdot R \cdot T_{Ref}}, \tag{2}$$

where index $i$ denotes the component, and subscript m stands for the mixture.

A corresponding state EoS typically has one or more reference components described very accurately by a reference EoS. In the corresponding states approach, the reference fluid volume $V_{Ref}$ and temperature $T_{Ref}$ are the reduced volume and temperature, $V_R$ and $T_R$, of the fluid or the mixture investigated. Here, subscript $R$ and Ref stand for reduced and reference, respectively.

### 2.3. The extended corresponding states principle

#### 2.3.1. Basic concept

In the extended corresponding states principle, the same principle is assumed. However, the mapping between the investigated fluid or mixture $T$ and $V$ and the reference fluid $V_{Ref}$ and $T_{Ref}$ is done via the scale factors $f_n$ and $h_n$ as

$$T_{Ref} = \frac{n \cdot T}{f_n}, \tag{3}$$

$$V_{Ref} = \frac{V}{h_n}. \tag{4}$$

These scale factors take into account how the fluids or the mixture in consideration differ from the reference fluid. As explained in Section 2.1, the thermodynamic properties are computed from the derivatives of the $F$ function. Therefore, from the definition of $F$, formulations for $f_n$ and $h_n$ and their derivatives are needed. The scale factors, $f_n$ and $h_n$, can be computed via scale factor functions, using semi-empirical functions, an accurate reference equation for each component, or using a simpler EoS. The work on shape factor functions started by Leach et al. (1968). Subsequently, many contributions were made. Examples are the work by Fisher and Leland (1970) and of Ely (1990), who has introduced the first exact shape factor concept. In addition, a substantial work on shape factor functions was conducted by Estela-Uribe and Trusler (1998). The computation of exact shape functions is computationally very expensive because they are implicit functions of the reference fluid $V_{Ref}$ and $T_{Ref}$. This is why the concept was left behind and thought to be impractical for use with numerical simulations. However, several implementations of the concept of extended corresponding states use simpler equations of state to compute shape factors and formulation that

**Table 3**
AAD [%] of water rich liquid phase densities averaged over the temperatures of each evaluated set of data.

| Data sets | Phase equilibrium | SPUNG | NH3 | R23 | R503 |
|---|---|---|---|---|---|
| King et al. (1992) | LLE | 20.5 | 3.4 | 5.8 | 8.8 |
| Chiquet et al. (2007) | SGLE | 21.6 | 5.3 | 9.9 | 14.7 |
| Hebach et al. (2004) | VLE | 20.1 | 4.3 | 7.2 | 8.7 |

**Table 4**
AAD [%] of the solubility of $CO_2$ and $H_2O$ in comparison with Valtz et al. (2004).

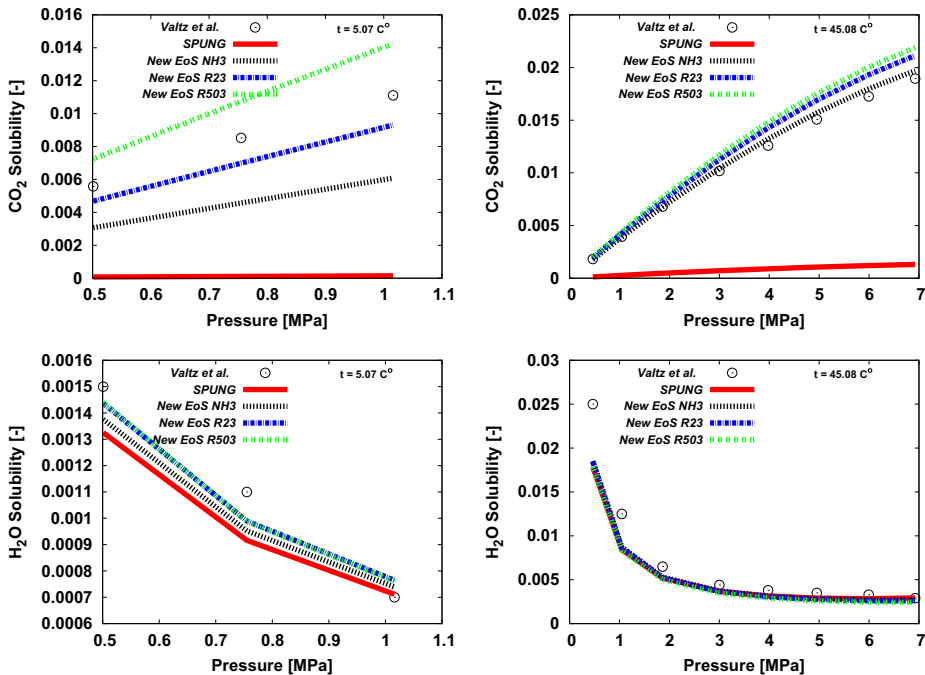| Component | Temperature (°C) | SPUNG | NH3 | R23 | R503 |
|---|---|---|---|---|---|
| $CO_2$ | 5.07 | 98.7 | 45.6 | 16.8 | 28.1 |
| | 25.13 | 96.8 | 15.9 | 4.9 | 25.0 |
| | 45.08 | 93.1 | 3.0 | 10.2 | 14.7 |
| $H_2O$ | 5.07 | 10.0 | 9.1 | 7.8 | 7.6 |
| | 25.13 | 17.8 | 15.4 | 15.4 | 18.1 |
| | 45.08 | 17.5 | 18.7 | 20.8 | 24.6 |



**Fig. 6.** $CO_2$ and $H_2O$ solubilities over low pressures and at temperatures of about 5 and 45 °C in comparison with Valtz et al. (2004) experimental data.
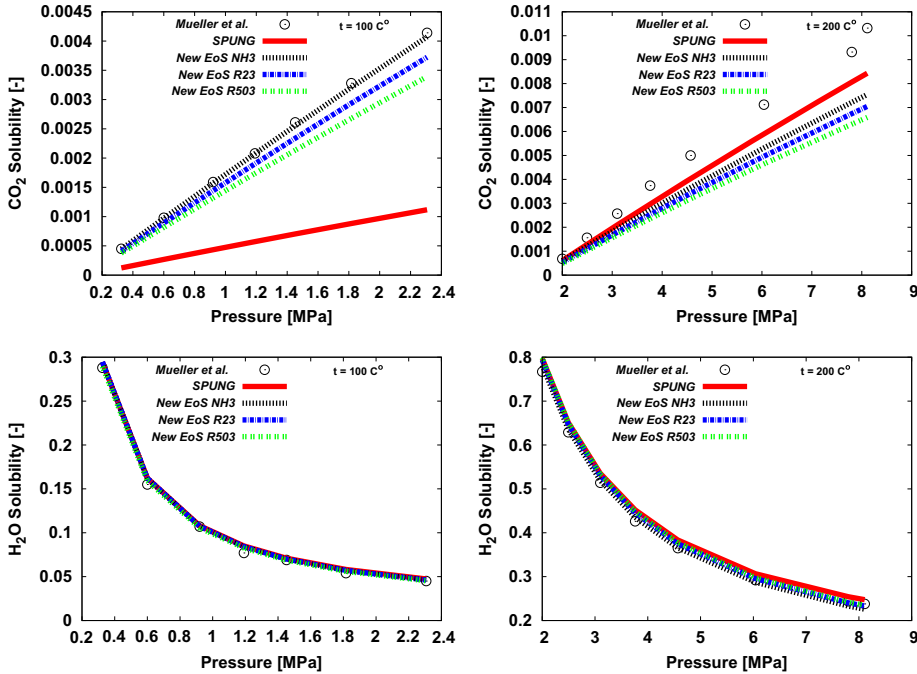
**Fig. 7.** $CO_2$ and $H_2O$ solubilities over low pressures and at temperatures of 100 and 200 °C in comparison with Mueller et al. (1988) experimental data.

**Table 5**
AAD [%] of the solubility of $CO_2$ and $H_2O$ in comparison with Mueller et al. (1988).

| Component | Temperature (°C) | SPUNG | NH3 | R23 | R503 |
|-----------|-----------------|-------|-----|-----|------|
| $CO_2$ | 100 | 72.8 | 1.3 | 9.5 | 17.3 |
| | 140 | 49.2 | 8.2 | 17.3 | 25.1 |
| | 200 | 17.0 | 23.6 | 29.5 | 34.4 |
| $H_2O$ | 100 | 4.9 | 3.7 | 3.8 | 2.3 |
| | 140 | 3.1 | 5.8 | 4.5 | 5.0 |
| | 200 | 4.5 | 2.2 | 2.7 | 3.0 |

is independent of $V_{Ref}$ and $T_{Ref}$, which showed a good compromise between accuracy and computation time. Among these are the SPUNG EoS that uses SRK EoS for the computation of the shape factors. The SRK EoS used in SPUNG EoS uses Soave's formulation for the computation of $\alpha(T)$ that appears in the equation of computing the $a_i$ parameter of pure components,

$$a_i = a_i^C \cdot \alpha(T). \tag{5}$$

Here, $a_i^C$ is the parameter $a$ for the pure component $i$ at critical conditions.

Using SRK EoS with Soave's formulation for $\alpha(T)$, Jørstad (1993) showed that $f_n$ and $h_n$ can be defined, respectively, as

$$f_n = \left( \frac{\sqrt{\frac{a_n}{a_{Ref}^C \cdot h_n}} + m_{Ref} \cdot \sqrt{\frac{n \cdot T}{T_{Ref}^C}}}{1 + m_{Ref}} \right)^2 \tag{6}$$

and

$$h_n = \frac{b_n}{b_{Ref}}, \tag{7}$$

where

$$m_{Ref} = \lambda + \beta \cdot \omega_{Ref} - \gamma \cdot \omega_{Ref}^2 \tag{8}$$

and $\lambda$, $\beta$ and $\gamma$ are constants that vary with the type of cubic EoS (e.g. 0.480, 1.574, and 0.176, respectively, for SRK). $\omega_{Ref}$ is the acentric factor of the reference component. The superscript $C$ means at critical conditions, and the subscript n means molar based. A similar discussion is made by Mollerup (1998) and Michelsen and Mollerup (2007).

From Eqs. (6) and (7) it is clear that to compute the derivatives of $f_n$ and $h_n$, a closure mixing rule formulation for the parameter $a_n$ and its derivatives are needed. The mixing rule to be selected or developed must be thermodynamically consistent.

### 2.3.2. The new EoS

In the new EoS we first introduce here, the Bender-MBWR EoS with 20 parameters of Polt (1987) was used for the reference fluid. The reference fluids recommended here are R23, R503 and NH$_3$. The R23 is CHF$_3$, and R503 is a mixture of R23 and R13 (CClF$_3$). The reference fluids are recommended after investigating several reference fluids including O$_2$, N$_2$, water, CO$_2$, C1–C9, and a set of refrigerants. Moreover, the cubic SRK-HV EoS was used to calculate the $a$ parameter in the scale factors. The parameter $a$ using Huron–Vidal mixing rules (Huron and Vidal, 1979) is defined as

$$a = b \left( \sum_{i=1}^{N_c} \left( x_i \frac{a_i}{b_i} \right) - \frac{G_\infty^E}{\ln(2)} \right), \tag{9}$$

where $b$ is the co-volume parameter defined as

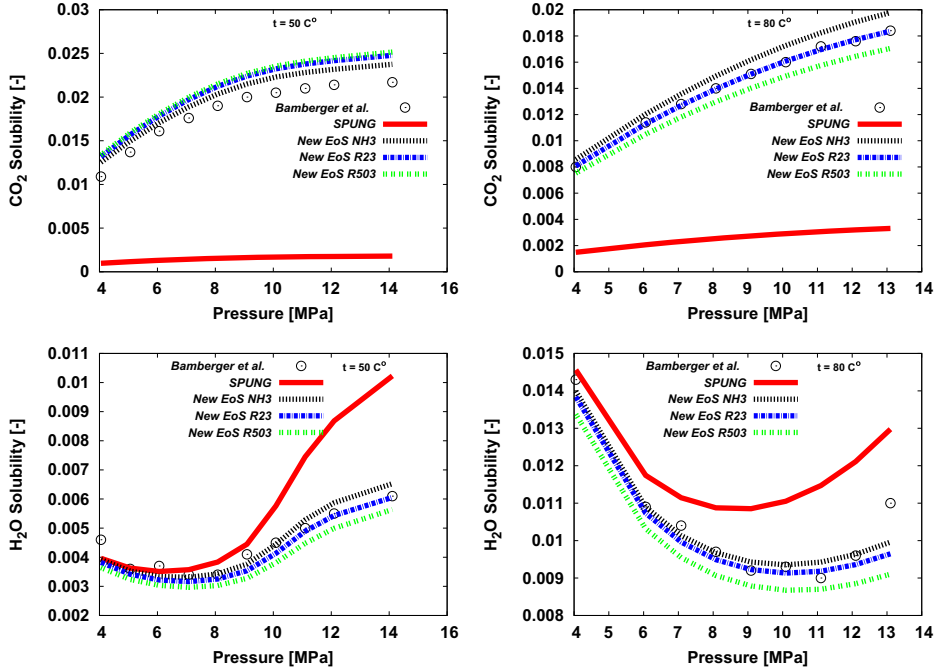$$b = \sum_{i=1}^{N_c} x_i \cdot b_i. \tag{10}$$

**Fig. 8.** $CO_2$ and $H_2O$ solubilities over moderate pressures and at temperatures of 50 and 80 °C in comparison with Bamberger et al. (2000) experimental data.

$G_\infty^E$ is the excess Gibbs free energy at infinite pressure,

$$\frac{G_\infty^E}{RT} = \sum_{i=1}^{N_c} x_i \cdot \frac{\sum_{j=1}^{N_c} \tau_{ji} b_j x_j C_{ji}}{\sum_{k=1}^{N_c} b_k x_k C_{ki}}, \tag{11}$$

where

$$\tau_{ji} = \frac{g_{ji} - g_{ii}}{RT}, \tag{12}$$

$$g_{ji} - g_{ii} = \Delta g_{ji} \tag{13}$$

and

$$C_{ji} = \exp(-\alpha_{ji}\tau_{ji}). \tag{14}$$

For a second order Huron–Vidal, $\Delta g_{ji}$ can be written as

$$\Delta g_{ji} = (d_{ji} + e_{ji} \cdot T + f_{ji} \cdot T^2) \cdot R, \tag{15}$$

where $\alpha_{ji}$ in Eq. (14) and $d_{ji}$, $e_{ji}$ and $f_{ji}$ in Eq. (15) are binary parameters to be fitted to experimental data. The used $d$, $e$, $f$ and the non-randomness parameter $\alpha_{ji}$ for $CO_2$–water are listed in Table 1.

A general discussion was made by Kontogeorgis and Coutsikos (2012), who reviewed the 30 years development of the activity coefficient models that are incorporated for cubic EoSs.

Here, for the ease of analysis and consistency with the work of Jørstad (1993), the molar based parameter $a_n = a \cdot n^2$ is used instead, defined as

$$a_n = b_n \left( \sum_{i=1}^{N_c} \left( n_i \frac{a_i}{b_i} \right) - \frac{G_{\infty n}^E}{\ln(2)} \right), \tag{16}$$

where $b_n = b \cdot n$ is defined as

$$b_n = \sum_{i=1}^{N_c} n_i \cdot b_i \tag{17}$$

and $G_{\infty n}^E = G_\infty^E \cdot n$.

Subsequently, the derivatives of $a_n$ needed to calculate the scale factors can be easily derived as follows:

$$\frac{\partial a_n}{\partial n_i} = b_i \cdot \frac{a_n}{b_n} + b_n \left( \frac{a_i}{b_i} - \frac{1}{\ln(2)} \cdot \frac{\partial G_{\infty n}^E}{\partial n_i} \right) \tag{18}$$

$$\frac{\partial^2 a_n}{\partial n_j \partial n_i} = b_i \cdot \left( \frac{a_j}{b_j} - \frac{1}{\ln(2)} \cdot \frac{\partial G_{\infty n}^E}{\partial n_j} \right) + b_j \cdot \left( \frac{a_i}{b_i} - \frac{1}{\ln(2)} \cdot \frac{\partial G_{\infty n}^E}{\partial n_i} \right)$$
$$- b_n \cdot \frac{1}{\ln(2)} \cdot \frac{\partial^2 G_{\infty n}^E}{\partial n_j \partial n_i} \tag{19}$$

$$\frac{\partial a_n}{\partial T} = b_n \left( \sum_{i=1}^{N_c} \left( \frac{n_i}{b_i} \frac{\partial a_i}{\partial T} \right) - \frac{1}{\ln(2)} \cdot \frac{\partial G_{\infty n}^E}{\partial T} \right) \tag{20}$$

$$\frac{\partial^2 a_n}{\partial T \partial n_i} = b_i \left( \sum_{i=1}^{N_c} \left( \frac{n_i}{b_i} \frac{\partial a_i}{\partial T} \right) - \frac{1}{\ln(2)} \cdot \frac{\partial G_{\infty n}^E}{\partial T} \right) \tag{21}$$
$$+ \frac{b_n}{b_i} \frac{\partial a_i}{\partial T} - \frac{b_n}{\ln(2)} \cdot \frac{\partial^2 G_{\infty n}^E}{\partial T \partial n_i}$$

$$\frac{\partial^2 a_n}{\partial T^2} = b_n \left( \sum_{i=1}^{N_c} \left( \frac{n_i}{b_i} \frac{\partial^2 a_i}{\partial T^2} \right) - \frac{1}{\ln(2)} \cdot \frac{\partial^2 G_{\infty n}^E}{\partial T^2} \right) \tag{22}$$

Once the $a_n$ and its derivatives are computed, the $f_n$ and $h_n$ and their derivatives can be computed.

## 3. Methodology

### 3.1. Numerical tools

The NTNU-SINTEF in-house thermodynamic library was used for the study presented. The new model was integrated to the library framework. The library is a tool for predicting the thermodynamic properties using various approaches that ranges in level of sophistication and underlying theory. The tolerance used for this study was $10^{-4}$ for both the multi-phase flash algorithm and the compressibility factor calculations.

### 3.2. Error definition

The errors of an EoS are measured here by the Relative Error (RE) and the Average of Absolute Deviation (AAD) defined for an arbitrary variable $C$ as

$$RE(C_r, \%) = \frac{|C_{s,r} - C_{\exp,r}|}{C_{\exp,r}} \times 100 \qquad (23)$$

and

$$AAD(C, \%) = \frac{100}{N} \times \sum_{r=1}^{N} \frac{|C_{s,r} - C_{\exp,r}|}{C_{\exp,r}} \qquad (24)$$

Here, $N$ is the total number of points, subscripts s and exp refer to simulation data and experimental data, respectively, and $r$ is a point index.

## 4. Results and discussion

### 4.1. Single phase density, high pressures

A set of conditions challenging for SPUNG and SRKs EoSs (Ibrahim et al., 2014b) at elevated pressures and various concen-

**Table 6**
AAD [%] of the solubility of $CO_2$ and $H_2O$ in comparison with Bamberger et al. (2000).

| Component | Temperature (°C) | SPUNG | NH3 | R23 | R503 |
|-----------|------------------|-------|-----|-----|------|
| $CO_2$ | 50 | 91.7 | 8.7 | 13.6 | 15.2 |
| | 60 | 88.9 | 9.9 | 9.5 | 7.0 |
| | 80 | 81.9 | 7.0 | 0.7 | 7.2 |
| $H_2O$ | 50 | 24.7 | 5.9 | 7.2 | 13.5 |
| | 60 | 20.5 | 5.9 | 5.7 | 9.9 |
| | 80 | 15.2 | 2.5 | 3.3 | 7.4 |

trations was evaluated using the new EoS with the different reference fluids R23, R503 and $NH_3$. The tested concentrations varied from 90% $CO_2$ to 90% of $H_2O$ over pressures that ranged from 10 to 100 MPa. The temperature at which the calculations were conducted was 400 °C. These conditions were consistent with the experimental data of Seitz and Blencoe (1999). The comparisons between the three tested reference fluids for the high-pressure data sets are plotted in Fig. 1. The figure shows the density change over molar fraction of $CO_2$ for the pressures of 14.94, 24.94, 39.94 and 99.93 MPa. The evaluation at low pressure data sets was excluded since all EoSs tested here and in Ibrahim et al. (2014b) were performing good for these conditions. This is obvious in Fig. 1 where at the lowest pressure of 14.94 MPa, all the new EoS and SPUNG EoS were very accurate over the entire range of concentrations.

The results showed very good matching and an improvement compared to SPUNG and SRKs EoSs results presented by Ibrahim et al. (2014b), especially as the pressure went up to 99.93 MPa. The mixing rules do not play a significant role, especially for the single phase, because they influence only the $a$ parameter calculations. Hence, improvement is argued to be mainly due to the use of the Bender 20 parameters MBWR EoS of Polt (1987) with the reference fluids R23, R503 and $NH_3$.

### 4.2. Rich phases

The new EoS was evaluated at conditions consistent with the experiments of Chiquet et al. (2007), King et al. (1992) and Hebach et al. (2004). Chiquet et al. (2007) measured densities of both $CO_2$-rich and water-rich phases when the $CO_2$-rich one was supercritical. The experiments were conducted at pressures that varied from 5 to 45 MPa, and the temperatures of $CO_2$-rich phases presented here were 35, 50, 90 and 110 °C. King et al. (1992) measured water-rich liquid-phase densities at pressures between 6 and 24 MPa. The temperatures at which the experiments were conducted were 15, 20, and 25 °C. The co-existing phase was $CO_2$-rich liquid phase. Hebach et al. (2004) data were used to evaluate the EoS for predicting water-rich liquid phase densities co-existing with $CO_2$-rich gas phase. The results of Chiquet et al. (2007) and Hebach et al. (2004) were measured at temperatures slightly around the listed values, although precisely fixed for each point.

The Supercritical Liquid Equilibrium (SGLE) $CO_2$-rich phase density predictions using the new EoS are presented in comparison to SPUNG and with the experimental data of Chiquet et al. (2007) in Fig. 2. The AAD of these predictions are shown in Table 2.
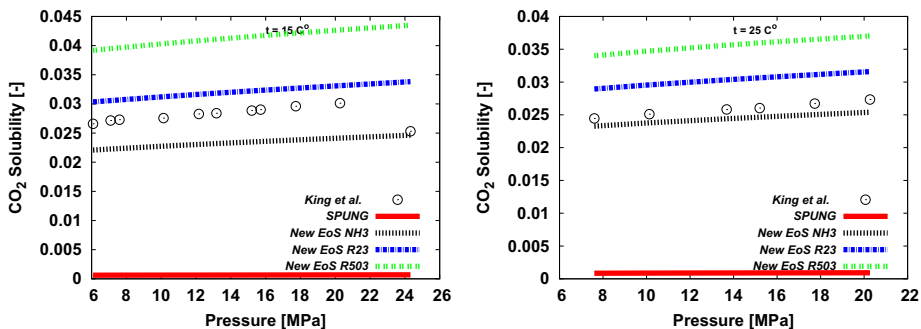
**Fig. 9.** $CO_2$ solubilities over moderate pressures and at temperatures of 15 and 50 °C in comparison with King et al. (1992) experimental data.
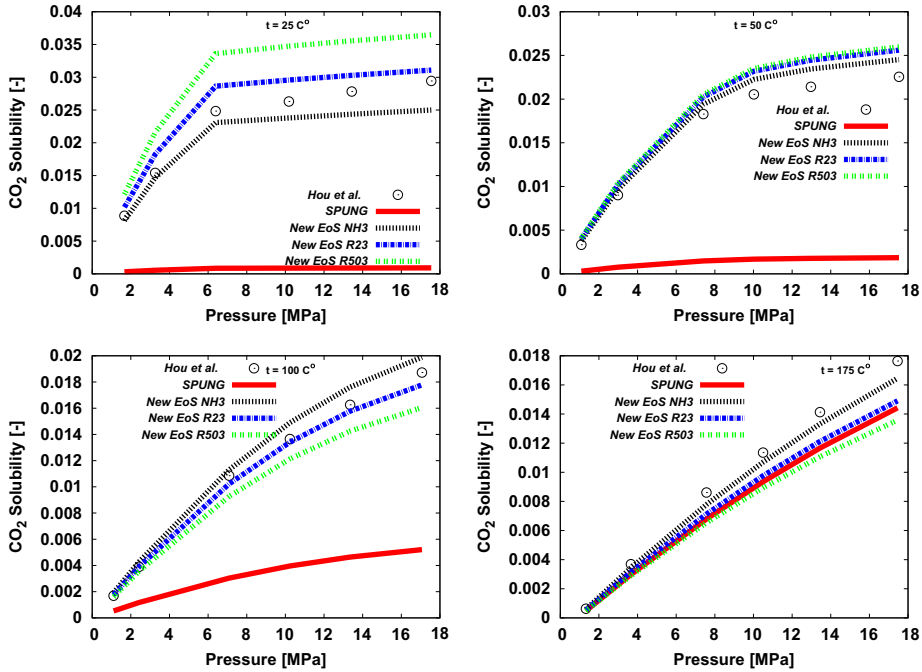
**Fig. 10.** $CO_2$ solubilities' computations in comparison with experimental data of Hou et al. (2013).

**Table 7**
AAD [%] of the solubility of $CO_2$ at different temperatures in comparison with King et al. (1992).

| Temperature (°C) | SPUNG | NH3 | R23 | R503 |
|---|---|---|---|---|
| 15 | 97.0 | 17.0 | 14.0 | 47.0 |
| 20 | 97.2 | 11.5 | 15.4 | 41.4 |
| 25 | 96.6 | 5.7 | 17.2 | 37.6 |

**Table 8**
AAD [%] of the solubility of $CO_2$ and $H_2O$ in comparison with Hou et al. (2013).

| Component | Temperature (°C) | SPUNG | NH3 | R23 | R503 |
|---|---|---|---|---|---|
| $CO_2$ | 25 | 96.6 | 9.5 | 12.6 | 32.7 |
| | 50 | 91.6 | 8.9 | 14.1 | 15.9 |
| | 75 | 82.9 | 13.3 | 7.5 | 2.4 |
| | 100 | 70.9 | 8.5 | 3.3 | 11.0 |
| | 125 | 57.4 | 2.3 | 12.0 | 21.0 |
| | 150 | 39.8 | 6.8 | 15.1 | 23.3 |
| | 175 | 19.3 | 6.9 | 15.3 | 22.5 |
| $H_2O$ | 25 | 52.7 | 27.1 | 28.9 | 30.9 |
| | 50 | 47.1 | 19.0 | 16.0 | 16.4 |
| | 75 | 24.4 | 4.6 | 3.5 | 4.8 |
| | 100 | 15.5 | 3.1 | 3.4 | 5.8 |
| | 125 | 12.0 | 5.7 | 4.8 | 6.5 |
| | 150 | 6.7 | 10.3 | 8.4 | 9.0 |
| | 175 | 5.5 | 9.5 | 7.0 | 6.8 |

**Table 9**
AAD [%] of the solubility of $CO_2$ and $H_2O$ at different temperatures in comparison with Wiebe (1941).

| Component | Temperature (°C) | SPUNG | NH3 | R23 | R503 |
|---|---|---|---|---|---|
| $CO_2$ | 50 | 92.0 | 6.8 | 11.7 | 12.0 |
| | 75 | 84.3 | 6.8 | 2.4 | 6.6 |
| $H_2O$ | 50 | 167.9 | 37.0 | 27.5 | 14.5 |
| | 75 | 148.0 | 32.4 | 24.8 | 13.3 |

are compared to the new EoS and SPUNG EoS in Fig. 4. Due to the similarity in trend between the results of 25 °C and 15 °C, the former are not shown here.

Density predictions using the new EoS of the liquid water-rich phase co-existing with gaseous $CO_2$-rich phase at a temperature of 29 °C are plotted in Fig. 5. The comparison at 19, 39 and 49 °C was similar, thus not presented here.

A summery of the water-rich phase AADs averaged over temperature is presented in Table 3.

Using the new EoS, the results for the $CO_2$-rich phase are slightly overshooting. However, the water-rich phase density predictions became very accurate. This can be attributed to the use of the reference fluids R23, R503 and $NH_3$. The results imply that R23 is the best compromise when $CO_2$–water is of concern.

### 4.3. Solubilities

The accuracies of the new EoS in predicting the mutual solubilities of $CO_2$ and $H_2O$ were validated against experimental data.

A review of the experimental data of $CO_2$–water system solubilities was given by Pappa et al. (2009). They recommended six sets of mutual solubilities data for model regression and validation. These six sets were those of Valtz et al. (2004), Mueller et al. (1988), Bamberger et al. (2000), King et al. (1992), Takenouchi and Kennedy (1964) and
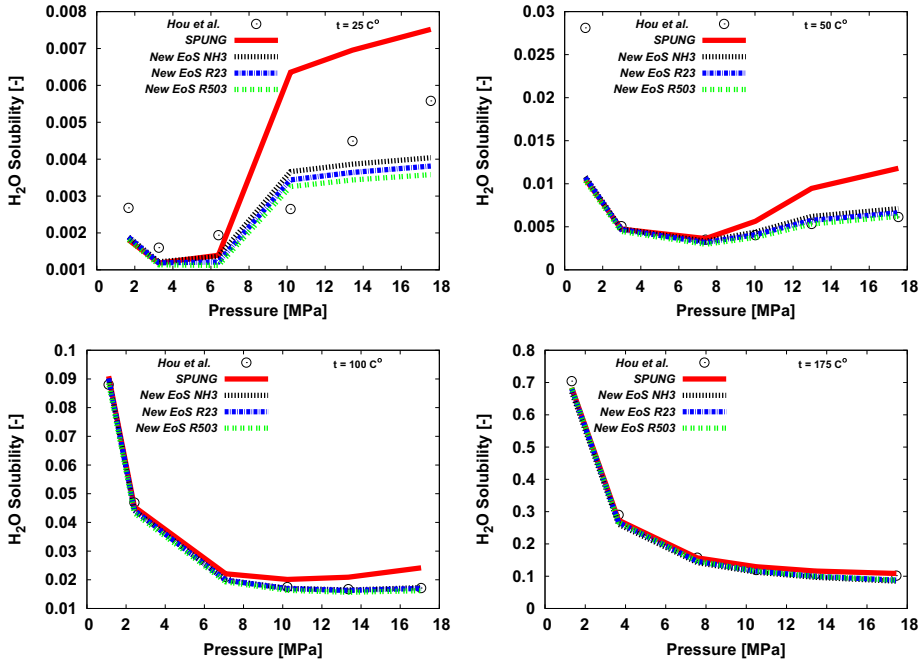
The density predictions using the new EoS of the liquid water-rich phase co-existing with a supercritical $CO_2$-rich phase at a temperature of 35 °C are presented in comparison with the experimental data of Chiquet et al. (2007) in Fig. 3.

The King et al. (1992) densities of the liquid water-rich phase co-existing with liquid $CO_2$-rich phase at a temperature of 15 °C

**Fig. 11.** H$_2$O solubilities' computations in comparison with experimental data of Hou et al. (2013).
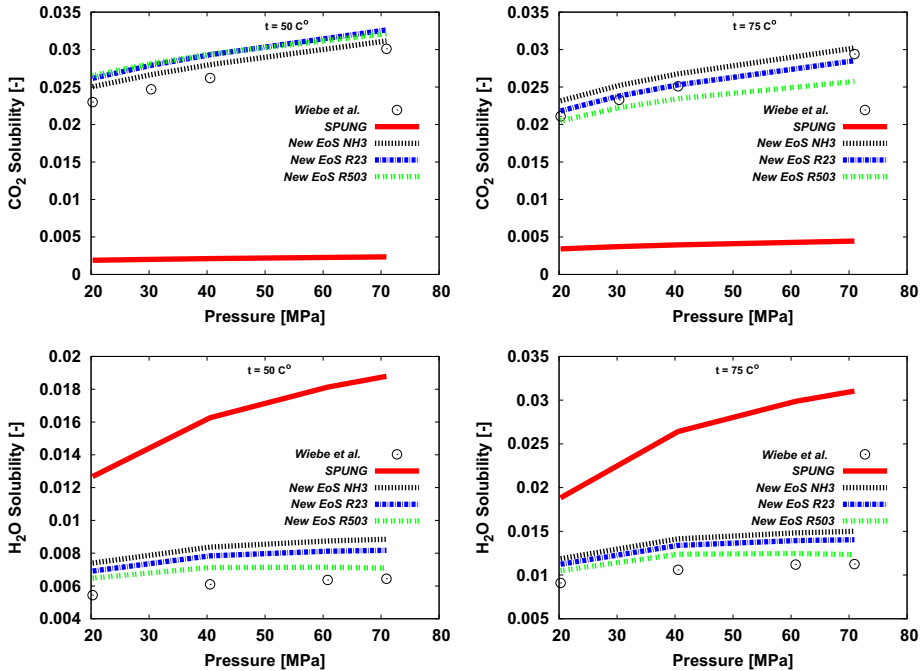


**Fig. 12.** CO$_2$ and H$_2$O solubilities over moderate pressures and at temperatures of 50 and 75 °C in comparison with Wiebe (1941) experimental data.

Wiebe (1941). The recent work by Hou et al. (2013) covered the available intermediate pressure data available in the literature at various temperatures and, in addition, filled in some gaps. Hou et al. (2013) also compared the new data against those of the literature and

found very good match. Takenouchi and Kennedy (1964) presented solubilities for very high pressures (10 to 70 MPa) between 110 and 350 °C. We only evaluated data at 110 °C, as higher temperatures are of minor relevance for CCS. Wiebe (1941) presented own data and
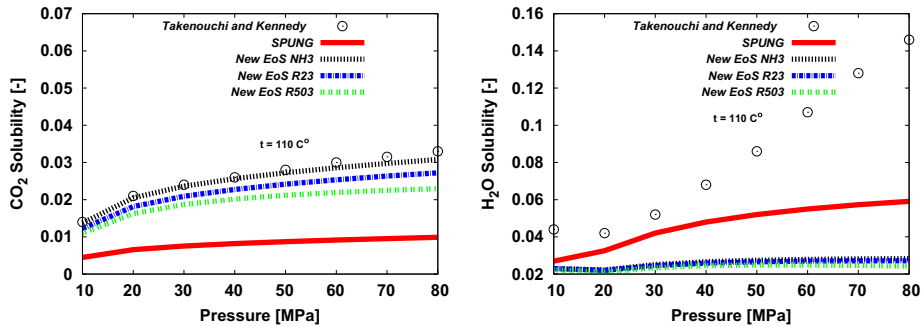
**Fig. 13.** $CO_2$ and $H_2O$ solubilities over very high pressures and at temperature of 110 °C in comparison with Takenouchi and Kennedy (1964) experimental data.

**Table 10**
AAD [%] of solubilities in comparison with Takenouchi and Kennedy (1964).

| Component | SPUNG | NH3 | R23 | R503 |
|---|---|---|---|---|
| $CO_2$ | 68.9 | 3.4 | 14.3 | 24.8 |
| $H_2O$ | 36.2 | 63.6 | 64.3 | 66.3 |

data from Wiebe and Gaddy (1939) for the pressure range of 1 to 70 MPa at temperatures from 25 to 100 °C. Owing to the fact that mutual solubility values were presented only for 75 and 100 °C, our calculations are limited to these data sets. The study of Bamberger et al. (2000) covered only pressures from 4 to 14 MPa at 50, 60, and 80 °C temperature values. The work of Valtz et al. (2004) investigated very low pressures at about 5, 25, and 45 °C. At 5 °C they measured pressures from 0.5 to 1 MPa. The pressures ranged approximately between 0.5 and 1 MPa. The span became wider as the temperature increased. At 45 °C, it was about 0.1 to 7 MPa. Mueller et al. (1988) published solubilities for another range; namely low pressures in conjunction with high temperatures (100–200 °C). The last study we compared with was Hou et al. (2013), which covered a large range of data for pressure values 1–17.5 MPa in conjunction with temperature values 25–175 °C.

We assessed the proposed EoS by comparing the predictions to SPUNG EoS and with the experimental works cited above. Fig. 6 shows our results with the data of Valtz et al. (2004). In addition, we assessed the solubilities at 25 °C, which yielded results similar to those shown in the figure. Table 4 gives the associated AADs.

Fig. 7 shows our results compared with Mueller et al. (1988) experimental data. In this figure we skipped the interim temperature, owing to the fact that those plotted were sufficient to illustrate the trend. However, Table 5 shows the AADs for the three assessed temperatures (Table 5).

For moderate pressures we chose the conditions to model according to Bamberger et al. (2000). Fig. 8 shows the comparison between our results and their experimental data, while Table 6 presents the AADs. We compare our results with the data of King et al. (1992) in Fig. 9 and Hou et al. (2013) in Figs. 10 and 11. Interim temperatures were left out with the same rationale as in the comparisons above. Table 7 for the former and Table 8 for the latter summarizes the AADs with respect to temperature. Fig. 12 and Table 9 compare our results with those of Wiebe (1941) experiments Fig. 12.

The proposed EoS was used to predict the mutual solubilities of $CO_2$ and $H_2O$ at very high pressures. The conditions are consistent with the work of Takenouchi and Kennedy (1964), namely between 10 MPa and 70 MPa, in conjunction with a temperature of 110 °C. Fig. 13 and Table 10 show our results and errors (in terms

of AADs), respectively, with reference to the work of Takenouchi and Kennedy (1964).

### 4.4. General discussion

The new EoS predicted the phase equilibrium very accurately. The comparison to SPUNG EoS showed large improvements. This is because the HV mixing rules have the advantage of handling asymmetric polar mixtures like $CO_2$–water, contrary to the symmetric quadratic mixing rule of van der Waals used in SPUNG EoS. We choose to derive the HV mixing rule for the shape factors calculation as it has the advantage of being a consistent mixing rule unlike the other asymmetric mixing rules that has the Michelsen–Kistenmacher syndrome (Michelsen and Kistenmacher, 1990). Moreover, in combination with the usage of the Bender-MBWR EoS parameters of Polt (1987) and the tested reference fluids, the new EoS predicted both densities and phase equilibrium for the polar mixture of $CO_2$–water accurately using the same set of parameters. The new EoS is of the same order of computational complexity as the SPUNG EoS. Therefore, the new ECS EoS is a similar compromise between computational time and accuracy. These achievements make the new EoS readily usable by CCS industry for its high accuracy and reasonable computational time.

### 5. Conclusions

A thermodynamically consistent extended corresponding states (ECS) EoS was developed for CCS industry. The new EoS can handle the phase equilibrium of the polar mixtures of $CO_2$–water with high accuracy. The high accuracy when compared with experimental data is achieved over a wide range of pressures and temperatures. This achievement is due to the proposed development of a Huron–Vidal mixing rules based approach computing the scale factors. The usage of R23, R503 and $NH_3$ as reference fluids allowed simultaneous accurate predictions of the density and phase equilibrium of the $CO_2$–water systems. This is achieved for the single phase at high pressures, supercritical-liquid, liquid–liquid, and vapor–liquid equilibrium.

# References

Bamberger, A., Sieder, G., Maurer, G., 2000. High-pressure (vapor+liquid) equilibrium in binary mixtures of (carbon dioxide+water or acetic acid) at temperatures from 313 to 353 K. J. Supercrit. Fluids 17 (2), 97–110.

Chapman, W.G., Gubbins, K.E., Jackson, G., Radosz, M., 1990. New reference equation of state for associating liquids. Ind. Eng. Chem. Res. 29 (8), 1709–1721.

Chiquet, P., Daridon, J.L., Broseta, D., Thibeau, S., 2007. CO$_2$/water interfacial tensions under pressure and temperature conditions of CO$_2$ geological storage. Energy Convers. Manag. 48 (3), 736–744.

Diamantonis, N.I., Economou, I.G., 2012. Modeling the phase equilibria of a H$_2$O–CO$_2$ mixture with PC-SAFT and tPC-PSAFT equations of state. Mol. Phys. 110 (11–12), 1205–1212.

Ely, J.F., 1990. A predictive, exact shape factor extended corresponding states model for mixtures. Adv. Cryog. Eng. 35, 1511–1520.

Estela-Uribe, J.F., Trusler, J.P.M., 1998. Shape factors for the light hydrocarbons. Fluid Phase Equilib. 150–151, 225–234.

Fisher, G.D., Leland, T.W., 1970. Corresponding states principle using shape factors. Ind. Eng. Chem. Fundam. 9 (4), 537–544.

Hebach, A., Oberhof, A., Dahmen, N., 2004. Density of water + carbon dioxide at elevated pressures: measurements and correlation. J. Chem. Eng. Data 49 (4), 950–953.

Hou, S.X., Maitland, G.C., Trusler, J.M., 2013. Measurement and modeling of the phase behavior of the (carbon dioxide + water) mixture at temperatures from 298.15 K to 448.15 K. J. Supercrit. Fluids 73, 87–96.

Huron, M.J., Vidal, J., 1979. New mixing rules in simple equations of state for representing vapour-liquid equilibria of strongly non-ideal mixtures. Fluid Phase Equilib. 3 (4), 255–271.

Ibrahim, M., Skaugen, G., Ertesvåg, I.S., 2012. Preliminary evaluation of the SPUNG equation of state for modelling the thermodynamic properties of CO$_2$–water mixtures. Energy Procedia 26, 90–97.

Ibrahim, M., Skaugen, G., Ertesvåg, I.S., 2014a. 2015. Modelling - water –water thermodynamics using spung equation of state (EoS) concept with various reference fluids. Energy Procedia, 51, 2014, 353–362, http://dx.doi.org/10.1016/j.egypro.2014.07.042.

Ibrahim, M., Skaugen, G., Ertesvåg, I.S., Haug-Warberg, T., 2014b. Modelling CO$_2$–water mixture thermodynamics using various equations of state (EoS) with emphasis on the potential of the SPUNG EoS. Chem. Eng. Sci. 113, 22–34.

Jørstad, O., 1993. Equations of state for hydrocarbon mixtures (Dr. Ing. thesis No. NTH 1993:92). Norwegian Institute of Technology, Trondheim, Norway.

King, M.B., Mubarak, A., Kim, J.D., Bott, T.R., 1992. The mutual solubilities of water with supercritical and liquid carbon dioxides. J. Supercrit. Fluids 5 (4), 296–302.

Kontogeorgis, G.M., Coutsikos, P., 2012. Thirty years with eos/ge models what have we learned? Ind. Eng. Chem. Res. 51 (11), 4119–4142.

Kontogeorgis, G.M., Voutsas, E.C., Yakoumis, I.V., Tassios, D.P., 1996. An equation of state for associating fluids. Ind. Eng. Chem. Res. 35 (11), 4310–4318.

Kunz, O., Klimeck, R., Wagner, W., Jaeschke, M., 2007. The GERG-2004 Wide-Range Equation of State for Natural Gases and Other Mixtures. GERG TM15, VDI Verlag, Düsseldorf, Germany.

Leach, J.W., Chappelear, P.S., Leland, T.W., 1968. Use of molecular shape factors in vapor–liquid equilibrium calculations with the corresponding states principle. AIChE J. 14 (4), 568–576.

Michelsen, M.L., Kistenmacher, H., 1990. On composition-dependent interaction coefficients. Fluid Phase Equilib. 58 (1–2), 229–230.

Michelsen, M., Mollerup, J., 2007. Thermodynamic Models: Fundamentals & Computational Aspects. Tie-Line Publications, Holte.

Mollerup, J., 1998. Unification of the two-parameter equation of state and the principle of corresponding states. Fluid Phase Equilib. 148 (1–2), 1–19.

Mueller, G., Bender, E., Maurer, G., 1988. Das Dampf-fluessigkeitsgleichwicht des ternaeren Systems Ammonik-Kohlendioxid-Wasser bei hohn Wassergehalten im Bereich zwischen 373 und 473 Kelvin. Ber. Bunsenges. Phys. Chem. 92, 148–160.

Pappa, G.D., Perakis, C., Tsimpanogiannis, I.N., Voutsas, E.C., 2009. Thermodynamic modeling of the vapor–liquid equilibrium of the CO2/H2O mixtures. Fluid Phase Equilib. 284 (1), 56–63.

Peng, D.Y., Robinson, D.B., 1976. A new two-constant equation of state. Ind. Eng. Chem. Fundam. 15 (1), 59–64.

Polt, A., 1987. Zur beschreibung der thermodynamischen eigenschaften reiner fluide mit "Erweiterten BWR-Gleichungen". Dissertation.

Seitz, J.C., Blencoe, J.G., 1999. The CO2–H2O system. I. Experimental determination of volumetric properties at 400 °C, 10–100 MPa. Geochim. Cosmochim. Acta 63 (10), 1559–1569.

Soave, G., 1972. Equilibrium constants from a modified Redlich–Kwong equation of state. Chem. Eng. Sci. 27 (6), 1197–1203.

Span, R., Wagner, W., 1996. A new equation of state for carbon dioxide covering the fluid region from the triple-point temperature to 1100 K at pressures up to 800 MPa. J. Phys. Chem. Ref. Data 25 (6), 1509–1596.

Takenouchi, S., Kennedy, G.C., 1964. The binary system H$_2$O–CO$_2$ at high temperatures and pressures. Am. J. Sci. 262 (9), 1055–1074.

Tsivintzelis, I., Kontogeorgis, G.M., Michelsen, M.L., Stenby, E.H., 2011. Modeling phase equilibria for acid gas mixtures using the CPA equation of state. Part II: binary mixtures with CO$_2$. Fluid Phase Equilib. 306 (1), 38–56.

Valtz, A., Chapoy, A., Coquelet, C., Paricaud, P., Richon, D., 2004. Vapour-liquid equilibria in the carbon dioxide–water system, measurement and modelling from 278.2 to 318.2 K. Fluid Phase Equilib. 226, 333–344.

Wiebe, R., 1941. The binary system carbon dioxide–water under pressure. Chem. Rev. 29 (3), 475–481.

Wiebe, R., Gaddy, V., 1939. The solubility in water of carbon dioxide at 50, 75 and 100°, at pressures to 700 atmospheres. J. Am. Chem. Soc. 61 (2), 315–318.

Wilhelmsen, Ø., Skaugen, G., Jørstad, O., Li, H., 2012. Evaluation of SPUNG and other equations of state for use in carbon capture and storage modelling. Energy Procedia 23, 236–245.